

GROWTH FACTOR ENRICHED MULTI-LUMINAL CONDUITS FOR AXONAL  
REGENERATION AND MATURATION ACROSS CRITICAL NERVE INJURIES

by

Geetanjali Shrirang Bendale

APPROVED BY SUPERVISORY COMMITTEE:

---

Dr. Mario I. Romero-Ortega, Chair

---

Dr. Joseph J. Pancrazio

---

Dr. Jennifer L. Seifert

---

Dr. Seth Hays

---

Dr. Danieli BC Rodrigues

Copyright 2019  
Geetanjali Shrirang Bendale  
All Rights Reserved

This work is dedicated to my husband, Varun Chheda, who represents those truly believing in  
and practicing equality in all areas of life.

GROWTH FACTOR ENRICHED MULTI-LUMINAL CONDUITS FOR AXONAL  
REGENERATION AND MATURATION ACROSS CRITICAL NERVE INJURIES

by

GEETANJALI SHRIRANG BENDALE, MS

DISSERTATION

Presented to the Faculty of  
The University of Texas at Dallas  
in Partial Fulfillment  
of the Requirements  
for the Degree of

DOCTOR OF PHILOSOPHY IN  
BIOMEDICAL ENGINEERING

THE UNIVERSITY OF TEXAS AT DALLAS

May 2019

## ACKNOWLEDGEMENTS

This dissertation is the result of many years of work and it would have never been possible without the amazing people that I have met during this journey. First and foremost, I would like to thank Dr. Mario Romero-Ortega for giving me this opportunity and for his mentorship and faith in me throughout. His training has shaped me into a creative, detail-oriented, persistent researcher. I would also like to thank Dr. Jennifer Seifert, for being an incredible mentor during my formative years as a graduate student. Her help and guidance has been invaluable throughout my time here. I would also like to thank my committee members, Dr. Joe Pancrazio, Dr. Seth Hays and Dr. Danieli Rodrigues, for their advice and valuable suggestions.

I couldn't have asked for a better group than the RNN Lab. I want to thank my brilliant group of undergraduate students, Brandon Tran, Jefferey Miyata and Fariel Rahman, who relentlessly worked with rabbits for over six months, and have added immensely to the successful completion of the experiments. I would also like to thank Ana Hernandez, for her help throughout these experiments, and the wonderful Tere Eddy, for helping manage everything effortlessly. Amongst the greatest things the lab has given me are my friends, Eileen Shimizu, Sanjay Anand and Aswini Kanneganti. Thank you for being my friends, mentors, critics and support network, all in one.

Most importantly, I would like to thank my family for supporting me throughout this tough journey. I want to thank my Baba for believing in me and my Aai for her countless "everything-will-be-okays." I am forever grateful for my amazing husband Varun, who I cannot thank enough for his constant encouragement and for being the anchor I needed to believe in myself all these years.

April 2019

# GROWTH FACTOR ENRICHED MULTI-LUMINAL CONDUITS FOR AXONAL REGENERATION AND MATURATION ACROSS CRITICAL NERVE INJURIES

Geetanjali Shrirang Bendale, PhD  
The University of Texas at Dallas, 2019

Supervising Professor: Mario I. Romero-Ortega

In the United States, about 900,000 peripheral nerve repair surgeries are performed every year, to treat traumatic and iatrogenic injuries. Despite the robust regenerative capacity of peripheral axons, studies have found that in nerve injuries resulting in substantial tissue damage ( $\geq 3\text{cm}$ ), as low as 25% patients gain full motor recovery and an even lower 3% gain complete sensory recovery. The current standard of care in clinic is surgical repair using an autologous nerve graft, extracted from a functionally less important nerve. While successful outcome depends on surgical precision and donor matching, in many cases, it can have deleterious co-morbid effects, formation of neuromas resulting in pain, in addition to loss of function in the donor nerve muscle. Although there are multiple biosynthetic nerve guides approved by the FDA, repair using autologous nerve grafts is still most preferred by surgeons, despite its risks. This is because currently available conduits have a hollow lumen, which fails to provide structural and biochemical support that is needed by peripheral axons to grow across long distances. Therefore, to enhance regeneration by mimicking the internal tubular architecture of the nerve, our lab previously designed a multi-luminal Biosynthetic Nerve Implant (BNI). The BNI is a polyurethane tube with an agarose scaffold consisting of multiple microchannels filled with collagen matrix. In a 10mm transection

sciatic nerve injury in a rat model, it was shown that the BNI provides structural support during regeneration, resulting in fascicular distribution of axons, and higher functional recovery, as compared to hollow lumen tubes. We next tested whether this effect can be further enhanced by the addition of growth factors, to repair critical nerve injuries with  $\geq 3$ cm tissue loss, and how that affects functional outcome. In this dissertation, we provide specific neurotrophic and pleiotropic cues to promote axon growth, increase maturation and re-myelination after injury, uncover possible mechanisms that affect axon pathfinding and functional recovery. We also developed 3D printed S-shaped conduits to determine the effect of geometry and topography on growing axons and mimic a critical gap in the rat model.

In Chapter 2, continuing from a previous study, we analyzed electron micrographs of distal end of nerve samples to determine the degree of myelination provided by pleiotrophin (PTN) and glial-derived neurotrophic factor (GDNF) treatments. Although we observed a moderate effect of PTN-GDNF in enticing axons and restoring function, there was a substantial lack of myelination, mainly contributed by abnormal radial sorting of the regenerating axons. We proposed that in addition to neurotrophic factors, incorporating biomolecules to stimulate Schwann cells into correctly sorting growing axons will improve re-myelination, and subsequent functional recovery.

In Chapter 3, we reasoned that since axonal derived Neuregulin1 Type-III signals Schwann cells to sort out large axons and myelinate them, incorporating it into the BNI will enhance re-myelination in a 4cm nerve gap. With an improvement in re-myelination and functional recovery, for the first time we show a neurotrophic effect of NRG1 Type-III alone. Here, we propose a possible signaling pathway wherein exogenous neuregulin binding to Schwann cells triggers release of endogenous growth factors from the Schwann cells, that bind to receptors on the nearest

axon, triggering growth and myelination, and further release of the membrane bound isoform NRG1 Type-III, in a two-way axo-glial signaling.

In Chapter 4, we developed 3D printed S-shaped nerve guide conduits (NGCs), to mimic a critical gap in the rat model and determine if axons can grow along curved paths. By comparing 10mm straight conduits with 13mm S-shaped conduits, we found that despite the 3mm difference in length, axons regenerated across the tubes within the same 7 week period, with no differences in the number, and with equal functional recovery. This model probes the importance of topological cues in axon guidance as well as provides a critical injury model that can be exploited for the standardized sensori-motor assessment techniques available for the rat.

Together, the work described here highlights the complexity of growth factor mediated peripheral nerve regeneration and re-innervation and its effect on restoring function, provides possible mechanisms of axon maturation that can be further exploited to enhance the intrinsic regenerative capacity of peripheral axons.



## TABLE OF CONTENTS

ACKNOWLEDGEMENTS .....	v
ABSTRACT.....	vi
LIST OF FIGURES .....	xi
LIST OF TABLES .....	xv
CHAPTER 1 INTRODUCTION .....	1
1.1 Clinical Significance.....	1
1.2 Organization of The Peripheral Nervous System .....	2
1.3 Peripheral Nerve Injury Classification .....	2
1.4 Cellular Response To Nerve Injury .....	4
1.5 Current Repair Strategies.....	7
1.6 Biosynthetic Nerve Implant (BNI) .....	17
1.7 Specific Aims .....	19
CHAPTER 2 EFFECT OF PLEIOTROPHIN AND GLIAL DERIVED NEUROTROPHIC FACTOR IN REPAIRING A CRITICAL NERVE GAP.....	20
2.1 Introduction .....	20
2.2 Materials and Methods .....	28
2.3 Results .....	30
2.4 Discussion.....	34
CHAPTER 3 ROLE OF NEUREGULIN 1- TYPE III IN AXON PATHFINDING, REGENERATION AND FUNCTIONAL RECOVERY IN A CRITICAL NERVE GAP IN THE RABBIT PERONEAL NERVE MODEL .....	37
3.1 Introduction .....	37
3.2 Materials And Methods .....	41
3.3 Results .....	48
3.4 Discussion.....	60
CHAPTER 4 EXTENDING THE MAXIMUM CRITICAL NERVE GAP IN THE RAT SCIATIC NERVE MODEL USING CURVED CONDUITS .....	65
4.1 Introduction .....	65
4.2 Materials And Methods .....	69
4.3 Results .....	73
4.4 Discussion.....	78

CHAPTER 5	DISSERTATION SUMMARY .....	81
5.1	Introduction .....	81
5.2	Limitations And Future Directions .....	84
5.3	Overall Summary And Dissertation Contribution .....	85
REFERENCES	.....	87
BIOGRAPHICAL SKETCH	.....	106
CURRICULUM VITAE	.....	107

## LIST OF FIGURES

Figure 1.1. Classification of nerve injury based on Seddon and Sunderland. Figure taken from[18] .....	4
Figure 1.2. Nerve conduits with luminal fillers used to mimic the internal architecture of the nerve. Incorporation of Schwann cells, neurotrophic factors, topographical cues like microchannels and ECM proteins provide structural and functional support to growing axons. Figure from [65].....	11
Figure 1.3. A&B) longitudinal view of the BNI with different number of microchannels. C &D) Figure 1.4Transverse view of the distal end of the BNI showing the successfully regenerated nerve, in fascicle like structures. E) Toluidine blue staining of the nerve section showing fascicles and F) abundant small and large myelinated axons inside the channels. Scale Bar: 50µm (Figure from[122] ) .....	18
Figure 2.1. Fabrication of the Biosynthetic Nerve Implant, characterization of growth factor microspheres and surgical implantation. (A) Cross section schematic of the BNI, showing its composition (B) The release profile of the PTN microspheres, showing a sustained release. Inserts: SEM images of the PTN-MPs and bioactivity assay showing axonal growth (C) BNI fabrication method, showing casting of the agarose scaffold and E) Cross section of the BNI showing the eight microchannels with luminal MP-collagen (insert). Scale bars: B) SEM: 5 µm, DRG: 1 mm, D) 1 mm, E) Device: 250 µm, Insert: 10 µm. F) 2 mm. ....	21
Figure 2.2. Effects of growth factors on neurite extension from DRG. (A) Confocal images of the DRG explants following treatments with different growth factor combinations. (B) Axonal length and C) number (density) indicated that PTN had a superlative effect on neurite growth, independently and in combination with GDNF and NT-3. Axonal density is reported as percentage of the negative control. *** = $p < 0.001$ , ** = $p < 0.01$ , * = $p < 0.05$ . Scale bar 100µm. ....	22
Figure 2.3. PTN-GDNF induces motor neurite outgrowth in ventral motor neuron of spinal cord explants in vitro. (A) Confocal images of neurite outgrowth in spinal cord explants. (B) A combination of PTN-GDNF showed a significant improvement in axon length and (C)number as compared to control, or individual growth factors. ***= $p \leq 0.001$ . ....	23
Figure 2.4. PTN-GDNF combination promote axon regrowth across a critical gap. (A) Images of explanted regenerated tissue, showing successful re-connection in all the BNI groups. (B) Immunofluorescent labelling of $\beta$ -III tubulin and P0 confirmed axons and myelination proximal (C) and distal (D) segments of the nerve tissue, with PTN-GDNF showing maximum number of axons in both, with a trend towards significance as compared to the PTN only group. ( $p=0.053$ ). Scale Bar: 50µm.....	25

Figure 2.5. Evoked compound action potentials from regenerated nerves. Stimulation of the regenerated nerves evoked a close to normal response in the A) Cut-resuture group, but failed in the B) BSA, PTN and GDNF groups.....	26
Figure 2.6. Modest recovery in Toe-Spread Index provided by PTN-GDNF. In the 4cm study, Toe-Spread Index (TSI) at the end of five months confirmed moderate recovery in TSI in the growth factor groups, but not comparable to the cut-resuture control. However, at the last time point, PTN-GDNF group was significantly better than the BSA control. *** = $p < 0.001$ , * = $p < 0.05$ .....	27
Figure 2.7. Radial sorting delay. Electron micrographs of axons in Remak bundles. (A) Compared to those with BSA, larger unmyelinated axons were present in the (B) PTN and (C) GDNF groups (arrowheads). (D) Some re-myelinated axons were present in the PTN-GDNF group. (E) Schematic representation of different diameter axons in the Remak bundles for each group. (F) Axon diameter distribution showed significantly smaller axons in the BSA, PTN and GDNF groups compared to the PTN-GDNF. Scale bar: 5 $\mu$ m. *** = $p < 0.001$ , ** = $p < 0.01$ ...	31
Figure 2.8. Re-innervation of the tibialis anterior muscle. (A) Co-labeling of axons (NF200) and AchR clustering ( $\alpha$ -bungarotoxin) demonstrated the successful target re-innervation. The intensity of axon/NMJs overlap was observed to be larger in the GDNF (D) and PTN-GDNF (E) compared to the BSA (B) and PTN (C) groups, but not as elaborate as the (cut-resuture) control. (F) Muscle mass did not improve significantly as compared to the positive control, indicating limited rescue of muscle atrophy. Scale bar: 5 $\mu$ m. * = $p < 0.05$ . ....	32
Figure 2.9. Muscle fiber area calculated from tissue sections revealed a significant atrophy in all BNI repaired animals as compared to the control, but a moderate rescue in the PTN-GDNF group over the BSA group. One way ANOVA, **** $p < 0.0001$ ** $p < 0.01$ . ....	33
Figure 3.1. Structural domains of the Neuregulin1 family of proteins. Type-I and II are soluble isoforms, whereas Type-III is a membrane bound isoform with a cysteine rich domain tethering it to the membrane. Figure adapted from [159] .....	38
Figure 3.2. A) Release profile of the neuregulin-1 microparticles, taken over 28 days showing the cumulative release of the growth factors over time. B) Characterization of the PLGA microsphere size and stability in terms of polydispersity index. C-F) Images of dorsal root ganglia explants at 10-days in vitro after treatment with either control, PTN, NRG1 type-III or combination of PTN-NRG1 type III microspheres. They are labeled for neurites ( $\beta$ -tubulin, green) or cell nuclei (DAPI, blue). Scale bar: All images; 100 $\mu$ m.....	43
Figure 3.3. Experimental design and timeline. Schematic of transection injury, indicating the two repair techniques, autograft and BNI conduit. Experimental timeline, indicating times of injury, behavioral assessment and terminal experiments, that included electrophysiological recordings and collection of tissue for histology. ....	45

Figure 3.4. Gross Anatomical pictures of the regenerated nerves. A) Tissue obtained from i) autograft group, and after removing the polyurethane tubes in the ii) Control, iii) NRG1 Type-III and the iv) PTN-NRG1 microsphere groups, showed robust growth and good vascularization (inset for each), for some tubes. v) Failed regeneration was observed in some tissue samples, as indicated by the intact agarose scaffold and no tissue presence in the middle segment of the regenerative bridge (inset). C) The success rate of each group, after excluding the tubes that showed no tissue growth. Scale Bar: 10mm. .... 49

Figure 3.5. Ultrastructural analysis of the distal end of the regenerated tissue. A) Electron micrographs of areas of myelination seen in the different treatment groups. B) Diameter of myelinated axons C) Analysis of g-ratios for myelinated axons observed in the different groups. Scale bar: A) All images; 5µm. \*=p<0.05 ..... 51

Figure 3.6. Analysis of Unmyelinated axons. A) Electron micrographs showing the axon distribution within bundles across the groups. B) Quantification of the number of unmyelinated axons present in the distal end of the regenerated nerves. C) Axon bundles consisting of more than 14 axons were compared between the groups. Scale Bar: A) All images; 5µm. .... 52

Figure 3.7. Compound nerve action potentials. Representative waveforms and respective group data for compound nerve action potential amplitudes at different stimulation intensities. A) Autografts ,B) Control C) Neuregulin Type-III and D) PTN-NRG1 Type III ..... 53

Figure 3.8. Compound muscle action potentials. Respective group data for compound muscle action potential amplitudes at different stimulation intensities and the corresponding motor force recruited for A) Autografts ,B) Control C) Neuregulin Type-III and D) PTN-NRG1 Type III. . 54

Figure 3.9. Immuno-histological labelling for axons. Images labelled for β-III tubulin showing axons in the proximal(A) and distal segments (C) of the regenerated nerve. Quantification of the number of axons in the B) Proximal and D) Distal segments using an automated software..... 56

Figure 3.10. Muscle Tissue analysis. A) Gross tissue images of the *Tibialis Anterior* muscles obtained after perfusion, and B) wet weight of these muscles in milligrams. C) Representative images of cross sections of muscle tissue, demonstrating the striking difference between the muscle fibers that is quantified in D. .... 58

Figure 3.11. NRG1 Type-III provides moderate functional recovery. A) Toe-Spread Index (TSI) for the different groups over the period of twenty eight weeks, demonstrating animals that crossed the recovery threshold of 0.6 TSI, indicated by dotted red line. B) Representative images of the method of measuring TSI, and examples of baseline, injury, recovery and no recovery toe-spread. C) Comparison of all groups throughout the study using 2 way ANOVA with Tukeys multiple comparison test, \*\*\*p<0.001, \*p<0.05. .... 60

Figure 3.12. Proposed pathway of neurotrophic effect of Neuregulin. ....64

Figure 4.1. Emphasis on the use of the rat as a model for nerve regeneration. A) Number of published experiments utilizing different animal models B) Molecular and physiological techniques available to examine nerve regeneration in different animal models. Data obtained from PubMed search and [193].....	67
Figure 4.2. A) An S-shaped conduit provides longer regeneration length within the same linear space available in a rat model. B) Digital model of the NGC designed using Onshape software.	70
Figure 4.3. Pilot Experiment Showing regeneration of the rat sciatic nerve across a 5mm curved conduit. A) Schematic of conduit geometry and surgical images after the nerve regenerated across the gap. Scale Bar: B) 2mm. ....	71
Figure 4.4. Micro-extrusion printing of the nerve guide conduits. A) Fabrication of the NGCs using a custom micro-extrusion 3-D printing system. B) Sample straight and S-shaped NGCs of varying length. Microscopic images of straight (inset, top) and S-shaped (inset, bottom) conduits showing the cross-sectional profile. The printing method results in a micro-groove profile along the conduit, thus providing topological cues for growing axons. Scale Bar: A) 10mm B) 5mm, inset;500 $\mu$ m. ....	74
Figure 4.5. Surgical implantation and gross regenerated nerve tissue from the straight (A) and S-shaped (B) NGCs. Quantification of the length (C) and thickness (D) of the regenerated nerve tissue. Scale Bar: A) 2mm. ....	75
Figure 4.6. A) Toe-spread index (TSI) calculated from treadmill videos was significantly different at week 7 as compared to week 1 after injury but showed no differences between the two conduit groups. Gait analysis showed that though swing time (B) was different at weeks 1, 5 and 7 within each group, there was no significant differences between the two conduit groups. Stance time (C) and stride length (D) were not different across time of between groups. ....	76
Figure 4.7. Immuno-histochemistry of the regenerated nerves. Transverse sections of the A) proximal and B) distal segments of the tissue were labelled for axons ( $\beta$ -III tubulin) and myelin (P0). Quantification using a cell counting software of the C&E) total axons and D&F) myelinated axons gave no significant differences between the straight vs the S-tube groups. Scale Bar: 100 $\mu$ m. ....	77
Figure 4.8. Threshold voltage values that evoked a motor response in the two groups, with an average of 1mV, with no significant differences between the two conduit groups. ....	78

## LIST OF TABLES

Table 1.1 Classification of Nerve Injury. Adapted from [14].....	3
Table 1.2 Commercially available FDA approved nerve guide conduits (Table adapted from [63], [64]).....	9
Table 1.3 Fabrication techniques for tissue engineered nerve guide conduits. Adapted from [83], [84].....	12
Table 1.4 Neurotrophic factors tested in pre-clinical studies of nerve repair. Table adapted from [129], [130] .....	16
Table 4.1 Assessment tests established in the Rat model that provide thorough understanding of the regenerative profile of nerves. Table adapted from [15] .....	67

# **CHAPTER 1**

## **INTRODUCTION**

### **1.1 Clinical Significance**

Peripheral nerve injuries result in loss of motor and sensory function along with formation of painful neuromas, and partial or complete paralysis [1], [2]. In the United States alone, approximately twenty million people suffer from peripheral nerve injuries resulting in about \$150 billion spent annually on medical care[3]. These injuries are either, crush and stretch injuries, or more severe such as complete transection. A recent clinical study indicated that 84.6% of peripheral nerve injuries were transection injuries, resulting from sharp objects, occupational accidents, or gunshot wounds [4]. Others have reported that 25% of sciatic nerve lesions are iatrogenic, typically caused during surgical repair of fractures or joint replacements [5]. It is also known, that tissue loss results in gap formation, and that the length of the gap is critical if longer than 3 cm. Further complicating the possibilities of functional recovery is the fact that denervated muscles atrophy over time, therefore, delays between the time of the injury and the surgical repair, greatly diminishes the degree of successful recovery [4]. Indeed, long term retrospective studies have shown that only 25% of the individuals with critical peripheral nerve gap injuries regain motor function, while only 3% experience any sensory recovery at all [6]. This results in permanent disability in most individuals, affecting their overall quality of life. The gold standard for the repair of nerve gap injuries is the autologous graft. However, the limited amount of donor tissue and deleterious co-morbidity, has motivated the development of biodegradable nerve conduits, several of which are FDA approved. Unfortunately, none of the available nerve guides match the quality and functional recovery achieved by autografts. Thus, the need of improved bioengineered nerve



strategies remains. In addition, the biological process of nerve regeneration is complex, and involves multiple cells types, which actions are tightly coordinated through molecular signaling, mediated both by releasable and surface-attached proteins. As our understanding of the biological and molecular processes involved in nerve injury and repair advances, it is imperative that such knowledge is incorporated into bioengineering approaches in order to achieve maximal functional recovery.

## **1.2 Organization of The Peripheral Nervous System**

The peripheral nerve trunk is cylindrical and contains bundles of axons, resident Schwann cells, and fibroblasts, all wrapped with a connective tissue layer called the epineurium. The individual axons are embedded in a protective connective tissue called the endoneurium. Bundled axons form fascicles which are in turn wrapped by specialized perineurial cells with tight-junctions between them, which then form a blood nerve barrier between the axons and the structures external to the epineurium [7], [8]. In the fascicles, 10% of the total cell population are fibroblasts, while macrophages account for 2-9% [9]. The remaining cell are all Schwann cells, present in multiple phenotypes, including pro-myelinating, myelinating, Remak, and senescent, based on location and function [10]. All these cells together provide trophic support to the axons, carry out signal conduction, and maintain neuroimmunology and homeostasis within this microenvironment [9], [11].

## **1.3 Peripheral Nerve Injury Classification**

Damage to the nerve is classified into severity categories based on the Sunderland and Seddon methods [12], [13] (Figure 1.1 and Table 1.1). Neurapraxia is described as mild type of nerve damage, affecting only the insulating layer of myelin that wraps some axons resulting in temporary

conduction block. Since the axon, endoneurium and epineurium are intact, no surgical intervention is necessary and, given the capacity of the PNS for spontaneous repair, full function recovery is expected. Axonotmesis occurs when nerve injury damage the axon fibers without affecting the perineurium or epineurium layers. This type of injury also regenerates with complete restoration of function. The most severe type of nerve damage is known as neurotmesis, which is characterized by complete disruption of the nerve trunk, with complete transection of all nerve layers and disconnection between a proximal and distal segment. This type of injury requires surgical intervention for repair, including the direct suture of the nerve segments or the use of an autograft for repair if the injury resulted in tissue loss and gap formation. This type of injury undergoes slow regeneration, with incomplete or lack of functional recovery. Sunderland further characterized axonotmesis into sub-classes based on severity of damage to the multiple layers and surgical outcomes [12]. Table 1.1 describe both types of nerve injury classifications and Fig. 1.1 illustrates the different types of injuries.

Table 1.1. Classification of Nerve Injury. Adapted from [14]

<b>Seddon Classification</b>	<b>Sunderland Classification</b>	<b>Degree of Damage</b>
Neurapraxia	I	Mild myelin damage Nerve bundle intact Full Functional Recovery
Axonotmesis	II	Axon damaged Endoneurium and Epineurium Intact Full regeneration
	III	Axon and endoneurium damaged Incomplete recovery

	IV	Axon, endoneurium and perineurium damaged Epineurium intact Surgical repair required Moderate recovery after repair
Neurotmesis	V	Complete transection of entire nerve Surgical repair required Recovery dependent on amount of tissue lost
	VI	Mix of any of the above

Upon injury, axons distal to the site of injury undergo a programmed process called Wallerian degeneration, resulting in loss of the axons at the distal end and denervation of the target muscle[2], [15], [16]. The process of Wallerian degeneration is also essential in creating a conducive microenvironment for regeneration of new axons[2], [17].

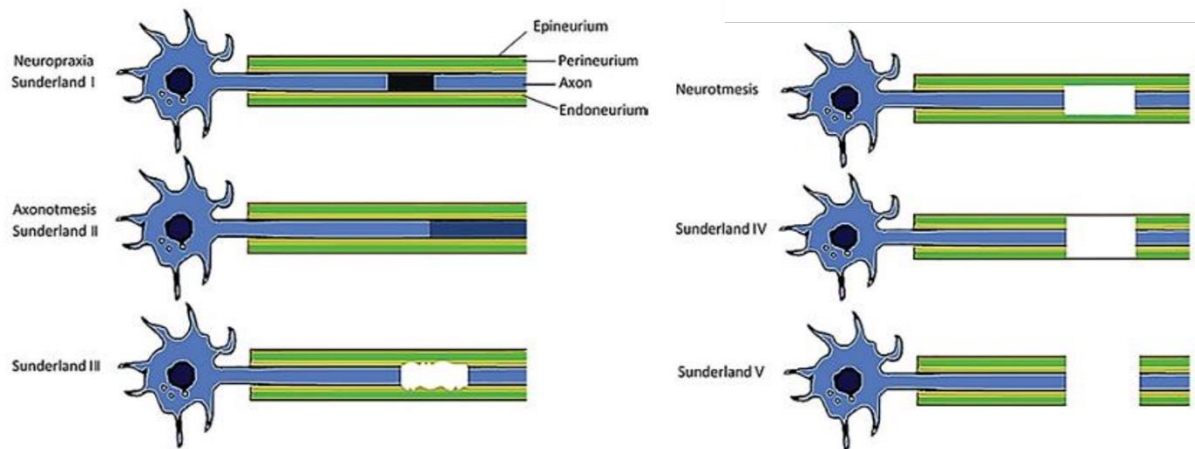


Figure 1.1. Classification of nerve injury based on Seddon and Sunderland. Figure taken from[18]

## 1.4 Cellular Response To Nerve Injury

### 1.4.1 Wallerian Degeneration

After injury, all cells in the peripheral nerve have an immediate reaction [19], [20]. Fibroblasts, Schwann cells and resident macrophages, participate in clearing axonal debris, while secreting

growth factors and inflammatory cytokines as part of the inflammatory response. Upon injury, axons distal to the site of injury undergo a programmed process called Wallerian degeneration (WD), where Schwann cells wrapping axons are activated to reabsorb the myelin, proliferate, migrate and form bands of Bungers, which serve as cellular scaffolds for regenerating axons, also releasing a number of growth factors to guide and entice their growth [2], [15], [16]. The process of WD is essential in creating a conducive microenvironment for regeneration of the affecting axons [2], [17], and was first described by August Volney Waller in the frog glossopharyngeal and hypoglossal nerves [19]. Studies in C57BL/Ola mice containing the slow Wallerian degeneration protein (WLD<sup>s</sup>), show intact axons at 35 days after injury, compared to wild type mice, which at that time show fully degenerated axons [21], [22]. Damage to the axonal membrane triggers microtubule fragmentation mediated by calcium-calpain, ubiquitin proteasome system (UPS) and the recently found sterile alpha- and armadillo-motif-containing protein-1 (SARM-1) [23]–[25]. It has been shown that extent of axonal regeneration and the rate of functional recovery was extremely slowed in the C57BL/Ola mice as compared to wild type, due to absence of WD related early regeneration associated genes [21]. Degrading axolemma and ECM proteins in the degenerating axons then activate the Toll Like Receptor (TLR) signaling of Schwann cell proliferation and differentiation [26]. Therefore, Wallerian degeneration plays a critical role in signaling breakdown of injured axons, invasion of immune cells and inducing proliferation of and growth factor secretion by Schwann cells.

#### **1.4.2 Neuronal Cells**

When a peripheral branch of the nerve is injured, retrograde signals are sent to the cell bodies in the dorsal root ganglion and the spinal cord, initiating a “positive injury signal” [27]. This signal

involves local activation and transport of mitogen activated protein kinases (MAPK) like Erk, c-Jun kinase as well as protein kinase G [28]–[32]. In turn, the activated kinases interact with dynein/dynactin to affect microtubule alignment and organization, that mediates the elongation of the growth cone of the axons during axonal regeneration [28]. Several immediate early genes are activated in the cell bodies, including cJUN, cFOS, ATF-3 and cAMP response element binding protein (CREB) which together trigger axonal death as well as initiation of regeneration [33], [34]. In the DRG, non-neuronal cells like macrophages and satellite cells have also been shown to migrate and proliferating around neuronal cell bodies [35]–[37].

#### **1.4.3 Schwann Cells**

Upon injury to the peripheral nerve, Schwann cells contribute to WD by endocytose fragments of myelin with autophagolysosomes that clear the debris [38]. Myelinophagy is regulated by the JNK/c-Jun pathway in these cells, and is distinct from those involved in repair mechanism [38], [39]. During the regeneration phase, STAT3 controls the fate of repair Schwann cells to maintain long-term survival [40]. Additionally, macrophages secrete VEGF which produces neo-vasculature in the regenerating bridge, thereby providing a path for SC migration [41]. After injury, SC dedifferentiation is regulated by TGF $\beta$ , which reprogram them into mesenchymal like cells in a wound healing like response [42].

#### **1.4.4 Macrophages**

TLR signaling of Schwann cells during WD activates recruitment of macrophages near the injury site for phagocytosis of axonal debris [43]. The immune complement system is known to activate the infiltration and proliferation of macrophages. Venom induced complement depletion reduced the number of macrophages recruited as well as delayed regeneration [44]. In addition to the injury

site, macrophage infiltration also occurs near the cell bodies of axotomized neurons [35], [37]. A recent study in rodents and human tissue demonstrated that macrophages are closely associated with Schwann cells after injury, and play a critical role in re-myelination and conduction velocity of the regenerated axons [45].

## **1.5 Current Repair Strategies**

### **1.5.1 Primary Repair**

The type of treatment for nerve repair mainly depends on the extent of injury as classified above. In injuries with minimal or no tissue loss, and a tensionless coaptation of the proximal and distal stump is possible, direct repair with micro-sutures is performed [46]. Good surgical outcome depends on fascicular matching, appropriate vascular support, and requires precision surgical technique for lining up the nerve bundle [47]. This type of direct repair is possible in approximately 85% of nerve trauma patients, while the rest require secondary repair methods [48]. This is due to the fact that stretching of nerve tissue over 10% has been shown to create a secondary injury, with permanent loss of 20% of normal blood flow [49], [50].

### **1.5.2 Secondary Repair with Nerve Autografts**

For the repair traumatic nerve injuries without a clean transection and with tissue loss, autologous nerve grafts are considered the gold standard. First extensively studied by Millessi, this repair technique involves the sacrifice of a healthy nerve in the patient, normally cutaneous branches that innervate the foot, in lieu of the injured nerve [51]. Autograft allow nerve repair without tension, which is needed as this avoids the possibility of compromised blood flow and regeneration failure. Common donor harvested nerves use for autografts include the sural nerve, the medial or lateral antebrachial cutaneous nerve and the superficial sensory branch of the radial nerve [52]. Autografts

contain the resident Schwann cells that provide neurotrophic factors as well as extra cellular matrix proteins like laminin and collagen that advance the growth cone of the regenerating axons. However, due to the limited availability of donor nerves, and the incidence of undesirable co-morbid effects including neuroma pain at the donor nerve site, off-the-shelf biosynthetic alternatives are highly desired and many have been proposed in the last two [53]. Despite this, a recent survey of surgeons reported that for large or critical gap injuries (those with  $\geq 3$ cm tissue loss), autologous grafts are preferred in 78.9% of the cases, due to lack of better alternatives[54].

### **1.5.3 Processed Nerve Allografts**

In nerve injuries where autologous nerve grafts are unavailable, donor nerves from cadavers are used for repair[53], [55], [56]. These donor nerves or allografts are processed in multiple freeze-thaw cycles and with detergents to decellularize them so they are non-immunogenic[57], [58]. Clinical studies have shown allografts to be safe and effective for the bridging of nerve gaps up to 50mm [53], [59]. However, despite decellularization, patients implanted with allografts are required to take immunosuppressants for as long as 18 months after implantation, with some patients still experiencing graft rejection[60]. Although chemically treated allografts eliminate the need for immunosuppressants, the Schwann cells present in them have been shown to express senescence markers like p16<sup>+</sup>, IL6 and senescence associated  $\beta$ -galactosidase[61], [62]. This process prevents the cells from proliferating, changes their secretory profile, further limiting axonal regeneration over longer injury gaps [61], [63].

### **1.5.4 Synthetic Nerve Guide Conduits**

Limitations of autologous nerve grafts and decellularized allografts in repairing long nerve defects calls for a need for developing biosynthetic nerve guides conduits that will mimic the internal

architecture of the nerve and provide chemical and topological cues that will drive the axons to regenerate over longer distances. Currently, there are multiple natural and artificial polymer tubes approved by the Food and Drug Administration (FDA), to be used as nerve guides [64], [65] (Refer to Table 1.2). These are hollow conduits made of Poly (lactic acid) (PLA), Poly (DL-lactide- $\epsilon$ -caprolactone) or collagen derived from animal tissue. Multiple pre-clinical studies indicate that these hollow conduits are as effective as autografts, but only to repair shorter gaps of up to 2 cm [66]–[68]. A recent industry analysis reported that surgeons and patients prefer autologous nerve grafts or allografts for repairing nerve gaps more than 3 cm [54].

### 1.5.5 Biomimetic Fillers for Nerve Guide Conduits

In order to increase the gap length that can be repair with nerve guides, several studies use intraluminal fillers to provide a more natural environment to regenerating nerves. Figure 1.2 is a schematic of the different alternatives that can be used, independently or in combination, to enhance axonal regeneration. These include transplantation of stem cells, growth factor releasing polymers, microchannels, porosity of the conduit wall, an internal scaffold for structural support, among others [65], [69].

Table 1.2. Commercially available FDA approved nerve guide conduits (Table adapted from [64], [65])

<b>Product Name and Manufacturer</b>	<b>Length Available</b>	<b>Material</b>	<b>Conduit Structure</b>
<b>Neurotube® (<u>Synovis</u>)</b>	<b>2-4cm</b>	<b>Polyglycolic Acid</b>	<b>Absorbable Mesh Tube</b>



<b>NeuraGen® (<u>Integra Life Sciences</u>)</b>	<b>2-3cm</b>	<b>Type-I Collagen</b>	<b>Semipermeable</b>
<b>Neuroflex™ (<u>Collagen Matrix</u>)</b>	<b>2.5cm</b>	<b>Type-I Collagen</b>	<b>Flexible, Semipermeable collagen matrix</b>
<b>NeuroMatrix™ (<u>Collagen Matrix</u>)</b>	<b>2.5</b>	<b>Type-I Collagen</b>	<b>Semipermeable tubular matrix</b>
<b>AxoGuard™ (<u>Axogen, Inc.</u>)</b>	<b>1cm</b>	<b>Porcine Submucosal Extracellular Matrix</b>	<b>Strong, flexible tube</b>
<b>Neurolac® (<u>Polyganics</u>)</b>	<b>3cm</b>	<b>Poly (DL-lactide-ε-caprolactone)</b>	<b>Transparent Tube</b>

Among these, adding Schwann cells have shown to improve regeneration across 12 mm gap in rats, although autologous SC were more effective than cultured cells [70], [71]. Adipose derived stem cells have also been shown to differentiate into neural cells, express neuronal markers and enhance nerve regeneration in the rat sciatic nerve [72], [73]. Forskolin-induced differentiation of bone marrow stromal cells into Schwann cell-like cells, similar to those of myelinating phenotype, increased the re-myelination after injury[74], [75].

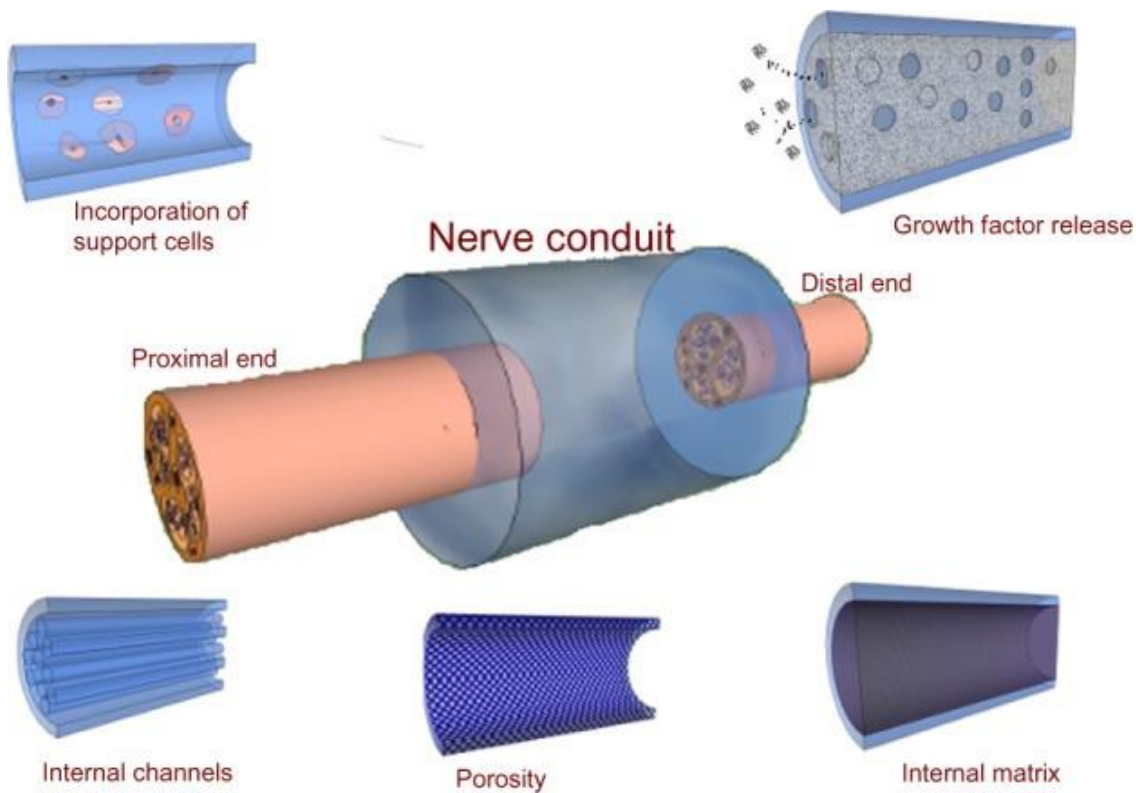


Figure 1.2. Nerve conduits with luminal fillers used to mimic the internal architecture of the nerve. Incorporation of Schwann cells, neurotrophic factors, topographical cues like microchannels and ECM proteins provide structural and functional support to growing axons. Figure from [65]

When reparative Schwann cells begin the process of regeneration, they aligned and form structures known as Bands of Büngner, which act as cellular scaffolds for the re-growing axons [76]. Use of aligned microstructures for guiding axons in the lumen of nerve guides, therefore offer a biomimetic regenerative support[77]. Our group and others have shown that introducing hydrogel microchannels filled with collagen, or aligned PLGA fibers into nerve guides, significantly improves axon guidance and migration of Schwann cells, further promoting nerve repair [78]–[81].

Material based advances in fabrication techniques have also contributed to design of novel nerve guide conduits. Electrospinning, freeze-drying and porogen-leaching techniques use

biocompatible polymer materials that allow control over porosity, fiber alignment as well as thickness of the conduit wall. Rapid proto-typing by use of 3-D printing further allow the potential of having complex geometrical luminal designs and improve manufacture reproducibility [82]. The following Table 1.3 covers the different fabrication techniques and the advantages offered.

Table 1.3. Fabrication techniques for tissue engineered nerve guide conduits. Adapted from [83], [84]

<b>Method of Fabrication</b>	<b>Materials Used</b>	<b>Advantages</b>
Electrospinning	Collagen, Chitosan PLLA, PLGA, Silk	Controlled porosity, High surface to volume ratio allowing cell adhesion
Porogen Leaching	Chitosan, PLLA, PLGA, PCL	Higher Porosity Permeability to Nutrients
Freeze Drying	Gelatin, Collagen	Allows use of natural polymers
Phase separation	Collagen, Chitosan PLLA, PLGA, Alginate	Produces an interconnected porous structure Scalable and controllable
Mandrel Based	Agarose, Chitosan, PLLA, PLGA	Aligned Microchannels Added structural support
Rapid Prototyping	Polyethersulfone, PLLA, PCL, Polyurethane	Form complex 3-D structures Reproducible pore size and distribution

### **1.5.6 Growth Factor Support**

Growth factors are proteins released primarily by Schwann cells and target cells, which attract and support the regeneration of injured axons. These are organized into protein families, among which are neurotrophins such as Nerve Growth factor (NGF), brain-derived growth factor (BDNF) and the glial-derived nerve factors include GDNF are known to mediate nerve regeneration preferentially of motor axons [85][17], [86]. GDNF was first extracted from rat glioma cell line as a tropic factor for the embryonic mid-brain[87]. Later it was found that GDNF also had trophic effects on the neurons of the periphery. After axotomy, GDNF level increased significantly and were at the highest concentration in the ventral root, until day 15 [88]. Myelinating and non-myelinating Schwann cells also secrete GDNF after injury, via purinergic receptors and downstream signaling of protein kinase D (PKD), which increases transcription of GDNF [89]. After regeneration of injured nerves, synthesis of GDNF is lowered, highlighting the critical role of this trophic factor in injury [90]. The use of GDNF in axon regeneration has been investigated by many groups. GDNF binds to its receptor GRF- $\alpha$  and then to Ret tyrosine kinase, with downstream effects resulting in phosphorylation [87]. In high concentrations, GDNF has shown to enhance proliferation of Schwann cells, resulting in myelination of previously unmyelinated axons [91]. In a delayed repair model of nerve injury, GDNF loaded PLGA microspheres and collagen conduits with functionalized GDNF, both improved motor nerve regeneration[92]–[95]. Activating Transcription Factor-3 (ATF-3) is produced as an injury marker in sensory and motor neurons. Exogenous GDNF applied after axotomy reduced expression of ATF3 in DRG cells by approximately 60% [96]. One study investigated the effect of GDNF fused with laminin binding domains injected inside an NGC, which improved recovery and axon fiber area in 5mm injury to

the recurrent laryngeal nerve of rats [97]. Similarly, GDNF expressing Schwann cells injected in an acellular nerve allografts, provided enhanced regeneration and muscle re-innervation [98][99]. Electrical stimulation of the muscle has been shown to elevate intramuscular BDNF and GDNF mRNA after nerve injury, which can then diffuse toward the growth cone, supporting axon regrowth [100]. Furthermore, treadmill exercise after nerve injury elevated levels of GDNF and BDNF in serum, nerve and muscle, implicating these molecules repair of damaged nerves [101]. Additionally, intramuscular delivery of GDNF acts synergistically with NGF and CNTF to restore functional recovery in rats[102], [103].

Pleiotrophin belongs to the heparin-binding growth factor family, and was first isolated from rat brain, suggesting their role in the CNS, involved in synaptogenesis, dendritogenesis and axonal outgrowth [104] [105]. PTN and its homolog midkine are known to be involved in liver regeneration [106]. Similar to other neurotrophic factors, PTN is also upregulated in denervated ventral root after axotomy, and persist up to 30 days after injury [107]. PTN also expressed in SC and endothelial cells immediately after injury, and one week later in macrophages[108]. In spinal cord cultures *in vitro*, PTN exhibits a neuroprotective effect, against glutamate excitotoxicity, and prevents denervation induced motor neuron death *in vivo*. This effect of pleiotrophin in motor neurons is mediated through the ALK receptor which induces phosphorylation of downstream effector molecules [109]. Pleiotrophin also binds to receptor protein tyrosine phosphatase (RPTP $\beta/\zeta$ ), important for cell proliferation, adhesion and transformation[110] and its effect is mediated by  $\beta$ -catenin that stabilizes the cytoskeleton via the cell adhesion molecule cadherin and the cytoskeletal protein actin [111]. Our group also recently showed that PTN increases the number of sensory axons in an amputee model of axon regeneration, highlighting its effect in selective

enticement of sensory fibers [112]. However Blondet et.al in 2006 showed that exogenous PTN in lesioned nerve impaired muscle reinnervation[113]. It is therefore important to investigate the efficacy of PTN in repairing long gap nerve injuries.

Other growth factors including insulin growth factor-2 (IGF), ciliary neurotrophic factor (CNTF), fibroblast growth factor-2 (FGF-2) and neurotrophin 3 (NT-3), are upregulated after injury in all nerve types[88], [107]. Table 1.4 lists the growth factors tested in pre-clinical injury models, and some of the effective different delivery methods used.

Table 1.4. Neurotrophic factors tested in pre-clinical studies of nerve repair. Table adapted from [114], [115]

Neurotrophic Factors	Delivery Method	Conduit Used	Injury Model	Regenerative Effect
BDNF	Cross Linked	Collagen Tube	Rat Sciatic nerve Transection Rabbit 15mm Nerve gap	Large myelinated axons Comparable to autograft
GDNF	Silk and PLGA Microspheres	Fibrin	Rat 8-15mm gap	More nerve tissue, SC migration and proliferation
NGF	Admix, Microspheres	Silicone, Amniotic membrane	Rats, 13mm gap Rabbits, 25mm gap Dogs, 30mm gap	High axon number and density Regeneration comparable to autograft
VEGF	Matrigel	Silicon	Rat, 10mm gap	Improved muscle weight and foot pad innervation
CNTF	Direct mixing	Silicon	Rat, 10mm gap	Better muscle weight, myelinated axons
NT-3	Direct Mixing	PHEMA, Collagen Matrix	Rat, 10mm gap	
FGF	Direct Loading	PHEMA, Collagen Matrix	Rat, 10mm gap	Comparable to autograft

### **1.5.7 Electrical Stimulation**

Muscle atrophy in two weeks following denervation, since target-derived growth factors are needed for targeted re-innervation, muscle atrophy limits the functional recovery [116], [117]. It has been reported that 60 min of electrical stimulation (ES) at 20 Hz following injury and immediate repair, significantly accelerated the rate of nerve regeneration [116], [118]–[120]. Furthermore, even after a 4 week delayed repair, ES provided a two-fold increase in muscle force [121]. It is known that ES activates a number of growth promoting molecules in the injured neurons, thus resulting in increased number and growth rate of axons [116]. In turn, ES of the denervated muscle has also shown promise in improving motor recovery, however, its effects in long gap repair is yet to be determined [119].

### **1.6 Biosynthetic Nerve Implant (BNI)**

We previously have developed a biosynthetic nerve conduit, which is a multi-luminal tube intended to provide chemical and topographical cues to growing axons[122]. It is fabricated using a polyurethane tube consisting of an agarose scaffold, with micro-channels consisting of collagen to support regenerating axons. Using a rat model of sciatic nerve transection, we were able to show the enhanced effect of the microchannels and agarose scaffold in repairing a 10mm gap. The regenerated nerve consisted of fascicle-like bundles of axons, confirmed from Toluidine blue staining.



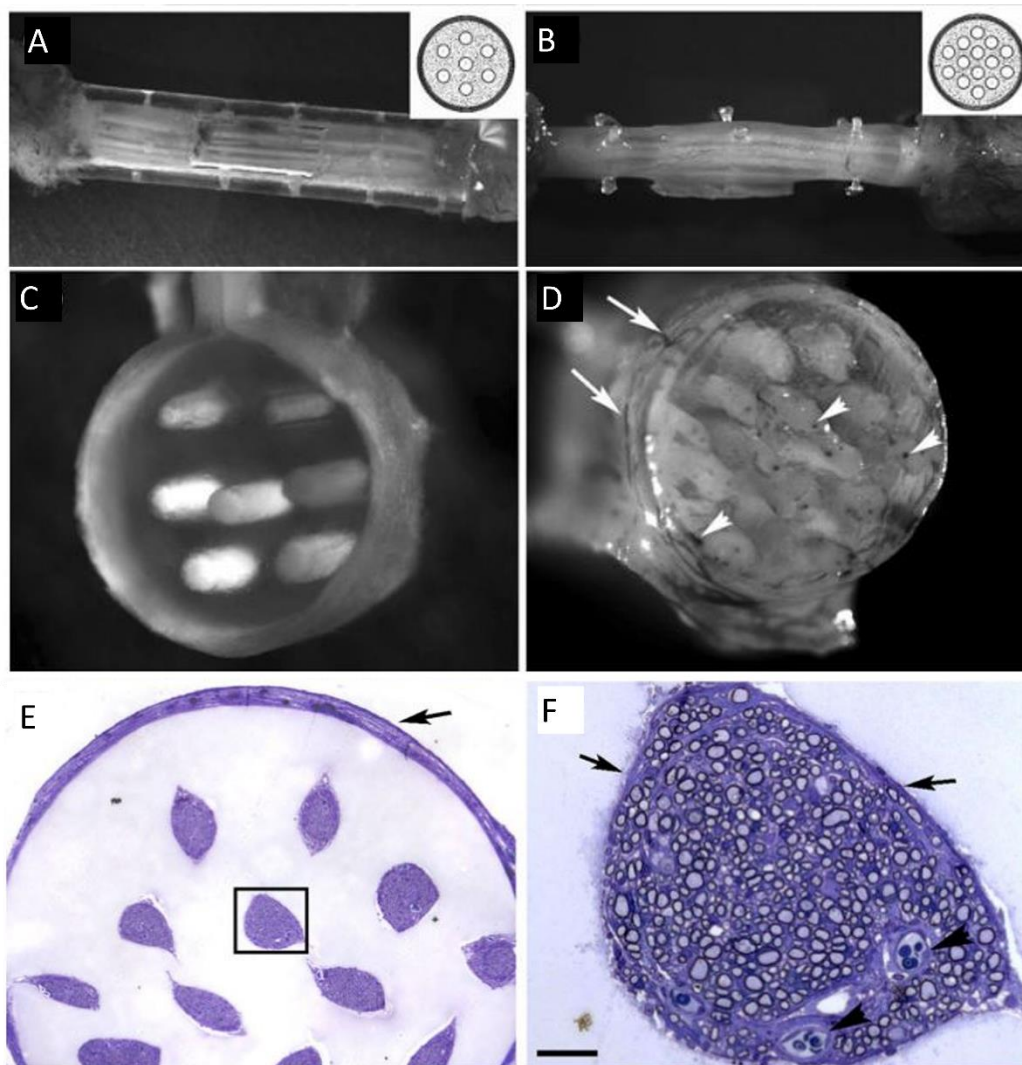


Figure 1.3. A&B) longitudinal view of the BNI with different number of microchannels. C &D) Figure 1.4 Transverse view of the distal end of the BNI showing the successfully regenerated nerve, in fascicle like structures. E) Toluidine blue staining of the nerve section showing fascicles and F) abundant small and large myelinated axons inside the channels. Scale Bar: 50µm (Figure from [122] )

Our results indicate that the BNI is a promising solution for bridging short gaps. However, its effectiveness in repairing nerves over longer gaps remains to be seen, given the nature of this complex process.

## 1.7 Specific Aims

The specific aims of this dissertation were focused on 1) Understanding the lack of functional repair despite abundant nerve regeneration with synergistic growth factors on long gap regeneration, 2) enhance re-myelination using growth factors to restore functional recovery and 3) to develop a rodent model of long gap nerve regeneration.

- *Specific Aim 1:* Using ultrastructural analysis (Chapter 2), determine the state of axonal maturation as affected by growth factor support across critical gaps and the level of muscle-re-innervation achieved.
- *Specific Aim 2:* As described in Chapter 3, we hypothesize that addition of Neuregulin1 type-III, will enhance radial sorting in the regenerating axons and subsequent re-myelination with improved function.
- *Specific Aim 3:* In the last aim (Chapter 4), we developed a rodent model of long gap nerve repair by designing an S-shaped, 3-D printed nerve guide conduit and evaluated the effect of topology on axon regeneration and its feasibility as a viable alternative to the use of larger animal models for the test of long gaps repair strategies, while taking advantage of the broad behavioral sensory-motor tests, and biochemical and cell biology techniques, that are well established in the rat model.

## CHAPTER 2

### EFFECT OF PLEIOTROPHIN AND GLIAL DERIVED NEUROTROPHIC FACTOR IN REPAIRING A CRITICAL NERVE GAP<sup>1</sup>

#### 2.1 Introduction

Although the peripheral nervous system has a robust regenerative capacity, repairing injuries involving large segment tissue loss are still a formidable challenge. Despite the availability of autologous nerve grafts, motor and sensory recovery is variable, and often incomplete [123], [124]. In addition, there is donor site morbidity, donor mismatch and the possibility of painful neuroma formation[53]. This in part is due to the complex, highly coordinated mechanism of axonal degeneration and regeneration after injury, involving multiple cellular populations, neurotrophic factors and extracellular matrix proteins. FDA approved biosynthetic alternatives like hollow nerve conduits and processed nerve allografts fail to fully mimic the internal environment of the nerve, and have shown sub-optimal results in clinic[125].

The main advantage of autologous grafts seems to be the presence of Schwann cells that secrete growth factors, extracellular matrix protein, as well as substrate for axonal growth. To that end, we have previously developed a multi-luminal Biosynthetic Nerve Implant (BNI), a polyurethane tube, consisting of an agarose scaffold with microchannels filled with collagen matrix loaded with growth factor encapsulated microspheres (Figure. 2.1 A&D).

---

<sup>1</sup> The data and figures included in this chapter are reprinted with permission from Acta Biomaterialia. Nesreen Zoghoul Alsmadi\*, Geetanjali S. Bendale\*, Aswini Kanneganti, Tarik Shihabeddin, An H. Nguyen, Elijah Hor, Swarup Dash, Benjamin Johnston, Rafael Granja-Vazquez, Mario I. Romero-Ortega. Glial-derived growth factor and pleiotrophin synergistically promote axonal regeneration in critical nerve injuries. Acta Biomaterialia, Volume 78, 2018, Pages 165-177, ISSN 1742-7061, <https://doi.org/10.1016/j.actbio.2018.07.048>.

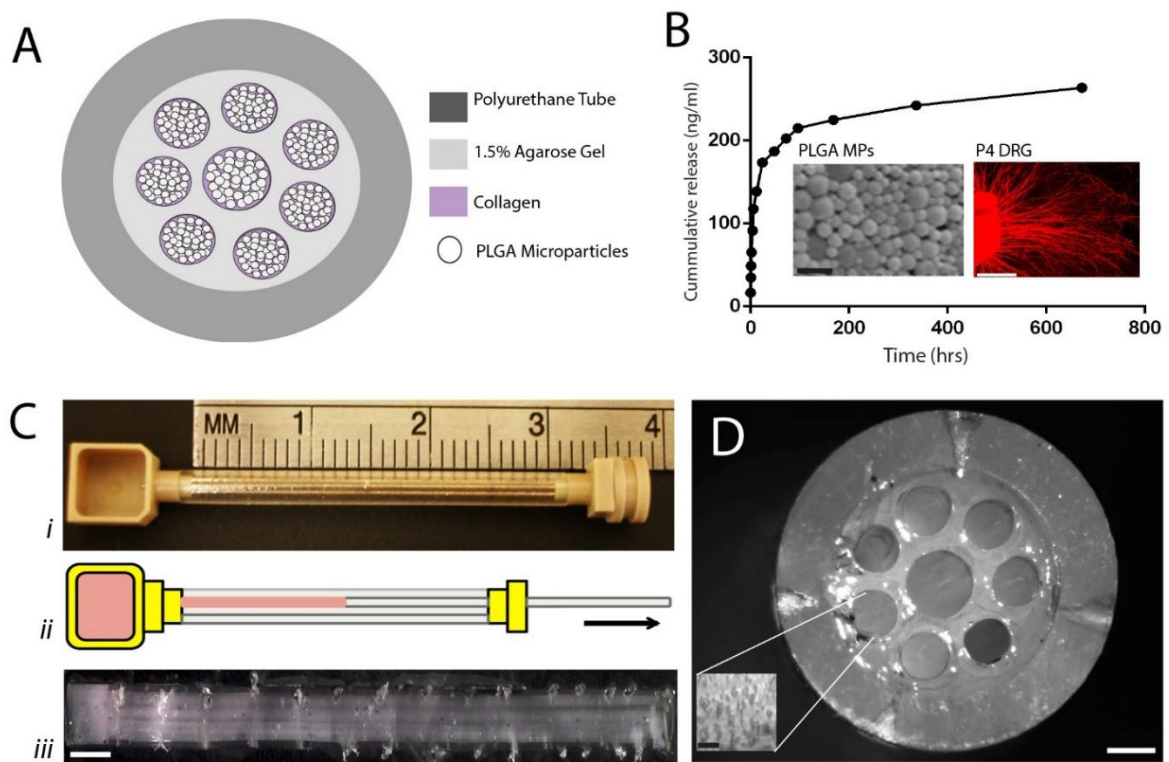


Figure 2.1. Fabrication of the Biosynthetic Nerve Implant, characterization of growth factor microspheres and surgical implantation. (A) Cross section schematic of the BNI, showing its composition (B) The release profile of the PTN microspheres, showing a sustained release. Inserts: SEM images of the PTN-MPs and bioactivity assay showing axonal growth (C) BNI fabrication method, showing casting of the agarose scaffold and E) Cross section of the BNI showing the eight microchannels with luminal MP-collagen (insert). Scale bars: B) SEM: 5  $\mu$ m, DRG: 1 mm, D) 1 mm, E) Device: 250  $\mu$ m, Insert: 10  $\mu$ m. F) 2 mm.

First, we systematically tested the effect of multiple neurotrophic factors on dorsal root ganglia (DRG) explants *in vitro*. The quantification of density and length of neurite outgrowth revealed that the combination of pleiotrophin (PTN) and glial-derived neurotrophic factor (GDNF) provided maximum growth, while addition of a third growth factor did not further enhance this effect (Figure 2.2).

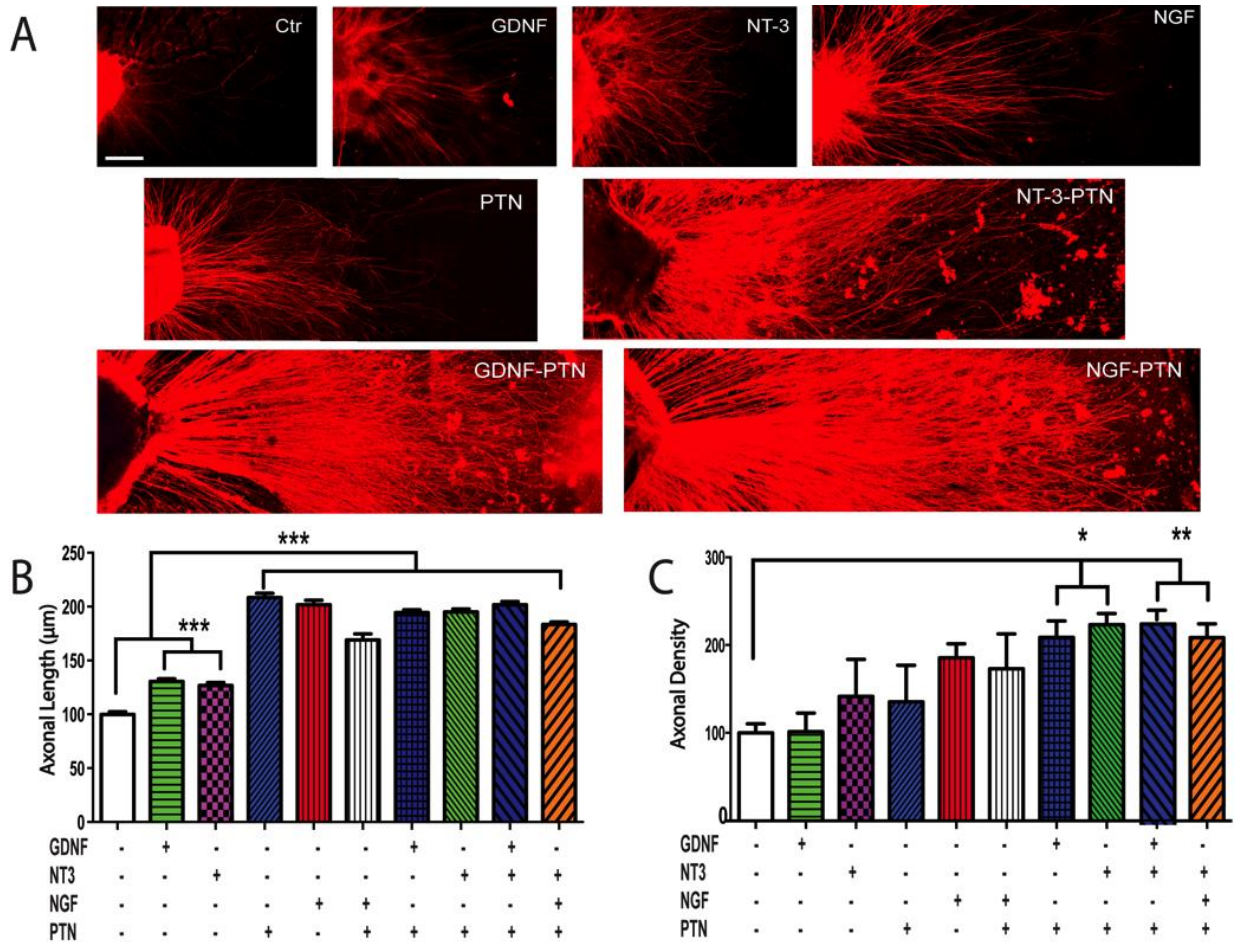


Figure 2.2. Effects of growth factors on neurite extension from DRG. (A) Confocal images of the DRG explants following treatments with different growth factor combinations. (B) Axonal length and C) number (density) indicated that PTN had a superlative effect on neurite growth, independently and in combination with GDNF and NT-3. Axonal density is reported as percentage of the negative control. \*\*\* =  $p < 0.001$ , \*\* =  $p < 0.01$ , \* =  $p < 0.05$ . Scale bar 100μm.

We further confirmed this neurotrophic effect on neurite extension from ventral motor neurons in the spinal cord (Figure 2.3 A). We observed that the combination of PTN-GDNF promoted maximum number and length of neurites as compared to the individual growth factors (Figure 2.3 B&C).



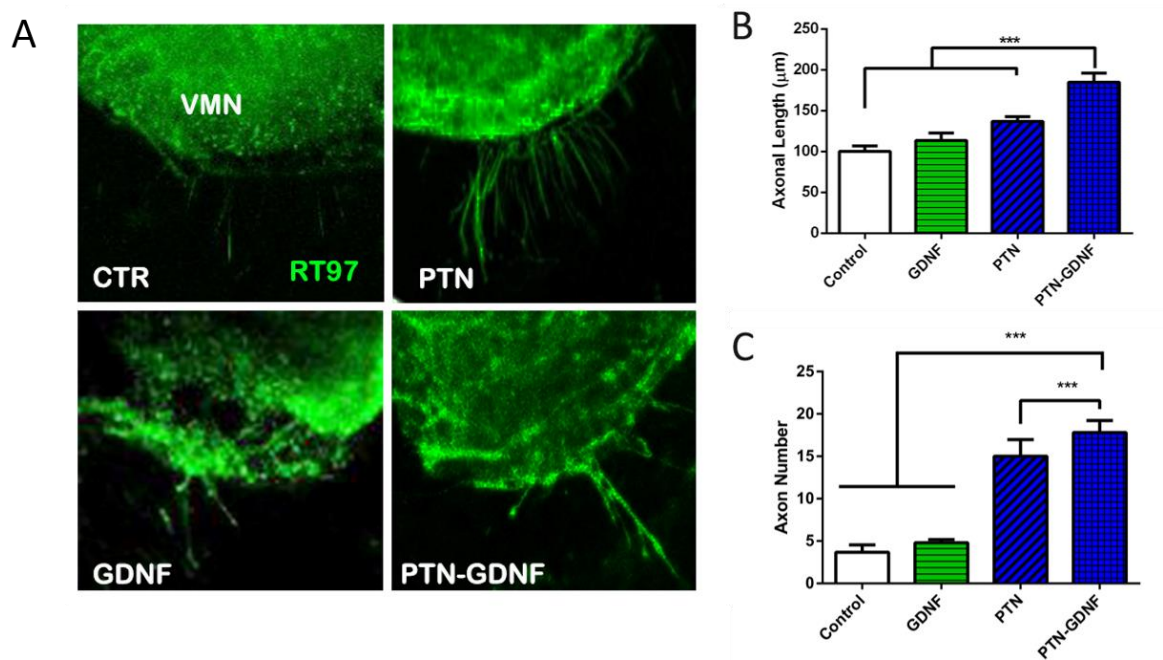


Figure 2.3. PTN-GDNF induces motor neurite outgrowth in ventral motor neuron of spinal cord explants in vitro. (A) Confocal images of neurite outgrowth in spinal cord explants. (B) A combination of PTN-GDNF showed a significant improvement in axon length and (C) number as compared to control, or individual growth factors. \*\*\*= $p \leq 0.001$ .

We then incorporated this combination within the BNI, and investigated its effect in promoting regeneration across 4cm nerve gap in a rabbit model of peroneal nerve transection, as compared to a cut-resuture control.

At five months post-surgery, gross evaluation of the explanted regenerated tissue, showed successful re-connection in all the BNI groups (Fig. 2.4A). The nerve tissue showed a more robust growth in the BNIs containing the growth factors as compared to those with BSA. Immunofluorescent labelling of  $\beta$ -III tubulin and P0 confirmed axons and myelination in the proximal segment of the regenerated nerves. The number of axons was similar in all the BNI groups ranging from 1350 to 1806, lower than those in the cut-resuture group ( $1412 \pm 186$ ; Fig. 2.4 C). Evaluation of the distal segment of the regenerated tissue showed that the number of axons

was reduced drastically in all the groups with BNIs. This indicates that most of the axons seen in the proximal segment were unable to reach the distal end of the nerve gap. As expected, the cut-resuture group had the highest number of axons ( $1885 \pm 247$ ), while those with BSA, PTN and GDNF had less than 25% of the control (361-394). However, those with a PTN-GDNF showed twice the number of axons distally ( $708 \pm 385$ ) as compared to the other BNI treatments, with a trend towards significance as compared to the PTN group ( $372 \pm 231$ ;  $p \leq 0.053$ ; Fig. 2.4 D).

To confirm re-innervation, we recorded compound motor action potentials evoked by stimulation, from the tibialis anterior muscle using needle electrodes. In the cut-resuture group, a response peak of  $0.70 \pm 0.20$  mV was recorded at 3X threshold (Fig. 2.5 A). Electrical stimulation failed to evoke a response in the other groups (i.e. BSA, PTN, GDNF, example shown in Fig. 2.5 B). However, in the PTN-GDNF groups, 1 out of 5 rabbits showed an evoked response of 0.05 mV, which was only 10% of the response observed in the cut-resuture group (Fig. 2.5 C). Interestingly, this was the only animal with few myelinated axons present in distal segment of the regenerated nerve. These results highlight the importance of remyelination, to improve conduction and re-innervation.

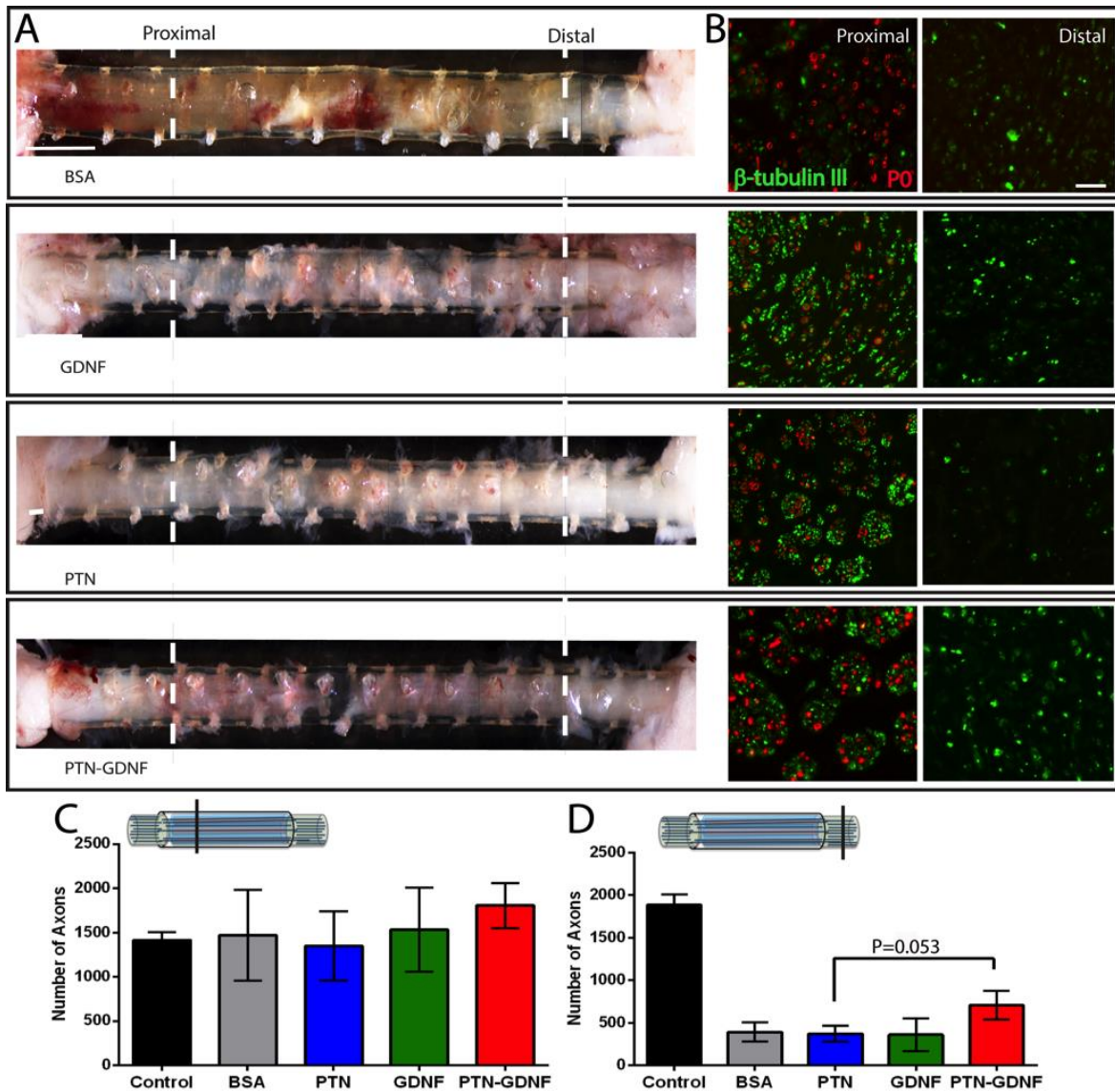


Figure 2.4. PTN-GDNF combination promote axon regrowth across a critical gap. (A) Images of explanted regenerated tissue, showing successful re-connection in all the BNI groups. (B) Immunofluorescent labelling of  $\beta$ -III tubulin and P0 confirmed axons and myelination proximal (C) and distal (D) segments of the nerve tissue, with PTN-GDNF showing maximum number of axons in both, with a trend towards significance as compared to the PTN only group. ( $p=0.053$ ). Scale Bar: 50 $\mu$ m.



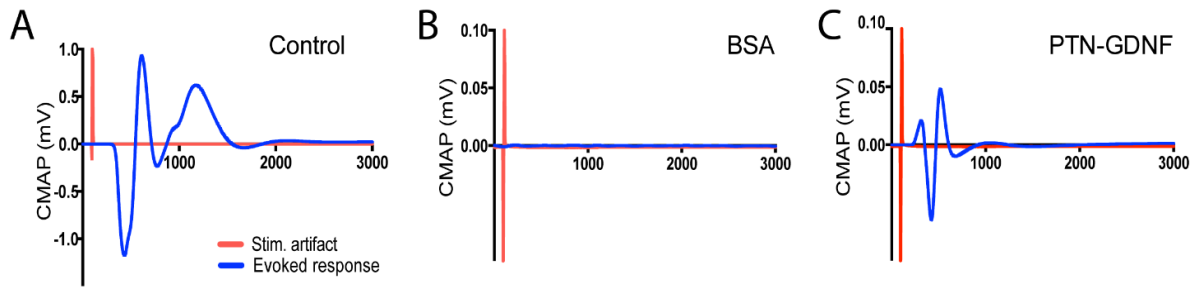


Figure 2.5. Evoked compound action potentials from regenerated nerves. Stimulation of the regenerated nerves evoked a close to normal response in the A) Cut-resuture group, but failed in the B) BSA, PTN and GDNF groups.

Behavioral assessment showed that the cut-resuture group recovered earlier, approximately 80%, starting at three months (Figure 2.6). At the end of five months, animals receiving BNIs with PTN-GDNF showed a significant 76% improvement as compared to the individual growth factors and the BSA group ( $p < 0.05$ ). Together, these results indicate that while PTN-GDNF promotes the growth of axons across a 4cm gap, the number of axons as seen from immuno-histochemistry is low, as compared to the cut-resuture control. Furthermore, while the combination provided moderate functional recovery, lack of evoked response indicated weak remyelination and/or incomplete muscle re-innervation.

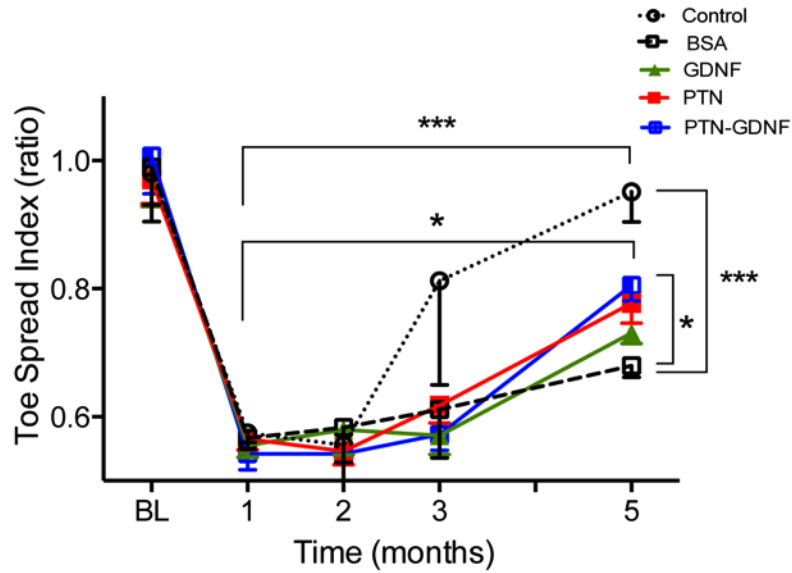


Figure 2.6. Modest recovery in Toe-Spread Index provided by PTN-GDNF. In the 4cm study, Toe-Spread Index (TSI) at the end of five months confirmed moderate recovery in TSI in the growth factor groups, but not comparable to the cut-resuture control. However, at the last time point, PTN-GDNF group was significantly better than the BSA control. \*\*\* =  $p < 0.001$ , \* =  $p < 0.05$ .

During development and after injury, axons share a close, 1:1 relationship with Schwann cells[33], [126]. As axonal growth cone proceeds, Schwann cells associate themselves with groups of axons and ensheath them within basement membranes[127]. Depending on diameter, the Schwann cells then sort these axons into myelinated or unmyelinated, via a highly coordinated mechanism known as radial sorting [127], [128]. Axons that cross the  $1\mu\text{m}$  diameter threshold, are sorted out by Schwann cells, which then switches to a pro-myelinating phenotype, wrapping the axon with myelin[127], [129], [130]. Abnormal radial sorting, associated with Schwann cell signaling, is known to affect axon caliber, maturation and subsequent myelination[131], [132]. In this chapter, we analyzed the ultrastructure of the regenerated tissue to determine the stage of axon maturation and its effect on muscle re-innervation.

## **2.2 Materials and Methods**

### **2.2.1 Surgical Procedures**

The biosynthetic nerve implant (BNI) conduits used in this study consists of a transparent polyurethane conduit (3 mm OD, 1.715 mm ID; Micro-Renathane®; Braintree Scientific Inc.) 3 or 4 cm in length, with 8 microchannels casted in 1.5% agarose in the lumen. These microchannels (7 of 0.35 mm and 1 in the center of 0.50 mm in diameter) comprised of 0.87 mm<sup>2</sup> total area, thus providing 36.18% of the nerve conduit lumen available for the regenerating axons. Each microchannel was filled with growth factor-loaded PLGA microparticles (MP) suspended in type I collagen releasing either bovine serum albumin (BSA), PTN, GDNF or PTN-GDNF. The MPs were prepared using double emulsion as previously described [133]. Sterilized polyurethane tubes were first filled with 1.6% agarose and metal mandrels were then drawn out to create microchannels filled with a collagen-microsphere mixture, as described previously [134]. The BNIs were then incubated at 37°C for 15 minutes to allow gelation of the collagen, before implanting in the animals. A cohort of twenty-four adult female New Zealand white rabbits, divided into two sub-cohorts, were implanted with biosynthetic nerve implants (BNI). Briefly, the peroneal nerve of the rabbit was exposed through a 6cm muscle-sparing incision in the biceps femoris muscle. The nerve was isolated from underlying connective tissue and a 30mm length was transected and replaced by a 40mm BNI filled with PTN(n=6), GDNF(n=6), PTN-GDNF(n=5) as compared with BNIs filled with BSA(n=3). As a positive control (n=5), the resected nerve section was cut and immediately sutured. The incision site was closed with staples and the animals received an analgesic (Buprenorphine SR, subcutaneous 1mg/kg, once every 72hours ) and antibiotic (Sulfamethoxazole/trimethoprim , 40mg/ml/8mg/ml, oral, daily for two-three weeks). All animal

experiments were performed in accordance with the guidelines of the Institutional Animal Care and Use Committee of the University of Texas at Arlington, according to the NIH guide for the care and use of laboratory animals.

### **2.2.2 Animal Perfusion and Tissue preparation**

At the study for each cohort, anesthetized animals were perfused with 0.9% saline and 4% paraformaldehyde. The regenerated nerve, with the implant tube intact, was harvested along with the respective *tibialis anterior* muscle. The tissue was then post-fixed in 4% PFA for 24-48 hours and then transferred to PBS solution. The regenerated nerve tissue was dissected, and the tube was separated carefully. The wet weight of the extracted *tibialis anterior* muscle was recorded in milligrams.

### **2.2.3 Immunohistochemistry**

For neuromuscular junction (NMJ) staining, the tibialis anterior muscle was harvested, wet weight recorded, fixed, and cryoprotected in 30% sucrose for 24-48 hours before embedding it in Tek OCT. Thin slices (40 $\mu$ m) were sectioned in the cryostat and co-labeled with the NF200 antibody (1:200; Sigma Aldrich) to visualize the heavy microfilament subunit in axons, and Alexa Fluor 488-labeled  $\alpha$ -bungarotoxin (1: 1000, Invitrogen) to visualize the nicotinic acetylcholine receptor (AChR). Images were taken with a 63X oil immersion objective in the confocal microscope (Nikon A1R). Grey scale images of the same sections were used to visualize muscle fiber boundaries to measure area of individual muscle fibers. Three regions of interest per sample were used to trace individual muscle fibers using ImageJ and area measurements were obtained. The data are presented as mean plus standard deviation.

#### **2.2.4 Electron microscopy**

A nerve segment 2.5 mm distal to the repair site was post-fixed in 2.5% glutaraldehyde in 0.1 M cacodylate buffer. The tissue was then embedded in epoxy resin, and 1  $\mu$ m thin sections were cut and stained with osmium and examined at 6000x magnification using a JEOL LEM 1200 EX II system. Ten regions across each sample were randomly selected for quantifying axon number and axon diameter using the Image J software.

#### **2.2.5 Statistical Analysis**

GraphPad Prism statistical analysis software was used to perform analysis of variance (ANOVA) to compare the different groups. Post-hoc Tukeys or Dunns tests were used for multiple comparisons. For axon diameter, the Shapiro-Wilk test indicated that the data was not parametric, and the Kruskal-Wallis test was used. All data values are represented as mean plus standard deviation unless noted otherwise. A value of  $p \leq 0.05$  was considered as statistically significant.

### **2.3 Results**

#### **2.3.1 PTN-GDNF mediates nerve regeneration across a 4 cm critical gap, but abnormal radial sorting prevents re-myelination**

As observed in Figure 2.4 B, the number of myelinated axons, present in the proximal segment of the BNI groups, reduced considerably at the distal end. This indicates that over longer lengths, the re-myelination effect of the growth factors was attenuated. To investigate this at the ultrastructural level, we evaluated distal regenerated segments of the nerve using electron microscopy. Electron micrographs allow a closer, more accurate measurements of axon diameter and myelination. Quantification showed that although present in large numbers, axons in the BSA groups were small in diameter ( $0.70 \pm 0.30 \mu\text{m}$ ), unmyelinated, and present within Schwann cell basement membranes (Fig.2.7 A). The axons present in the GDNF ( $0.84 \pm 0.48 \mu\text{m}$ ) were similar in diameter as compared

to the PTN ( $0.80 \pm 0.21\mu\text{m}$ ) group (Fig.2.7 B, C), also present in Remak bundles. Interestingly, larger diameter axons ( $0.96 \pm 0.35\mu\text{m}$ ) were found in the PTN-GDNF group within Remak ensheathing as well as some re-myelination of large axons (Fig.2.7 D). As expected, the mean fiber size in the cut-resuture control was  $1.01 \pm 0.47\mu\text{m}$ , with large axons up to  $7\mu\text{m}$  in diameter. These data suggest that the presence of axons, albeit important, is not adequate for successful reinnervation, and that the differentiation of Schwann cells resulting in normal axonal sorting and myelination is critical. Although PTN-GDNF treatment moderately influenced axon diameter, the extent of remyelination was poor, indicating a limitation in the pro-regenerative properties of the neurotrophic factors.

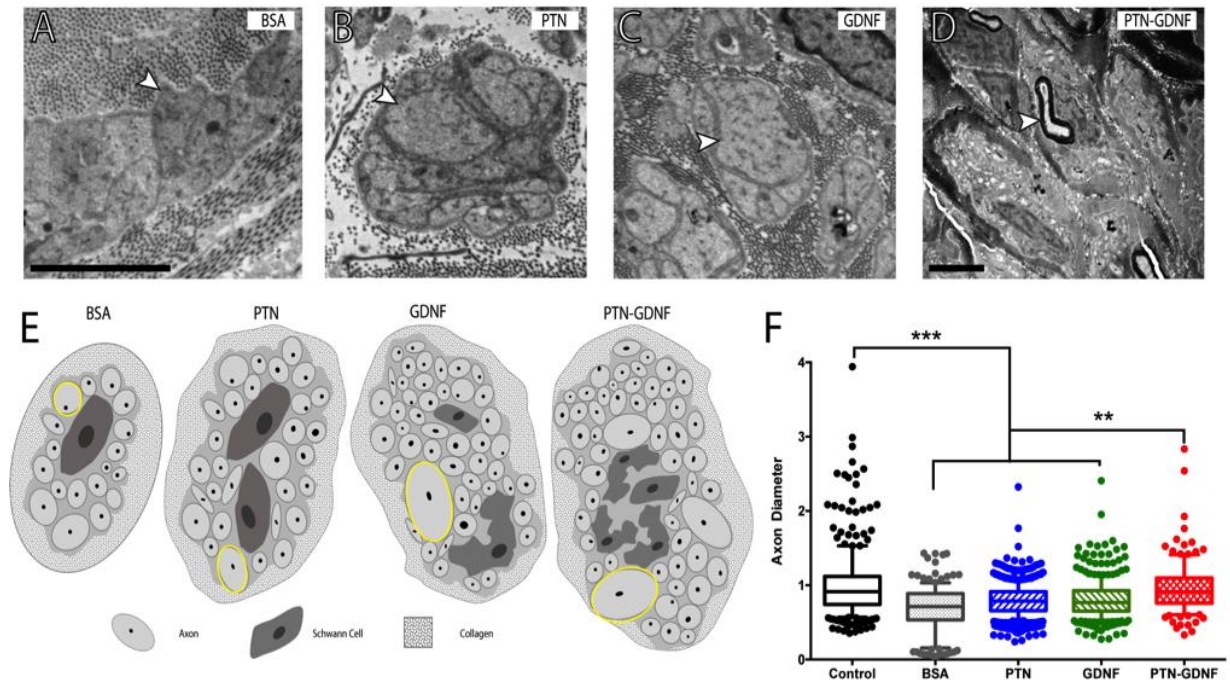


Figure 2.7. Radial sorting delay. Electron micrographs of axons in Remak bundles. (A) Compared to those with BSA, larger unmyelinated axons were present in the (B) PTN and (C) GDNF groups (arrowheads). (D) Some re-myelinated axons were present in the PTN-GDNF group. (E) Schematic representation of different diameter axons in the Remak bundles for each group.

group. (F) Axon diameter distribution showed significantly smaller axons in the BSA, PTN and GDNF groups compared to the PTN-GDNF. Scale bar: 5 $\mu$ m. \*\*\* =  $p < 0.001$ , \*\* =  $p < 0.01$ .

### 2.3.2 PTN-GDNF moderately rescues muscle atrophy, mediates neuro-muscular re-innervation

To determine target reinnervation by the regenerated axons, we labelled the neuromuscular junctions in the TA muscle with  $\alpha$ -bungarotoxin (for acetylcholine receptors) and NF-200 (for axons). The intensity of axon/NMJs overlap was observed to be larger in the GDNF and PTN-GDNF compared to the BSA and PTN groups, but not as elaborate as the (cut-resuture) control (Fig. 2.8 A-E). The GDNF and PTN-GDNF showed a range of 3-5 NMJ with evident NF200/AchR co-labeling, indicating that these were re-innervated muscles. However, quantification of the tibialis anterior muscle mass was significantly larger in the cut-resuture control ( $6 \pm 0.41$  g) compared to all others with a growth factor ( $3.2$ - $3.6 \pm 0.4$  g) or BSA ( $2.67 \pm 0.7$ g; Fig.2.8 F).

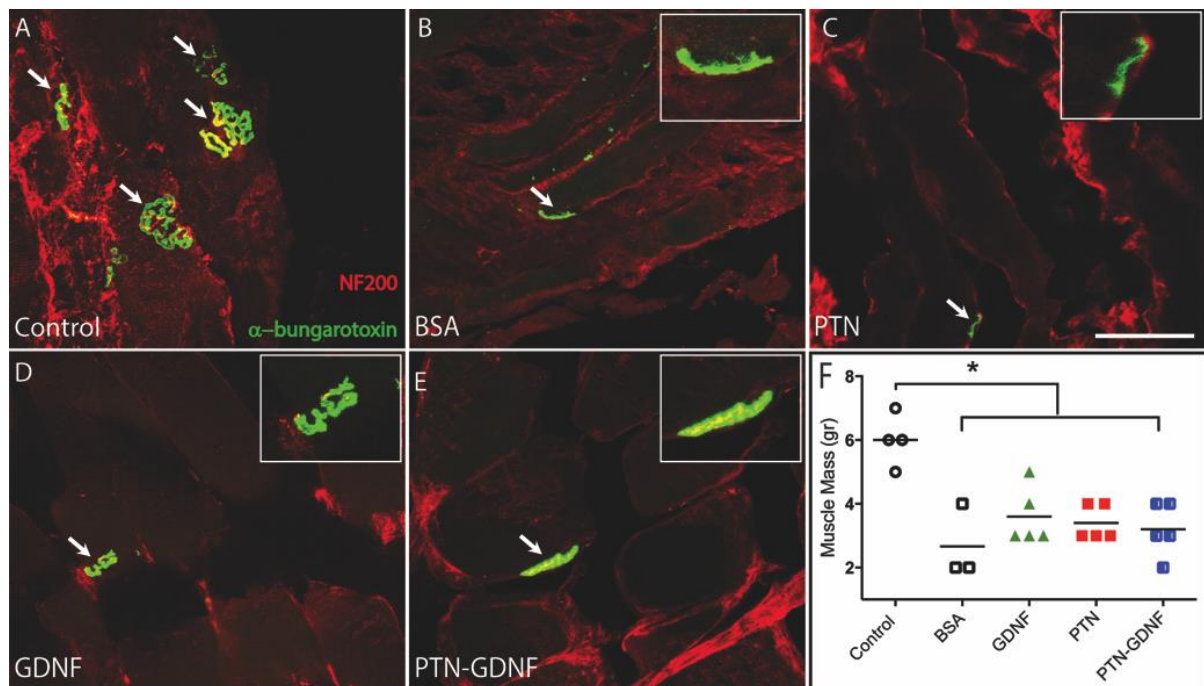


Figure 2.8. Re-innervation of the tibialis anterior muscle. (A) Co-labeling of axons (NF200) and AchR clustering ( $\alpha$ -bungarotoxin) demonstrated the successful target re-innervation. The intensity of axon/NMJs overlap was observed to be larger in the GDNF (D) and PTN-GDNF (E)

compared to the BSA (B) and PTN (C) groups, but not as elaborate as the (cut-resuture) control. (F) Muscle mass did not improve significantly as compared to the positive control, indicating limited rescue of muscle atrophy. Scale bar: 5 $\mu$ m. \* =  $p < 0.05$ .

In addition, muscle fiber area showed atrophy in all the BNI groups as compared to the control (Figure 2.9,  $p < 0.0001$ ). However, PTN-GDNF showed a moderate rescue as compared to the BSA and GDNF ( $p < 0.01$ , Figure 2.9). This data suggests that although PTN-GDNF provided re-innervation, re-establishment of neuromuscular junctions was weak, which explains the lack of evoked activity.

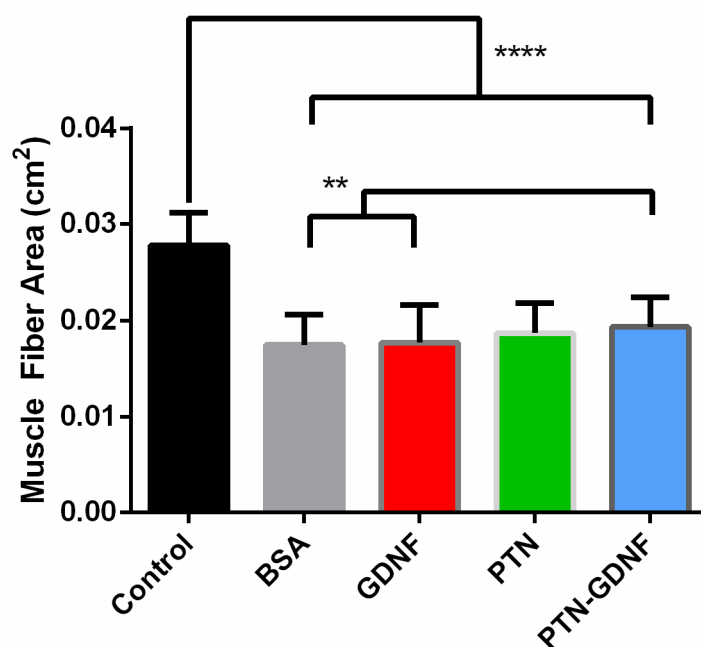


Figure 2.9. Muscle fiber area calculated from tissue sections revealed a significant atrophy in all BNI repaired animals as compared to the control, but a moderate rescue in the PTN-GDNF group over the BSA group. One way ANOVA, \*\*\*\* $p < 0.0001$  \*\* $p < 0.01$ .

The results from this study demonstrate that multi-luminal conduits provide pro-regenerative conditions for the injured nerve, and addition of PTN and GDNF further enhance regeneration and provide moderate recovery across a 4cm critical nerve gap.



## 2.4 Discussion

In this study, we characterized the synergistic effect of PTN and GDNF in successfully repairing critical nerve gaps. Our results indicate that PTN does not induce abnormal growth of cells but in fact improves number of regenerated large axons. In addition, the combination of PTN and GDNF highly enhances axons as well as moderate remyelination with significant functional recovery. The main findings presented here suggest that a combination of GDNF and PTN do have a synergistic effect resulting in nerve regeneration across a 4 cm gap injury.

Our in vitro studies show that the combination of GDNF and PTN significantly enhanced axonal outgrowth over the other treatment groups. After injury, PTN and GDNF are known to be highly expressed in Schwann cells as well as in the ventral motor neurons[135]. While PTN is known to be specific for motor neurons, GDNF facilitates both motor and sensory survival [88], [107]. Previous studies have shown that mouse lacking GDNF or its receptors die right after birth[136]. Reports show that exogenous administration of GDNF promotes axon sprouting after transection of sciatic nerve[137]. GDNF binding to receptors Ret and GFR $\alpha$  stimulate neural progenitor cells to differentiate[138]. Activation of GDNF receptors leads to intracellular changes initiated by phosphorylation of a tyrosine subunit present on Ret resulting in a cascade of intracellular activations leading to activation of the Ras-ERK pathways[139]. Additionally, PTN has shown to be mitogenic, angiogenic and acts on Schwann cells, macrophages and endothelial cells, suggesting its role in nerve regeneration [108], [113]. PTN has been shown to promote nerve elongation, cell proliferation and angiogenesis in regenerating skeletal muscle[140]. Developing embryos have been found to express PTN in the peripheral nervous system and have been shown to convey neurotropic support for motor neurons[109]. In fact, embryonic sensory neurons lacking

the PTN receptor undergo apoptosis despite NGF support [141]. It is associated with the protection, promotion and guidance of neural regeneration. In addition to skeletal muscle reinnervation, PTN is also known to induce mitogenesis in different cells types, such as epithelial, endothelial, mesenchymal, and neuronal cells[110] . Some reports suggested that PTN and its receptor ALK have high expression level in cancer cells[142]. Our histology results, however, show that PTN successfully regenerates axons after transection as indicated by the presence of  $\beta$ -III tubulin positive axons even in the distal end. In addition, gross anatomy also shows that there was no abnormal growth of cells in the repaired nerve. A previous study by Blondet et al in 2006 delivered exogenous PTN to the nerve and muscle and showed that high concentrations(1mg/kg) of this peptide impairs nerve regeneration[113].However, in our study, we used very low(20 $\mu$ g/mL), physiologically relevant concentrations of PTN and showed successful regeneration. Our results indicate no tumor formation and for the first time, PTN was used to bridge a critical gap.

Next, we tested a combination of PTN-GDNF in a 4 cm critical gap in a rabbit common peroneal nerve injury model. We observed axonal regeneration in the distal end of the tube in all animals that after five months post injury, the average number of axons at the distal section of the regenerated nerve was two folds higher for the combination of PTN and GDNF group in comparison to the BSA, PTN, and GDNF groups. This demonstrates the improved regenerative capacity when growth factors act synergistically, however no myelination was present at the distal section. This result was further confirmed by electron micrographs (EM). EM showed presence of many unmyelinated axons in these groups, but a lack of myelinated axons. Our results point towards a delay in axonal sorting during regeneration, which is visible by the presence of large,

unsorted axon bundles. It has been long known that axonal diameter is a critical factor in determining the extent of myelination and an axon on exceeding a diameter of 1 $\mu$ m will be detected by the Schwann cell and be myelinated [143]. The Schwann cells play a critical role in this signaling and the neuregulin-1 family of ligands has shown to regulate Schwann cell proliferation, differentiation and migration and eventual myelination[127], [144], [145]. Specifically, neuregulin-1 type III which is the axon derived sub-type is responsible for myelinating mature, large diameter axons, by signaling the pro-myelinating Schwann cells [144]. It is also known that axonal derived neuregulin regulates the Schwann cell derived neuregulin (type I) signaling. As observed in our results, the presence of large axons but failed myelination suggests the need for exogenous application of neuregulin along with the combination of trophic factors to enhance regeneration with increased remyelination. In addition, to prevent muscle atrophy, nerve regeneration across critical gaps can be accelerated through electrical stimulation of the nerve and/or muscle as well as exercise therapy[116], [118], [146]–[150].

Our results demonstrate that PTN and GDNF act synergistically to bridge a 4 cm long gap across nerve defect as confirmed by the toe spread index, electrophysiology, and histology more effectively than either BSA, PTN, or GDNF. While the combination of the topographical multilaminar structural design of the BNI with the co-administration of growth factors PTN and GDNF promotes the regeneration of axons across a 4 cm gap injury, delayed radial sorting inhibits re-myelination. Further addition of growth factors that regulate Schwann cell directed axonal sorting and promote maturation and re-myelination, could be an effective strategy to restore maximum functional recovery.

## CHAPTER 3

### ROLE OF NEUREGULIN 1- TYPE III IN AXON PATHFINDING, REGENERATION AND FUNCTIONAL RECOVERY IN A CRITICAL NERVE GAP IN THE RABBIT PERONEAL NERVE MODEL

#### 3.1 Introduction

##### 3.1.1 Neuregulin 1 family of proteins

The neuregulin 1 family of proteins, encoded by the *nrg1* gene, contain an epidermal growth factor (EGF)- like domain and signal via the ErbB receptors. There are six types of NRG1 proteins (Type I-VI), and about 31 isoforms of these proteins, some of which are neuro differentiation factor (NDF), heregulin, glial growth factor (GGF), acetylcholine receptor inducing factor (ARIA), sensory and motor differentiation factor (SMDf) [151], [152]. *Nrg1* knockout mice have shown to exhibit abnormalities in neural development, axonal sorting and myelination as well as synaptogenesis and glial cell development in the central and peripheral nervous system[151]–[154]. These proteins all interact with the ErbB tyrosine kinases along their EGF-like domains, mainly due to the homology between ErbB receptors and EGF receptors. The binding of the *nrg1* domain induces dimerization in the ErbB resulting in downstream phosphorylation of the intracellular domains of the ErbB receptors. Through this signaling, NRG activates the phosphoinositide 3-kinase (PI3K) and phosphorylates MAPK and Akt to promote SC survival, migration and differentiation[155], [156]. An extensive isoform specific study in animals heterozygous for *neuregulin* <sup>$\Delta$ EGF-lacZ</sup> allele by Meyer et. al in 1997 describes specific roles for the different NRG1 isoforms. NRG1 Type-I was abundant in the endocardium of the developing ventricle, with some Type-III present. In the cranial ganglia, undifferentiated cells express Type I, regulating development and survival.

Additionally, motoneurons and cells in the cranial and dorsal root ganglia express NRG1 Type-III that profoundly regulates Schwann cell fate and axon pathfinding[151]. In spinal cord motor neurons, NRG1 is localized in the post synaptic regions, associated with C-bouton proteins like vesicular acetylcholine transporter. The expression of these proteins is disrupted on axotomy, suggesting a role in injury and repair [157]. Additionally NRG1 Type-I shows a two fold increase in distal Schwann cells, sustained for 2 weeks after injury, suggesting a ‘de novo’ compensatory effect due to loss of axonal contact [158]. The different types of proteins encoded by the *NRG1* gene are illustrated in Figure 3.1.

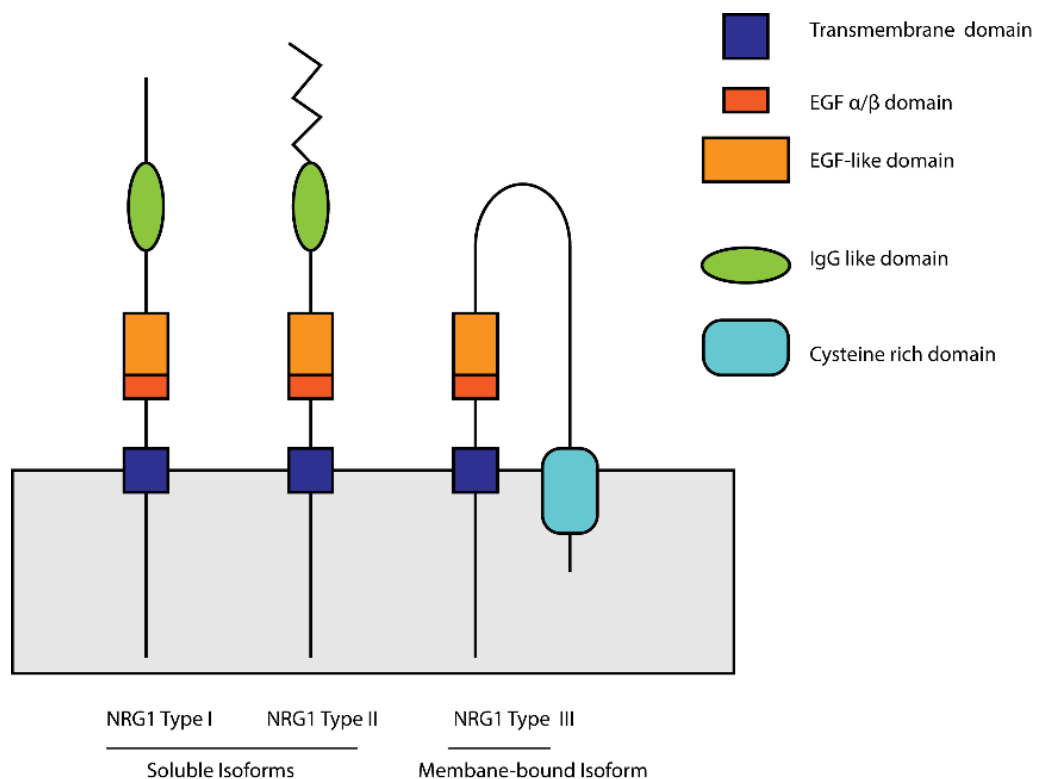


Figure 3.1. Structural domains of the Neuregulin1 family of proteins. Type-I and II are soluble isoforms, whereas Type-III is a membrane bound isoform with a cysteine rich domain tethering it to the membrane. Figure adapted from [159]

### 3.1.2 Role of Neuregulin 1 Type-III in Peripheral Nerve Development and Injury

Of the many isoforms coded by the *nrg1* gene, NRG1 Type-III is known to play a significant role in Schwann cell maturation and subsequent myelination of axons in the peripheral nervous system (PNS), during development and after injury[127], [160]. In the PNS, NRG1 Type-III is the axonal derived isoform that binds to the ErbB2/3 receptors on the Schwann cells, triggering a signaling cascade inducing conversion of pre-cursor Schwann cells into pro-myelinating or Remak type[127], [144], [161]. After injury, this protein signals the Schwann cells to incorporate laminin along the regenerative bridge facilitating axonal growth[162]. Levels of NRG1 Type-III in axons differentially determines myelination or ensheathment within Remak bundles, as well as number of axons associated with one Schwann cell forming the bundle. In axons, NRG1 Type III is the only ligand that dictates this type of SC signaling.[127], [144]. Mutation of NRG1 Type-III in zebra fish demonstrated that Schwann cell migration is profoundly affected along the nerve, and that these cells trespass into the spinal cord when NRG1 type-III is overexpressed. This highlights the potential instructive role of neuregulin in development of axons, as well as after injury[163]. Immediately after axotomy, there is a marked downregulation of ERBb2/3 receptors, which is then upregulated up to 28 days after injury. In striking similarity, mRNA levels of NRG1 Type-III stays upregulated after injury and up to 28 days, suggesting the role of this ligand and its cognate receptor in degeneration and regeneration [164]. NRG1 Type-III drives remyelination after injury by upregulating myelin related proteins like myelin basic protein, myelin protein zero and myelin associated glycoprotein for up to two weeks. During this initial stage, mutation of neuregulin impairs re-myelination, for about 2 months, but is later rescued by compensatory mechanisms[129]. However, in critical nerve transection injuries, we and others have shown that

such mechanisms fail due to long term denervation and Schwann cell senescence, emphasizing the importance of NRG1 type-III in re-myelination and subsequent functional recovery[61], [134]. In superior cervical ganglion axons, inhibition of ErbB receptors or knocking out NRG type III resulted in reduced SC proliferation and migration and markedly increased apoptosis of existent cells, implicating NRG1 Type-III in development of sympathetic axons as well[165]. GTPase dynamin 2 regulates membrane remodeling, fission and vesicular trafficking and deletion of Dnm2 in development, impairs axonal sorting and onset of myelination while in adults, causes peripheral neuropathy and demyelination [166]. Ablation of dnmn2 in mouse skeletal muscle results in muscle atrophy, fiber loss, abnormal NMJ formation and peripheral nerve degeneration [167].

In our previous work (described in Chapter 2), we have shown successful regeneration of the peripheral nerve across a 40mm peroneal nerve gap, using glial-derived neurotrophic factor (GDNF) and pleiotrophin (PTN)[134]. Although the combination of these growth factors resulted in maximum functional recovery and highest number of axons as compared to the negative control, there was lack of myelination and inadequate neuromuscular contact[134]. The electron micrographs of the regenerated nerves showed abnormal axonal sorting, with large ( $>1\mu\text{m}$  diameter) axons ensheathed within a Schwann cell basement membrane. It is known that during development and/or after injury, growing axons that surpass the  $1\mu\text{m}$  diameter threshold, are sorted out by a pro-myelinating Schwann cell, and subsequently myelinated, proportional to the levels of NRG1 type-III present on the axon[10], [168]. The smaller axons are bound within a single basement membrane in groups of 12-14, thus forming a Remak bundle[10], [169]. Based on our previous results, we propose that NRG1 type-III, in combination with PTN will enhance axonal

sorting and regeneration, promote myelination and subsequent neuro-muscular reinnervation, in a 4cm critical peroneal nerve gap.

## **3.2 Materials And Methods**

### **3.2.1 Microparticle fabrication and characterization**

The growth factors pleiotrophin (PTN) and neuregulin 1 type-III (NRG1 Type-III) were encapsulated in 50% polylactic: 50% Co-glycolic acid (PLGA, Sigma Aldrich) using a previously described double emulsion method [133]. Briefly, 20 $\mu$ g of NRG1 Type-III (R&D Biosystems) and 20 $\mu$ g of PTN (Invitrogen) were dissolved in DI water separately and added to a mixture of dichloromethane (DCM) and PLGA. After multiple sonication cycles, the DCM could evaporate from the solution over the course of four hours. Thereafter, the remaining solution was centrifuged at 5000 rpm for 15 minutes and the precipitate was frozen at -20°C overnight followed by lyophilization. The loading efficiency of the microspheres was calculated to be 68%. A zeta potential analyzer was used to measure the size of the resulting microspheres and the stability of the microspheres was determined from their polydispersity index. As a no growth factor control, PLGA microspheres loaded with DIW were prepared using the same method. As determined from the zeta potential analyzer, the size of the microspheres was 3098.25 $\pm$  0.185nm for the NRG1 Type-III microspheres and 2436  $\pm$ 0.529nm for the PTN microspheres. The stability of the microspheres as determined from their polydispersity index was 0.185 and 0.529 for the NRG-1 and PTN microspheres respectively (Figure 3.2). For the control microspheres, the particle size was 2465 $\pm$  91 nm with a polydispersity index of 0.7 (Figure 3.2). The long term sustained release of the growth factors was determined by suspending 1g microspheres in 1ml PBS at 37°C and collecting the solution at regular intervals spanning one month. The growth factor content in the



release samples were quantified using commercially available ELISA kits (NRG-1, PTN) and read at 550nm using an EPOCH 2 microplate reader (BioTek). The PLGA microspheres provided a sustained release of protein over a period of twenty-six days (Figure 3.2 A), with a 1500ng/ml concentration by the last day, which has been shown to be optimum for Schwann cell proliferation and differentiation[156].

### **3.2.2 Bioactivity Of Encapsulated Protein *In Vitro***

To assess whether the encapsulated growth factors were biologically active, dorsal root ganglia (DRG) explants were incubated with the microspheres and neurite growth was quantified. Briefly, neonatal mice (P0-P4) were used to harvest dorsal root ganglia explants. After cleaning the connective tissue, the DRG were placed on PDL and laminin coated glass bottom wells and stabilized in place using 15µl collagen (EMD Millipore#ECM675). Microspheres mixed with collagen solution were placed in each well and incubated at 37°C for 15 minutes to allow the collagen to polymerize. Thereafter, 400µl neurobasal A media supplemented with 2% B27, 0.5% penicillin/streptomycin, and 0.75% L-glutamine was added to each well and incubated at 37°C, 5% CO<sub>2</sub> for 7 days. Every 72 hours, 200µl of the media was replaced from each well with freshly made media. After 7 days, the DRG explants were fixed using 400µl of 4% paraformaldehyde for 15 minutes on a shaker and rinsed with PBS. After rinsing, the explants were permeabilized using 0.5% Triton X100 in PBS and blocked with normal goat serum for one hour. The DRGs were then incubated with mouse anti-β-III (Abcam #78078) tubulin overnight on a shaker at 4°C. The next day, the explants were rinsed three times in PBS and then labelled with goat anti mouse 594 for one hour and counterstained with DAPI to visualize cell nuclei. As seen in Figure 3.2, neurite growth was observed in all groups supplemented with growth factor encapsulated microspheres.

While NRG1 Type-III alone stimulated the growth on longer neurites, the combination of pleiotrophin and NRG1 Type-III had the highest density of neurite outgrowth (Figure 3.2 C-E).

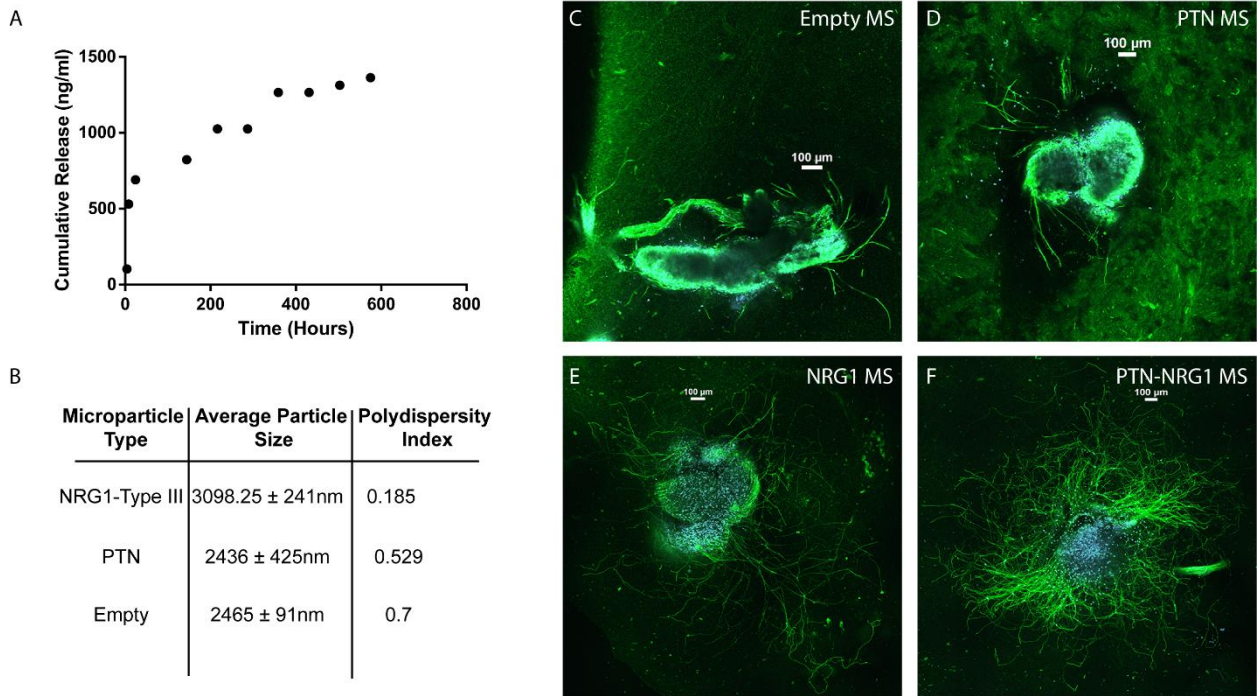


Figure 3.2. A) Release profile of the NRG1 Type-III microparticles, taken over 28 days showing the cumulative release of the growth factors over time. B) Characterization of the PLGA microsphere size and stability in terms of polydispersity index. C-F) Images of dorsal root ganglia explants at 10-days in vitro after treatment with either control, PTN, NRG1 type-III or combination of PTN-NRG1 type III microspheres. They are labeled for neurites ( $\beta$ -tubulin, green) or cell nuclei (DAPI, blue). Scale bar: All images; 100 $\mu$ m.

### 3.2.3 Surgical Procedures

After confirming the sustained delivery and biological activity of the microspheres, a cohort of twenty-four adult female New Zealand white rabbits were implanted with biosynthetic nerve implants (BNI) as described previously. Briefly, the peroneal nerve of the rabbit was exposed through a 6cm muscle-sparing incision in the biceps femoris muscle. The nerve was isolated from underlying connective tissue and a 30mm length was transected and replaced by the BNI conduit filled with either Control (n=6), NRG1 (n=6) or PTN-NRG1 (n=6) microspheres (Figure 3.3A).

As a positive control (n=5), the resected nerve section was reversed and sutured to the nerve stumps by adding a 10mm empty tube to compensate for nerve retraction, at the distal end (Figure 3.3A). Intramuscular application of 2  $\mu$ l of NRG  $\beta$ 1 has been shown to improve Schwann cell proliferation and differentiation, and to promote regeneration in an end-to-side neurorrhaphy model[156]. Since NRG1 Type-III has not been previously applied *in vivo*, we used the NRG  $\beta$ 1 concentration as reference for loading the microspheres in the BNI conduits. The biosynthetic nerve implant (BNI) conduits consists of a transparent polyurethane conduit (3 mm OD, 1.7 mm ID; Micro-Renathane $\text{\textcircled{O}}$ ; Braintree Scientific Inc.) 3 or 4 cm in length, with 8 microchannels casted in 1.5% agarose in the lumen of the conduit (7 of 0.4 mm and 1 in the center of 0.5 mm in diameter) providing a total of 0.9 mm<sup>2</sup> or 36.2% of the nerve conduit lumen available for nerve regeneration. Sterilized polyurethane tubes were first filled with 1.6% agarose and metal mandrels were then drawn out to create micro-channels filled with a collagen-microsphere mixture, as described previously[134]. In this study, the 4cm BNI conduits were loaded with a total volume of 3.6 $\mu$ l of the NRG-MP suspension, estimated by ELISA to release 2.16 ng/ $\mu$ l/day for a total of 52 days. This concentration is comparable to that used for Schwann cell stimulation at the neuromuscular junction, and thus considered adequate for stimulating axon remyelination. The 52 days of NRG release in the microchannels was estimated to provide sustained remyelination support for the critical gap, since regenerating axons are known to growing at a rate of 1.5mm/day and will take 60 days to cross the 4cm gap. The BNIs were then incubated at 37°C for 15 minutes to allow gelation of the collagen, before implanting in the animals. The study was double blinded and randomized, and all animal experiments were performed in accordance with the guidelines of the

Institutional Animal Care and Use Committee of the University of Texas at Dallas, according to the NIH guide for the care and use of laboratory animals.

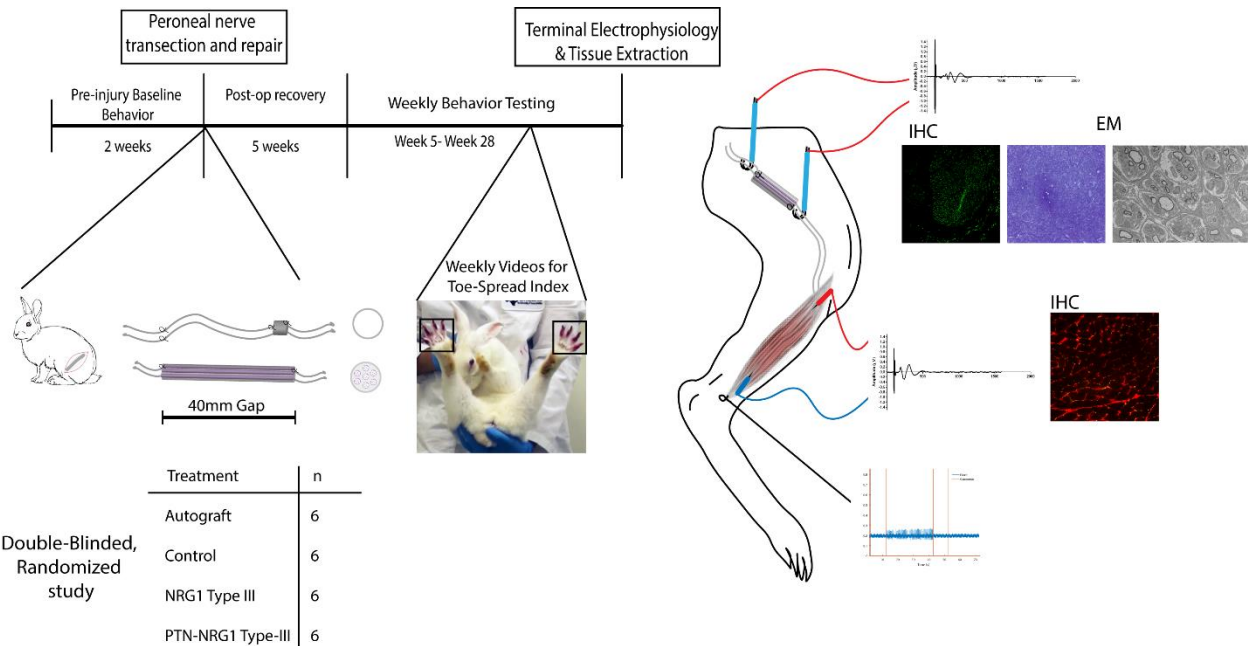


Figure 3.3. Experimental design and timeline. Schematic of transection injury, indicating the two repair techniques, autograft and BNI conduit. Experimental timeline, indicating times of injury, behavioral assessment and terminal experiments, that included electrophysiological recordings and collection of tissue for histology.

### 3.2.4 Toe-Spread Index (TSI) Assessment

The toe-spread index is the standard behavioral assessment used to evaluate the re-innervation of the peroneal nerve muscle group and is an indicator of functional recovery. When the animals are held loosely at the scruff of the neck and lowered suddenly, they extend their toes as a reflex to land (Figure 3.10). Videos for each animal were once taken before surgery and weekly starting 5 weeks post-surgery. For each time point, one frames (from three different trials) were selected to compare the toe-spread between the injured and the un-injured foot. The ImageJ software was

used measure the distance between the first and the last toe. The TSI is the ratio of the of the injured over the uninjured toe-spread.

### **3.2.5 Electrophysiological and Muscle Force Measurements**

In addition to recording compound motor action potentials (CMAPs) and compound nerve action potentials (CNAPs), measurement of muscle force is known to be a good indicator of functional motor recovery and successful re-innervation. Animals were sedated with ketamine (35mg/kg) and Xylazine (5mg/kg) combined in a single syringe and administered intraperitoneally. After that, the surgical plane of anesthesia was maintained using 2% isoflurane in oxygen. In a sterile field, the muscle was re-opened using a scalpel and the repaired nerve was re-exposed. After carefully isolating from surrounding tissue, two pairs of hook electrodes (FHC) were placed proximal and distal (at 6cm between them) to the repair site for stimulation and recording respectively. Using a sterile scalpel, the group of muscles innervated by the peroneal nerve was exposed and a pair of needle electrodes was placed for recording CMAPs. A nylon suture was connected to the tendon protruding at the ankle for attachment to a force transducer (RB-Phi-117, RobotShop, Mirabel, QC) to record isometric force from the muscles[170].The proximal end of the repaired peroneal nerve was stimulated to obtain CNAPs and CMAPs using the OmniPlex Neural Data acquisition system whereas the corresponding force exerted by the muscle was recorded using a custom interface programmed in MATLAB.

### **3.2.6 Animal Perfusion and Tissue Preparation**

At the end of twenty- eight weeks, anesthetized animals were perfused with 4% paraformaldehyde. A 6cm length of the regenerated nerve, with the implant tube intact, was harvested along with the respective *tibialis anterior* muscle. The tissue was then post-fixed in 4% PFA for 24-48 hours and

then transferred to PBS solution. The regenerated nerve tissue was dissected, and the tube was separated carefully. Gross tissue analysis was performed to determine the extent of regeneration across the injury gap. The tissue was divided into six sections, proximal (P), middle (M1& M2) and distal (D1, D2 & D3), and processed for histological analysis.

### **3.2.7 Immunohistochemistry**

The harvested nerve tissue sections labelled P, M1, D1 and D3 were embedded in paraffin and 10µm thin transverse sections were obtained using a microtome (Leica RM 2235). The muscle tissue was cryopreserved in 30% sucrose overnight and then embedded in OCT solution. The frozen tissue was then cut into 40µm thick sections. A heat induced antigen retrieval method was used to recover the epitopes and the tissue sections were deparaffinized. The tissue sections were then labelled with primary antibodies for axons ( $\beta$  tubulin III; 1:400; Abcam #78078) and myelination (P0; 1:200; EMD Millipore #AB9352). After overnight incubation at 4°C, the sections were rinsed and then labelled with Cy2-and Cy3 conjugated secondary antibodies for one hour (1:400; Sigma Aldrich). After rinsing, mounting media (Shandon™ Immu-Mount) was used to cover-slip the slides. Images were taken using a Nikon A1R confocal microscope and number of axons and myelination was quantified using an automated image analysis software, CellC version 2.5 (<http://en.bio-soft.net/draw/CellC.html>). For neuromuscular junction (NMJ) staining, the tibialis anterior muscle was harvested, wet weight recorded, fixed, and cryoprotected in 30% sucrose for 24-48 hours before embedding it in Tek OCT. Thin slices (40µm) were sectioned in the cryostat and co-labeled with the NF-200 antibody (1:200; Sigma Aldrich#N4142) to visualize the heavy microfilament subunit in axons, and Cy3-labeled  $\alpha$ -bungarotoxin (1: 1000, Invitrogen) to visualize the nicotinic acetylcholine receptor (AChR). Images were taken with a 40X oil

immersion objective in the confocal microscope (Nikon A1R). Co-labelling of NF-200 and  $\alpha$ -bungarotoxin were identified as active, re-innervated neuromuscular junctions. Three regions of interest per sample were used to trace individual muscle fibers using ImageJ and area measurements were obtained. The data are presented as mean plus standard deviation.

### **3.2.8 Transmission Electron Microscopy**

Tissue sections M2 and D3 were post-fixed in 2.5% glutaraldehyde in 0.1 M cacodylate buffer and embedded in epoxy resin. Thin, 1 $\mu$ m sections were obtained and imaged using a JEOL 1400X transmission electron microscope. Six regions per animal were selected for quantification of axon number, axon diameter and g-ratio, using the ImageJ software. Axon diameter was calculated as an average of two diameter measurements at 90° from each other.

### **3.2.9 Statistical Analysis**

GraphPad Prism statistical analysis software was used to perform two way analysis of variance (ANOVA) with repeated measures to compare the different groups for the toe-spread index (TSI). One way ANOVA was used to compare axon and muscle quantification. Post-hoc Tukeys tests were used for multiple comparisons. A value of  $p \leq 0.05$  was considered as statistically significant.

## **3.3 Results**

### **3.3.1 Gross Anatomical Analysis**

The explanted nerves were inspected for tissue growth and bridging of the nerve stumps, to confirm regeneration. There was observable tissue growth in all the BNI tubes, with apparent regeneration in most of them. However, after removing the polyurethane tubes, only some of the nerves were confirmed to have fully regenerated with robust tissue growth and vascularization as seen in Figure 3.4. In some tubes, the agarose was intact with little to no tissue present in the regenerative bridge,

suggesting either collapsing of microchannels during implantation, or presence of air bubbles produced during the fabrication of the BNIs. Although inspected before implantations, given the manual fabrication of these conduits, micro-defects persist, which is one of the limitations of this conduit. For each group, samples were classified as success or failure based on gross regeneration observed across the injury gap. Based on these results tabulated in Figure 3.4 C, only those animals showing robust regeneration were considered for further data analysis.

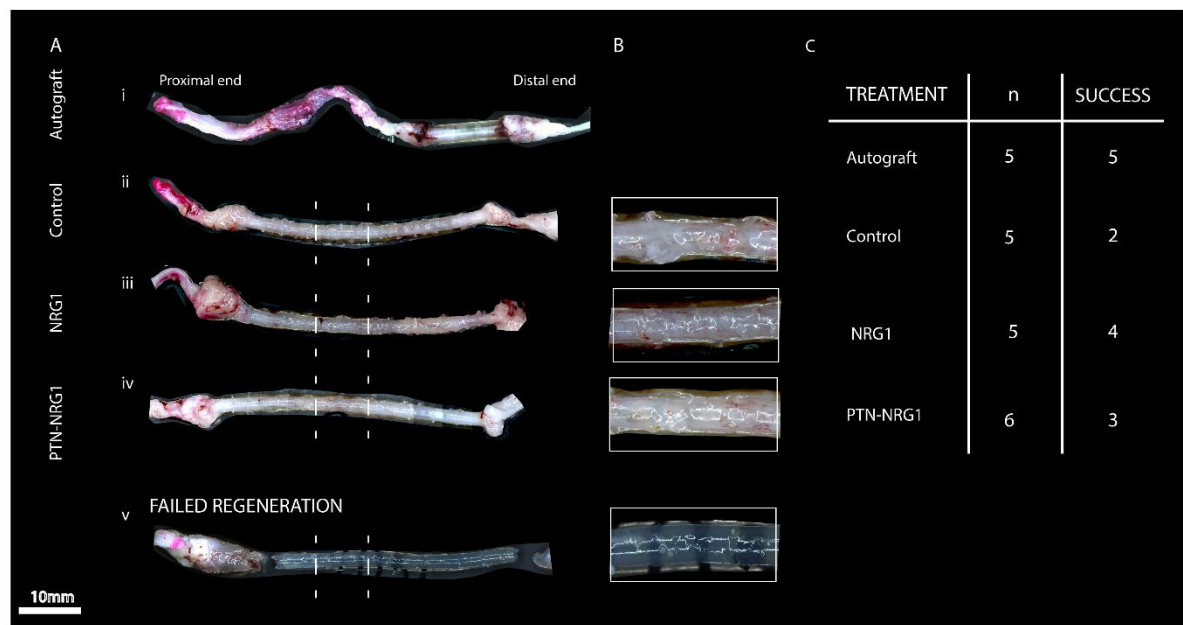


Figure 3.4. Gross Anatomical pictures of the regenerated nerves. A) Tissue obtained from i) autograft group, and after removing the polyurethane tubes in the ii) Control, iii) NRG1 Type-III and the iv) PTN-NRG1 microsphere groups, showed robust growth and good vascularization (inset for each), for some tubes. v) Failed regeneration was observed in some tissue samples, as indicated by the intact agarose scaffold and no tissue presence in the middle segment of the regenerative bridge (inset). C) The success rate of each group, after excluding the tubes that showed no tissue growth. Scale Bar: 10mm.

### 3.3.2 Nrg1 Type-III promotes axonal sorting of large caliber axons

Toluidine blue labelled sections were used to evaluate the overall tissue growth at the distal end of the regenerated nerves, which showed a robust growth in the autograft group, while those in the



BNI groups showed more of a fascicular structure, with epineural tissue around these fascicles (Figure 3.5 A). Higher magnification EM images were obtained to quantify the number diameter and g-ratios of axons. As seen in Figure 3.5A, the autograft group had a wide distribution of large and small axons with different degrees of myelination, with an average diameter of 5.8  $\mu\text{m}$ . In the BNI groups, the myelinated axons were of similar diameter; control (2.3  $\mu\text{m}$ ), NRG1 Type-III(2.3  $\mu\text{m}$ ) and PTN-NRG1 (2.1  $\mu\text{m}$ ). Myelination analysis revealed that the NRG1 Type-III and PTN-NRG1 Type-III groups with better myelination (average g-ratio  $0.69 \pm 0.1$  and  $0.66 \pm 0.1$  respectively), as compared to those of the Control group (average g-ratio  $0.74 \pm 0.10$ , Figure 3.5 B&C). While the autograft had well distributed large and small myelinated axons, the g-ratios were significantly different as compared to the Control group ( $p < 0.001$ ), suggesting that the absence of neurotrophic factors, specifically neuregulin, impacts the myelination thickness of small axons. Furthermore, as expected, the autograft group had a significantly greater number of myelinated axons as compared to the BNI groups, with no differences within the BNI groups.

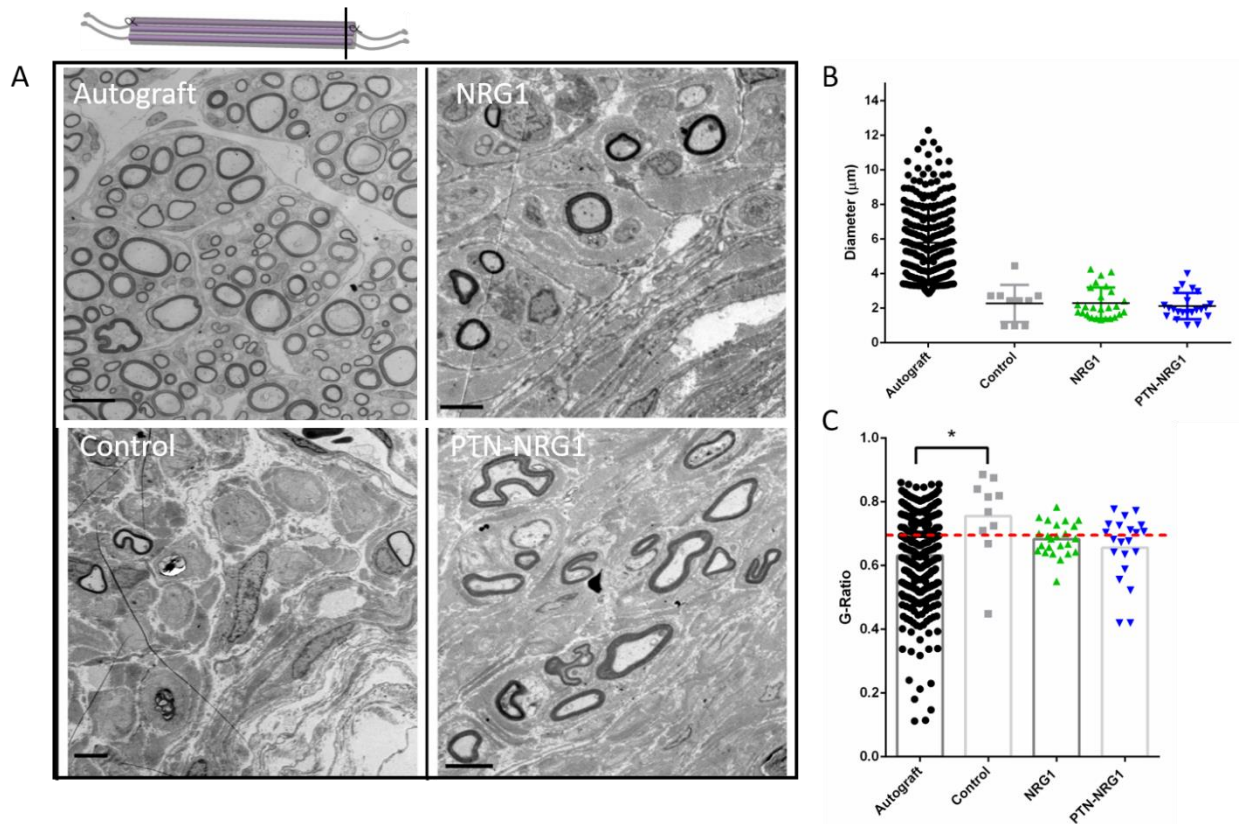


Figure 3.5. Ultrastructural analysis of the distal end of the regenerated tissue. A) Electron micrographs of areas of myelination seen in the different treatment groups. B) Diameter of myelinated axons C) Analysis of g-ratios for myelinated axons observed in the different groups. Scale bar: A) All images; 5μm. \*= $p < 0.05$

We then evaluated the unmyelinated axons to determine the diameter and stage of sorting that these axons were in. Diameter quantification indicated that the control group the NRG1 only and PTN-NRG1 group had similar number of axons larger than 1 μm, with the autograft group with the lowest number (Figure 3.6 B). We then quantified how many of these axons were within bundles, and compared only those bundles that consisted of more than 14 axons, indicating an abnormal state[171] The control group consisted of large number of abnormal bundles with an average of 21 axons/bundle (Figure 3.6 C). The NRG1 type-III group and autograft group had an average of 15 axons/bundle with the lowest in the PTN-NRG1 Type III group (12 axons/bundle).

This suggested that while most of the large unmyelinated axons in the control group were arrested within bundles, those in the growth factor and autograft groups were sorted out of the bundles. Since all these axons were still unmyelinated, it is possible they are further along in the radial sorting phase as compared to the control group. This is analogous with developmental radial sorting where axons crossing the 1 $\mu$ m threshold get sorted out by individual, pro-myelinating Schwann cells, and then myelinated[127]. These results indicate that addition of neuregulin may be contributing to axonal sorting, further advancing separation of large axons, and subsequent target pathfinding[172].

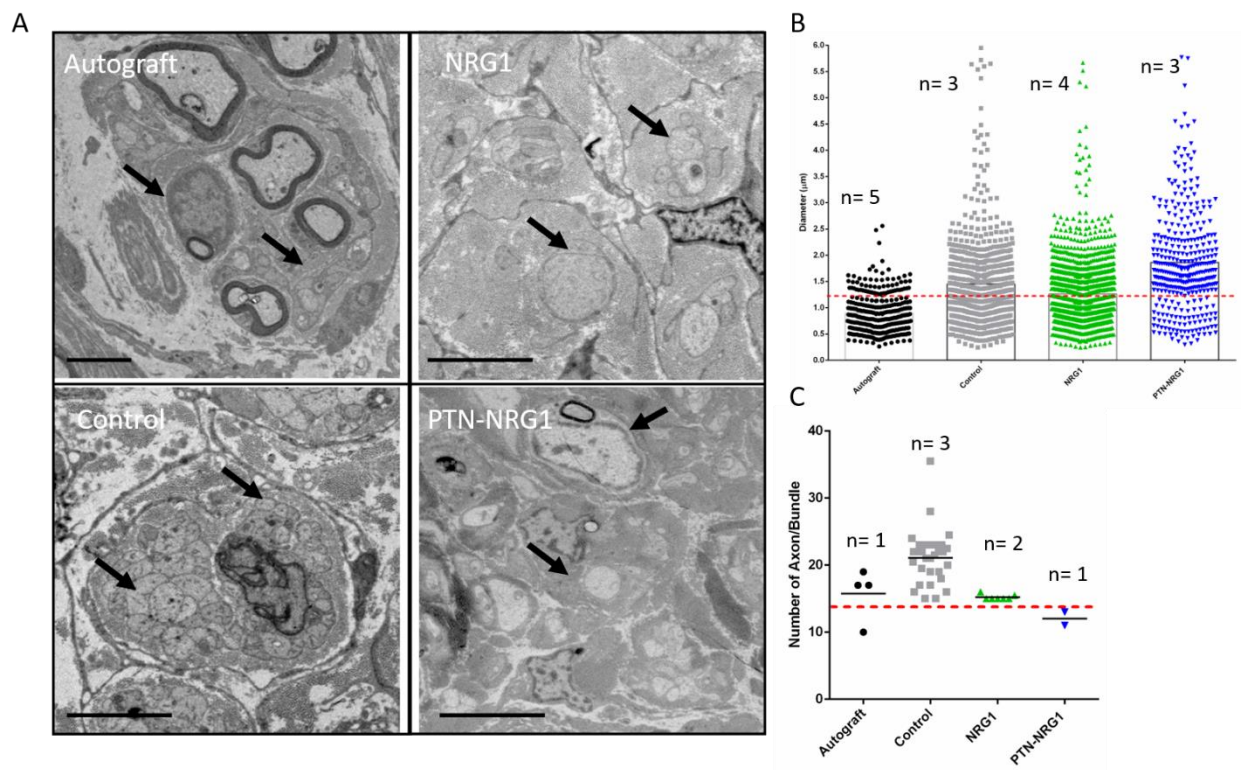


Figure 3.6. Analysis of Unmyelinated axons. A) Electron micrographs showing the axon distribution within bundles across the groups. B) Quantification of the number of unmyelinated axons present in the distal end of the regenerated nerves. C) Axon bundles consisting of more than 14 axons were compared between the groups. Scale Bar: A) All images; 5 $\mu$ m.

### 3.3.3 NRG1 Type-III induces evoked muscle response at low thresholds, and higher force recruitment

To evaluate conduction properties of the regenerated nerves, the proximal side of the injured nerve was stimulated using hook electrodes, while recording action potentials from the distal stump and the tibialis anterior muscle, and force recruited by the muscle using a force transducer. We observed that while the autograft repaired nerves had higher evoked responses, the NRG1 Type-III group had the lowest thresholds of activation close to that of the autografts (between 800 $\mu$ V-1200 $\mu$ V, Figure 3.7 A). At threshold of activation, the NRG1 Type-III group had greater average amplitude of 140.3 $\pm$ 89.5  $\mu$ V, as compared to that of the control group (84.7  $\mu$ V), and the PTN-NRG1 group (134.2 $\pm$ 84.9 $\mu$ V, Figure 3.7 B-D). Although these values were lower than those of the autograft (501 $\pm$  433.9  $\mu$ V), it suggests that the axons were correctly guided to the target muscle, re-innervating it.

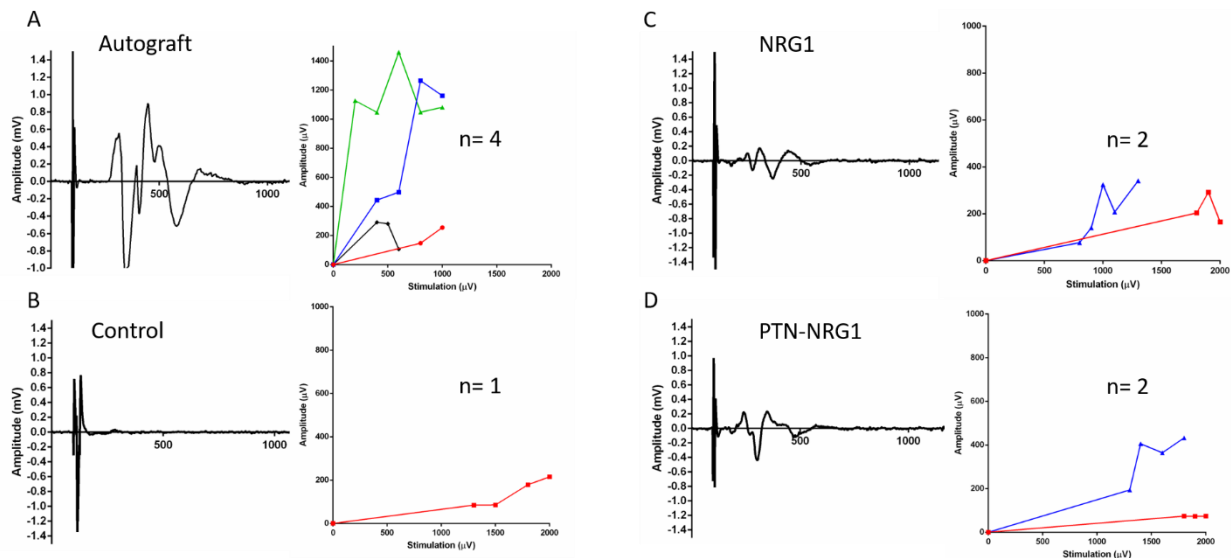


Figure 3.7. Compound nerve action potentials. Representative waveforms and respective group data for compound nerve action potential amplitudes at different stimulation intensities. A) Autografts ,B) Control C) NRG1 Type-III and D) PTN-NRG1 Type III

For compound muscle activation, similar trend was observed with greater force recruited at lower thresholds for the growth factor treated groups (Figure 3.8). The autograft group had the highest maximum amplitude (962  $\mu$ V), followed by the PTN-NRG1 group (353  $\mu$ V) and NRG1 group (108.72  $\mu$ V), and was lowest in the control group (37  $\mu$ V, Figure 3.8). Similarly, the maximum muscle force recruited was highest in the autograft (0.5V) followed by the NRG1(0.13V) PTN-NRG1(0.1V) and the lowest in the control group (0.04V, Figure 3.8).

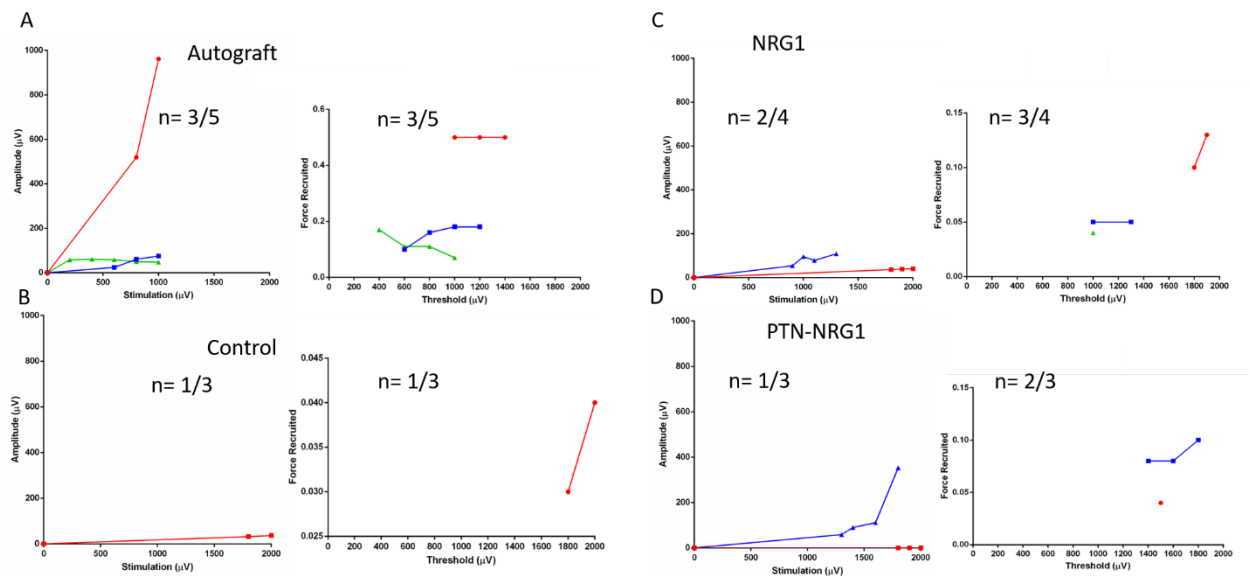


Figure 3.8. Compound muscle action potentials. Respective group data for compound muscle action potential amplitudes at different stimulation intensities and the corresponding motor force recruited for A) Autografts ,B) Control C) NRG1 Type-III and D) PTN-NRG1 Type III.

### 3.3.4 Neuregulin1 Type-III provides axon regeneration across 4cm nerve gap

In addition to EM analysis, the proximal and distal sections of the nerves were labelled with  $\beta$ -III tubulin, to quantify the number of axons regenerated across the 4cm bridge. In the proximal segment, sections were taken from the first 2cm length of nerve tissue that had grown into the BNI conduit. As expected, the autograft sections consisted of the maximum number of axons ( $2907 \pm 1057$ , Figure 3.9 A, B). The BNI group with NRG1 Type-III consisted of more axons

(1701±1182) as compared to those in the control (670 ±78) or PTN-NRG1 group (1120.600±1964.827), however, due to internal variability, there was no significant difference within these groups. These results indicate that whether growing across an autograft or a multi-luminal nerve conduit, axons can grow to distances up to 2cm, regardless of the treatment type. As these axons progress towards the distal end, this number reduces, based on the treatment type. While the autograft has significantly greater number of axons( $p<0.0001$ ), the NRG1 Type-III group had slightly more axons (1395.250±1077.187), as compared to the control (656.800±689.360) or the PTN-NRG1 Type-III (744.3333±908.7784, Figure 3.9 A, C). The loss in number of axons between the proximal and distal end can be attributed to reduced regenerative potential as compared to autografts, possibly due to a smaller number of Schwann cells or neurotrophic support. However, greater number in the NRG1 Type-III group may indicate added neurotrophic support for axons to grow across critical gaps, correctly guiding them to the distal end. It would be interesting to investigate whether providing higher concentrations of NRG1 Type-III, will further enhance this effect.

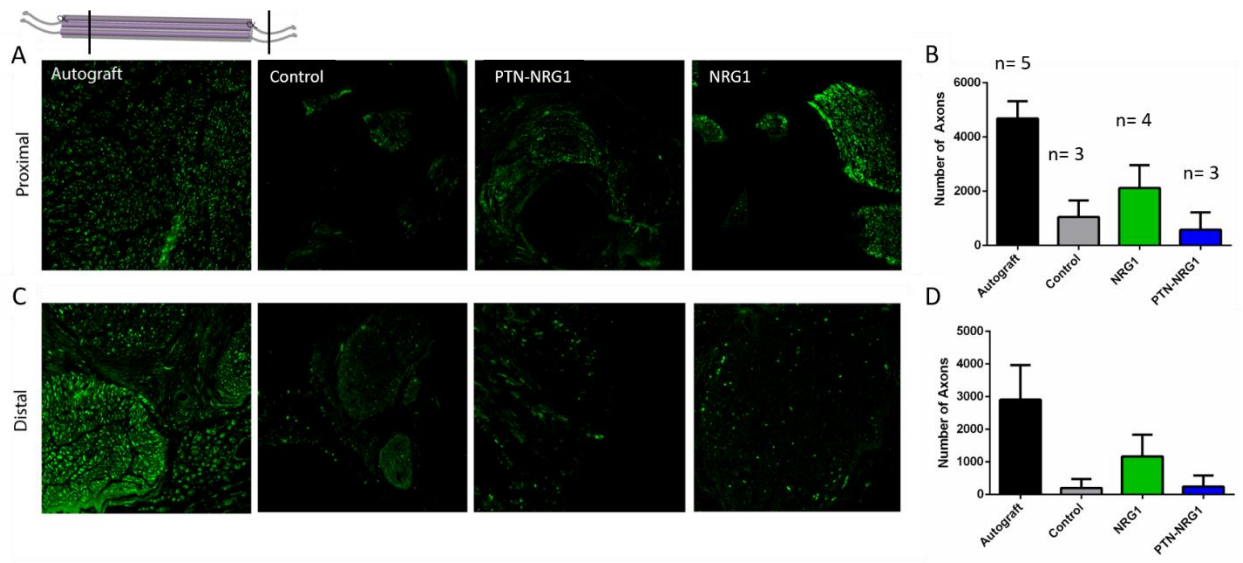


Figure 3.9. Immuno-histological labelling for axons. Images labelled for  $\beta$ -III tubulin showing axons in the proximal(A) and distal segments (C) of the regenerated nerve. Quantification of the number of axons in the B) Proximal and D) Distal segments using an automated software.

### 3.3.5 NRG1 Type-III moderately rescues muscle atrophy

To evaluate the degree of re-innervation gained through regeneration, we measured the wet muscle mass of the tibialis anterior muscle explanted after perfusion. As compared to healthy muscles ( $10588.890 \pm 974.6386 \text{ mg}$ ), all groups had a significant loss of muscle mass ( $p < 0.0001$ ), indicating atrophy due to long term denervation (Figure 3.7 A). Although the autograft group ( $6537.606 \pm 1479.026 \text{ mg}$ ) was higher than the other BNI conduit groups, there was no statistical significance due to variability within that subset (Figure 3.7 B). Within the BNI groups, muscle mass was similar, with control ( $5458.808 \pm 525.6611 \text{ mg}$ ), PTN-NRG ( $5194.474 \pm 735.6979 \text{ mg}$ ) and NRG1 Type-III ( $5536.232 \pm 893.4038 \text{ mg}$ ). We further quantified the area of the muscle fibers from images taken for the neuromuscular junctions (Figure 3.7 C). The autograft groups had the largest area of muscle fibers ( $1364 \pm 796.0 \mu\text{m}^2$ ), indicating robust re-innervation, as compared to the conduit groups (Figure 3.7 D). While similar in number, the NRG1 Type-III ( $465.2 \pm 183.2 \mu\text{m}^2$ ),

and the Control ( $461.4 \pm 166.5 \mu\text{m}^2$ ) groups had slightly higher fiber areas as compared to the PTN-NRG1 group ( $399.2 \pm 121.8 \mu\text{m}^2$ ). This indicates that despite the presence of large number of myelinated axons, and conduction of motor action potentials, muscle atrophy substantially affects reinnervation. Although not statistically significant, NRG1 Type-III does increase muscle mass and muscle fiber area to some extent, suggesting that it might be accelerating re-innervation. This agrees with the lower activation thresholds and higher muscle force recruited, as well as faster conduction, demonstrating a modest neurotrophic effect of NRG1 Type-III. This indicates that although the control group had detectable number of myelinated and unmyelinated axons, there wasn't enough reinnervation to improve function.



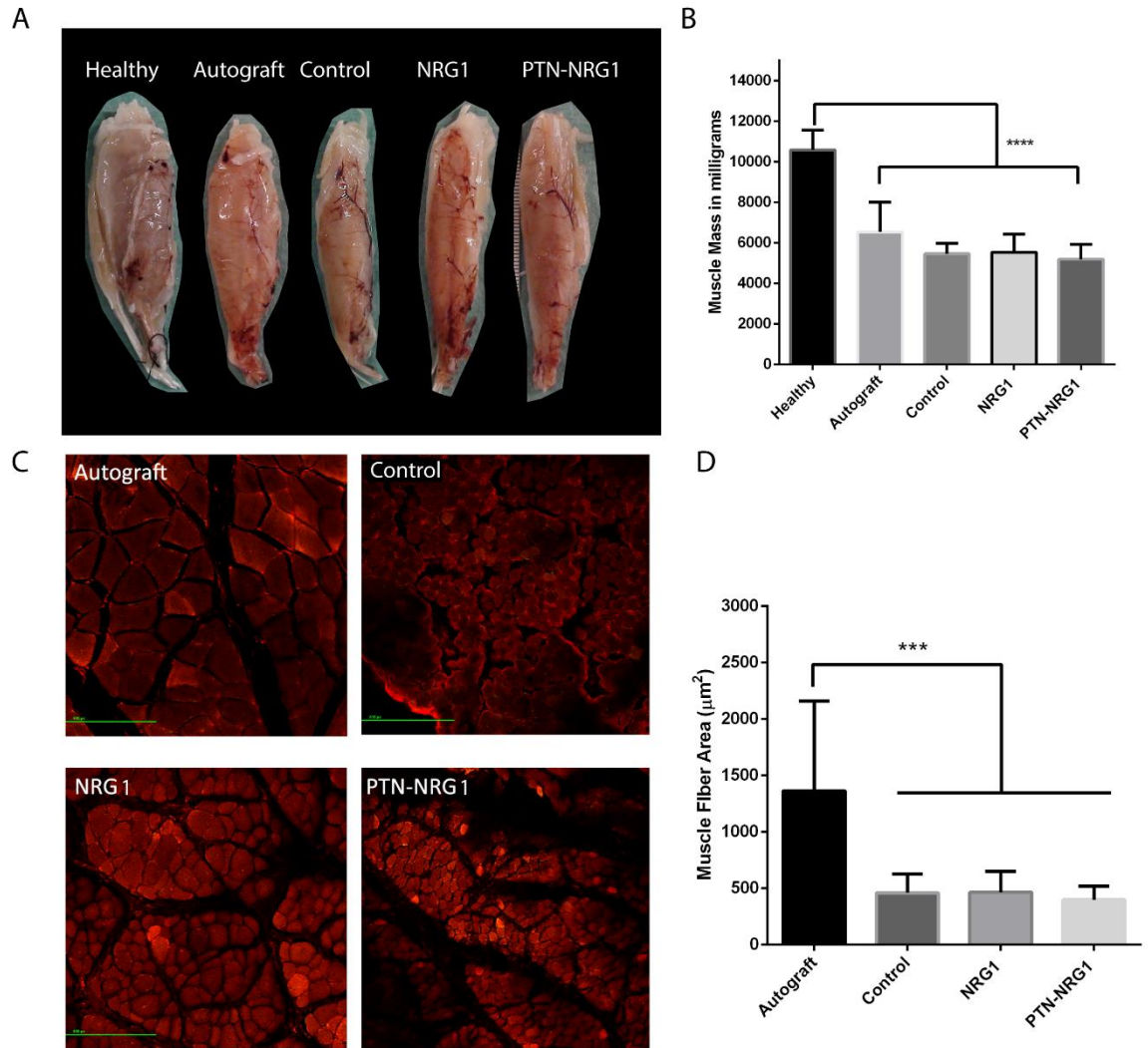


Figure 3.10. Muscle Tissue analysis. A) Gross tissue images of the *Tibialis Anterior* muscles obtained after perfusion, and B) wet weight of these muscles in milligrams. C) Representative images of cross sections of muscle tissue, demonstrating the striking difference between the muscle fibers that is quantified in D. \*\*\*\* $p < 0.0001$

### 3.3.6 NRG1 Type-III promotes early, sustained functional recovery

Over the 28 weeks, toe-spread index was obtained by measuring the distance between the first and the last toe, as seen by the startle response in the rabbits. At five weeks post-injury, all animals had functional deficits as compared to baseline, although some animals in the autograft exhibited signs

of recovery. At the end of 28 weeks, the autograft group had an average TSI of  $0.8066 \pm 0.06$ , significantly higher than that of the control and PTN-NRG1 group ( $p < 0.001$ ). Interestingly, the NRG1 Type-III only group had more animals showing functional recovery with an average TSI of  $0.75 \pm 0.05$  as compared to only two from the PTN-NRG1 group ( $0.642 \pm 0.04$ ). Surprisingly, despite the presence of myelinated axons seen in this group, none of the animals with the control group showed substantial recovery, with a mean TSI of  $0.4936 \pm 0.05$ , lower than the NRG1 Type-III group. However, muscle fiber area of this group was close to that of the NRG1 Type-III group, and higher than that of the combination. It is possible that due to abnormal pathfinding, these axons may have a delayed growth and re-innervation, and would restore function at later stages. There were no significant differences between the autograft and NRG1 Type-III group. These results highlight the significance of targeted reinnervation in addition to axonal regeneration at the injury site, indicating that albeit moderate, effect of NRG1 Type-III in proliferation and migration of Schwann cells may have contributed to the superior functional recovery. Additional sensory assessment techniques and neuro-muscular markers may provide insight into the mechanisms of this effect.

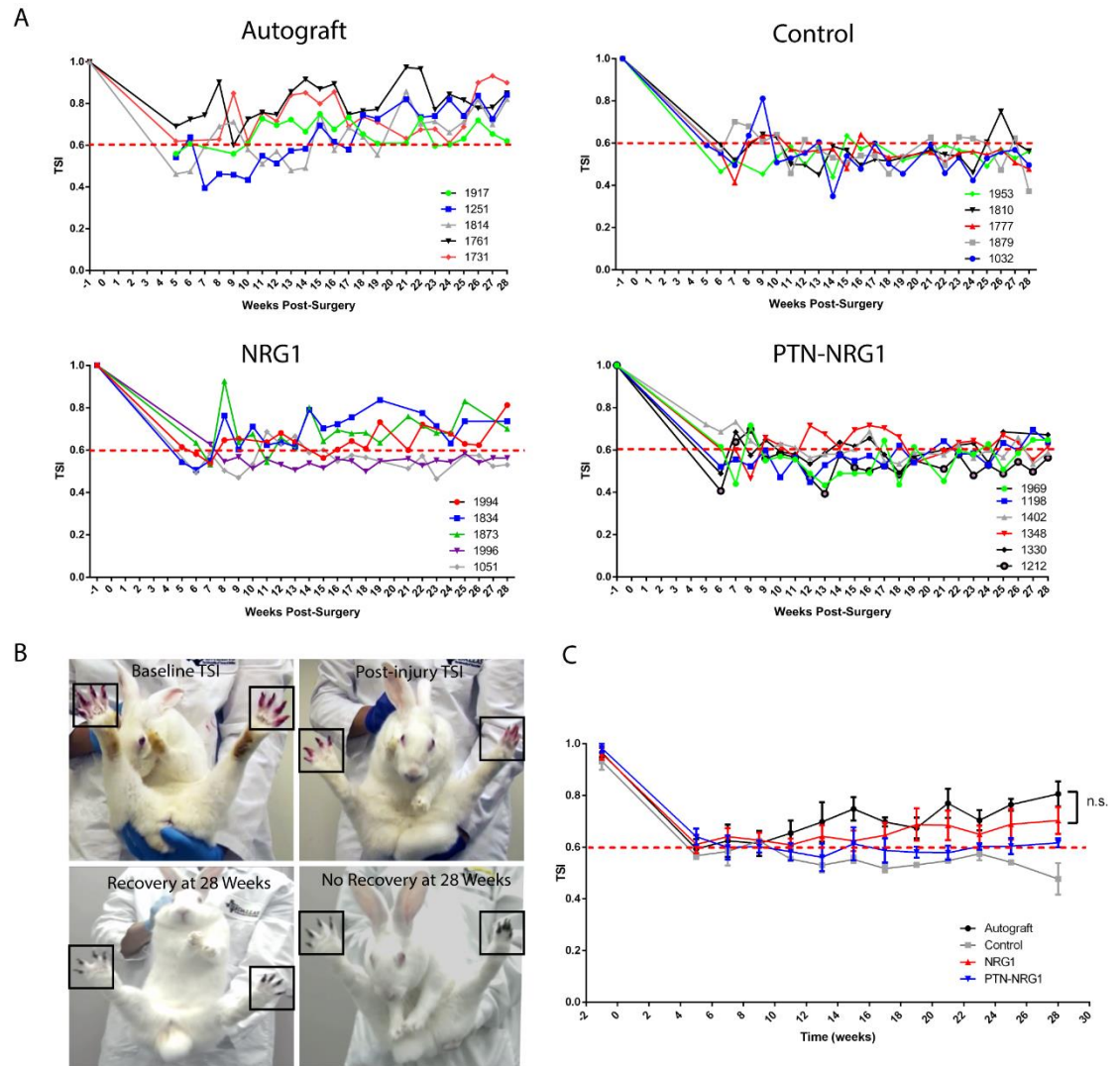


Figure 3.11. NRG1 Type-III provides moderate functional recovery. A) Toe-Spread Index (TSI) for the different groups over the period of twenty eight weeks, demonstrating animals that crossed the recovery threshold of 0.6 TSI, indicated by dotted red line. B) Representative images of the method of measuring TSI, and examples of baseline, injury, recovery and no recovery toe-spread. C) Comparison of all groups throughout the study using 2 way ANOVA with Tukeys multiple comparison test, \*\*\* $p < 0.001$ , \* $p < 0.05$ .

### 3.4 Discussion

Evidence of neurotrophic factors like BDNF, GDNF, NGF, expressed during development and after injury makes them ideal candidates for use in nerve conduits to facilitate regeneration[107], [109], [173], [174]. We and others have shown the efficacy of growth factor loaded multi-luminal

nerve guide conduits in repairing short transection injuries[122], [134], [175]. However, in our previous work we observed that while growth factor does entice growth of axons across critical gaps, lack of myelination severely affects motor conduction and functional recovery. Neuregulin 1 Type-III, an axonal derived neuregulin, has been implicated in myelination via proliferation and differentiation of Schwann cells[176], [177]. Levels of NRG1 Type-III, secreted as a function of axon diameter, directs Schwann cells to ensheath the axon, determining its fate as unmyelinated or myelinated[127], [178], [179]. We hypothesized that NRG1 Type-III enriched BNI conduits will direct radial sorting of axons, furthering re-myelination and providing functional recovery comparable to that by the autologous nerve graft, across a 4cm peroneal gap. We also combined NRG1 Type-III with PTN to investigate whether addition of PTN provided an additional neurotrophic effect, augmenting function. Induced Neurite outgrowth from dorsal root ganglia explants was enhanced by the presence of NRG1 Type-III and markedly increased by addition of PTN. Our results suggested that while NRG1 Type-III enticed longer axons, addition of trophic factors like PTN induces further growth, in a possible combinatorial effect. However, despite being implicated in axon regeneration, PTN did not provide an additional effect *in vivo*. Gross anatomical analysis suggested that the Biosynthetic Nerve Implant may be supporting nerve growth by itself, as seen from the robust tissue growing in the no growth factor group. However, all BNI groups had some subjects that failed to show any regeneration at all, which can be a consequence of the manual fabrication of these conduits. In the future, this can be circumvented by automated 3-D fabrication techniques like printing or molding, that provide precise control over geometry as well as loading of biological components like cells and growth factors[180], [181]. To examine whether NRG1 Type III promotes radial sorting and subsequent myelination, we performed TEM

analysis. Surprisingly, NRG1 Type-III alone enticed comparably greater number of large unmyelinated axons, which appeared to be sorted out from axon bundles and associated with individual Schwann cells.

Electrophysiological analysis revealed that conduction strength along the axons in the NRG1 Type-III group was faster and greater in amplitude, with greater muscle recruitment as compared to the NRG1-PTN combination as well as the non-growth factor group. At threshold of activation, the NRG1 Type-III group had greater average amplitude of  $140.3 \pm 89.5 \mu\text{V}$ , as compared to that of the control microsphere group ( $84.680 \mu\text{V}$ ), and the PTN-NRG1 group ( $134.155 \pm 84.84573 \mu\text{V}$ ). A similar effect was observed after a transection injury in rats, where NRG1 accelerated Schwann cell proliferation and migration to the distal stump of the nerve, via the ErbB2/3- FAK pathway, guiding axons to the appropriate target muscle, improving conduction[156].

On the contrary, muscle mass and fiber area for the growth factor groups were significantly lower than that of the autografts, with weaker neuromuscular junction formation (Figure 3.9). Due to long term denervation resulting in significant atrophy, it is possible that despite the axons reaching the right target muscle, the muscle fibers were too weak to restore neuromuscular connections. However, this did not affect the significant functional recovery observed in NRG1 Type-III, suggesting that more experiments may be needed to investigate its function in muscle re-innervation. A recent study demonstrated that treatment with NRG1 isoforms  $\alpha$  and  $\beta$  downregulate atrophy proteins atrogen and FoxO3, rescuing atrophic conditions *in vitro*[182]. It will be interesting to investigate whether the exogenous application of NRG1 Type-III to injured

nerves affects expression of other NRG1 isoforms in the muscle, as a mechanism to rescue atrophy in long term denervated muscles.

Despite these mixed results, the functional recovery in the NRG1 Type-III group was the most significant, almost comparable to the autograft. It can be observed from Figure 3.9, that while the autograft group begins to recover at the earliest time point, the NRG1 Type-III soon follows, with comparable recovery by week 28. Conversely, most of the animals in the control group remained at an average low throughout the recovery period, while only one animal in the PTN-NRG1 Type-III shows recovery by the last week. Although similar effects in the myelination and electrophysiology, it is possible that axons enticed by NRG1 Type-III alone were directed to the target muscle, and innervated the dorsal dermatome of the rabbit foot, resulting in the improved toe-spread. In future experiments, histological labelling of this tissue will provide additional insight into how re-innervation is modulated at the neuro-muscular junction, and whether there are differential effects on sensory versus motor recovery.

Here we propose a pathway by which exogenously applied NRG1 Type-III binds to Schwann cells, triggering a release of neurotrophic factors from the cells (Figure 3.11). The traditional mechanism of axo-glial signaling between the axons and Schwann cells, first demonstrated by Esper and Loeb in 2004 (Figure 3.11 A), where neurotrophic factors secreted by SC binds to respective receptors on the developing axons, which further phosphorylates and cleaves the membrane bound NRG1 Type-III via the activation of protein kinase C $\delta$ [183][184]. Here we propose the opposite (Figure 3.11 B), wherein exogenously applied NRG1 Type-III acts in two ways; 1) It binds to the ErbB2/3 receptors, and via activation of Akt, FAK and Erk, promotes survival, migration, proliferation and differentiation of SC. 2) This also activates secretion of

neurotrophic factors from the SC which then bind to the nearest axon, further activating growth and survival of those axons and via PKC $\delta$ , increases expression of membrane bound NRG1 Type-III.

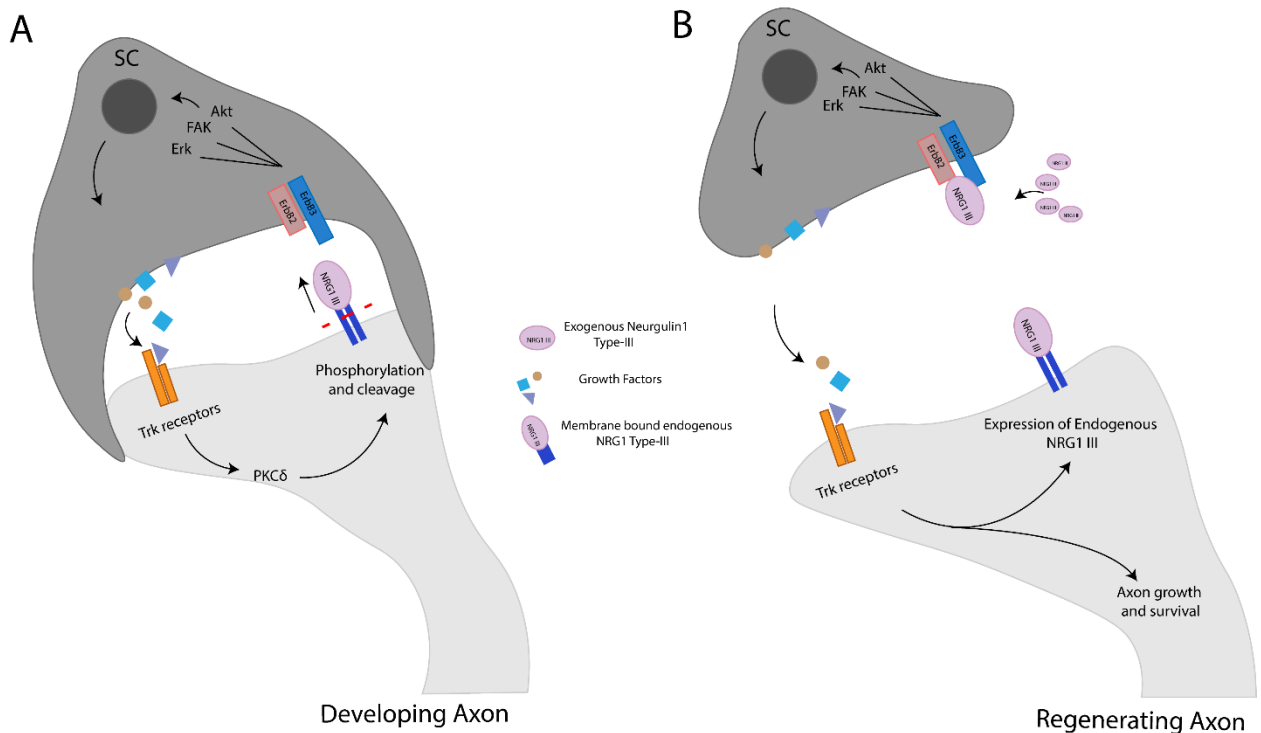


Figure 3.12. Proposed pathway of neurotrophic effect of NRG1 Type-III

Western blot analysis of injured nerves repaired using NRG1 enriched BNI conduits, at different time points will provide quantitative confirmation of this proposed pathway. Overall, these results suggest a neurotrophic role for NRG1 Type-III, and possibly other isoforms of neuregulin that may play interchanging roles in long gap regeneration.

## CHAPTER 4

### EXTENDING THE MAXIMUM CRITICAL NERVE GAP IN THE RAT SCIATIC NERVE MODEL USING CURVED CONDUITS

#### 4.1 Introduction

Although the peripheral nervous system has a robust regenerative capacity, injuries that result in extensive tissue loss ( $\geq 3$  cm), require surgical repair to bridge the long gap defect. Autografts remain the clinical “gold standard” for surgical repair of long gap nerve injuries, albeit, with limited success, as sensory and motor deficits persist in 17% of patients [185], and the co-morbid formation of painful neuromas at the donor site [1], [186]. The Food and Drug Administration (FDA) has approved biosynthetic conduits to repair nerve gap defects, which are hollow tubes and only used to repair short ( $< 2$  cm) nerve defects. However, the regenerative capacity of the hollow conduits is limited and likely due to the lack of luminal structural and biological support, [187]. These limitations continue to motivate further research on alternative repair methods including allografts and nerve guides[187]. Yet, despite the availability of polymer nerve guides and allografts, about 78.9% of critical nerve injuries are repaired using autografts [188].

Nerve repair involves complex multicellular and molecular mechanisms which if delayed or altered, also contribute to poor functional recovery [170], [189]. After axonal injury, the cell bodies in the dorsal root ganglia (DRG) and the ventral spinal cord up-regulate the expression of regeneration associated genes (RAGs) such as cJUN, GAP-43 and Cap-23 [190]. These genes, in turn, upregulate proteins that mediate axon cone growth. The direction of axon extension is guided by topographical cues and growth factors secreted by Schwann cells. Many groups have investigated the effects of exogenous as well as genetically expressed growth factors on long gap



regeneration. Our group recently tested the synergistic effect of GDNF and pleiotrophin in repairing a 4cm peroneal nerve gap in a rabbit model[134]. Although our results showed successful regeneration across the bridge, it was insufficient to translate into complete functional recovery due to lack of re-myelination. It has also been shown that long gap regeneration across acellular nerve allografts fails because Schwann cells present in the regenerating microenvironment become senescent before axonal contact, resulting in failed re-myelination. Furthermore, these regenerated axons need to reach their target muscles and reinnervate the end plates, which often fails due to muscle atrophy and insufficient acetylcholine receptors[157].

Although the mechanisms of development and regeneration of peripheral axons are well characterized, the events of repair and recovery after severe long gap injuries are still poorly understood, making it difficult to translate into successful therapeutic strategies.

#### **4.1.1 The rat as a model in peripheral nerve regeneration**

The laboratory rat model has been well established and is typically the first model for *in vivo* testing. It is well characterized for nerve transection injury and assessment[191]. A PubMed search for “peripheral nerve repair”, as of March 5, 2019 indicates a total of 8385 articles that have been published on peripheral nerve regeneration in the last three decades, of which 5603 were listed as rat models. A detailed literature review in 2012 noted that of the total long gap nerve repair studies, 74% were published for the rat model, all of them investigating gaps  $\leq 2$ cm (Figure 4.1A)[191]. This also highlights the emphasis on using the rat as a model for understanding the regenerative profile of peripheral nerves, primarily due to standardized techniques available for rat, and lacking in most other pre-clinical models (Figure 4.1B).

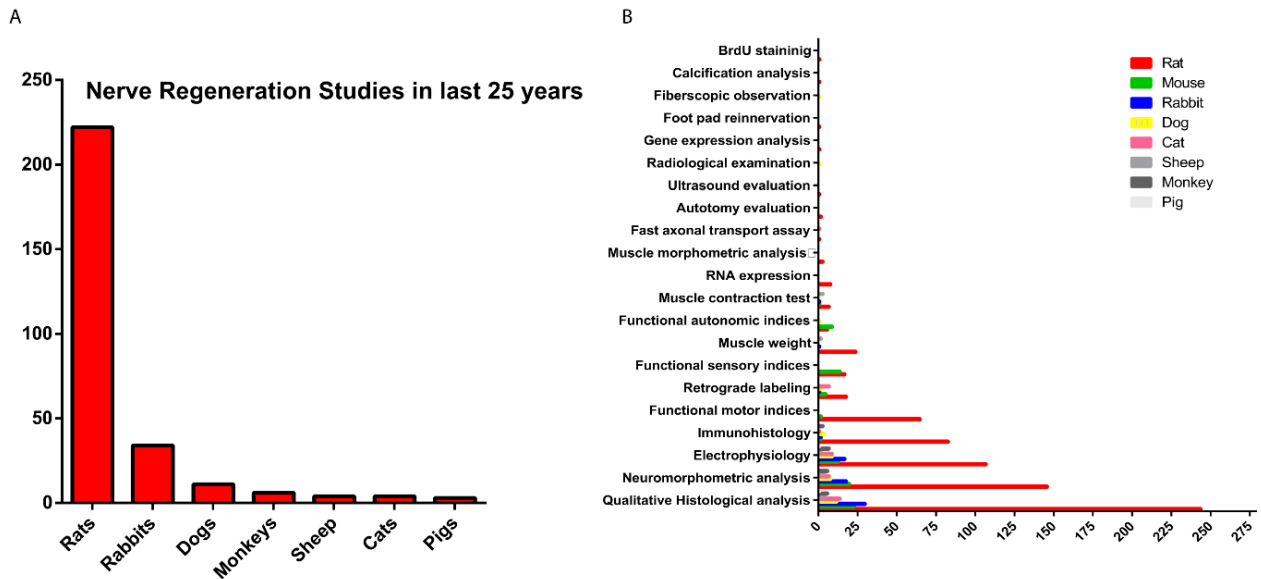


Figure 4.1. Emphasis on the use of the rat as a model for nerve regeneration. A) Number of published experiments utilizing different animal models B) Molecular and physiological techniques available to examine nerve regeneration in different animal models. Data obtained from PubMed search and [191].

The following table provides a list of the assessment tools most commonly used in rat models, and are well standardized, that inform about important aspects of motor and sensory axon regeneration, providing critical clues to intrinsic mechanisms of injury and repair.

Table 4.1. Assessment tests established in the Rat model that provide thorough understanding of the regenerative profile of nerves. Table adapted from [15]

Assessment	Type of Modality	Regenerative Outcome
Pinch Test	Sensory	Distance and Rate of Regeneration
Retrograde Tracing	Sensory, Motor, Autonomic	Number of Neurons, Specific Distance
Pin-prick test, foot flick test	Sensory	Skin re-innervation
Toe-Spread Index	Motor	Muscle re-innervation

Nerve Conduction	Sensory, Motor	Re-innervation
Motor Unit Number, Muscle tension, Muscle weight	Motor	Muscle force recovery, muscle reinnervation
Algesimetry	Sensory	Mechanical, Thermal Nociception
Silicone mould test	Sympathetic	Re-innervation of sweat glands
Grasp/Pull Force test	Motor	Grasp strength
Gait and Kinematic analysis, Sciatic Index	Motor, Sensory	Foot placing, pattern during locomotion
EMG	Motor	Muscle activation
Staircase test	Sensory-motor	Forelimb dexterity
Evoked potentials	Sensory-motor	Central pathway changes

#### 4.1.2 Topographical cues promote nerve regeneration

Topographical cues like micropatterns, filaments and microgrooves alter cell shape by providing a physical substrate for cellular filaments to progress. It has been shown that when neurites of growing axons extend forward, topographical cues promote this progression of cells via transient activation of the mTORC2 pathway, and have the ability to override inhibitory stimuli *in vitro*[192]. It has also been shown that aligned poly-caprolactone fibers guide Schwann cell to elongate and migrate as well as upregulate myelin associated proteins[193]. Three dimensional polycaprolactone fibers produced by electrospinning have shown excellent neurite outgrowth by

changing cell morphology and extending longer processes and inducing migration of Schwann cells[80].

Here, we designed 3-D printed S-shaped conduits, to provide topological support to growing axons as well as provides a longer regeneration length within a smaller linear space. We show that this model allows successful regeneration of the sciatic nerve, comparable to that of a conventional straight hollow conduit, while providing a clinically relevant injury model.

## **4.2 Materials And Methods**

### **4.2.1 Design and Manufacturing of 3D Printed S-Shaped Conduits**

The digital models for linear and S-shaped nerve guidance conduits were designed using a computer-aided design software Onshape (Figure 4.2). The models were then sliced along the diameter of the NGC to generate a toolpath based with conduit radius which incorporated microgrooves along the S-shaped conduits and the straight conduits [181]. The conduits were fabricated using a custom micro extrusion 3D printing system as previously reported [194], [195]. Briefly, the system uses a three-axis robot (MPS75SL; Aerotech), a digital pressure regulator (Ultimus V; Nordson), a motion controller (A3200; Aerotech), and a microscope with a camera for imaging (OM99-V7; Omano) [82], [196]–[200]. The silicone (SI 595 CL, Loctite) was printed using a 10 cc syringe barrel and 27 gauge tapered tip (Nordson) using the extrusion pressure at 43 psi and printing at 1.2 mm/s. The total build time of S-shaped and linear conduits were 5 min and 3.5 min, respectively. Following printing, the conduits were subsequently cured at room temperature and manually released from the glass substrate using a sterile razor blade. Before implantation, the NGCs were washed with ethanol and sterilized under UV light for 45 minutes. The printed conduits were manually sectioned along the axial direction using a razor blade to

generate 500  $\mu\text{m}$  thick slices, and brightfield micrographs were obtained (Axiozoom.V16, Zeiss), for visual confirmation of the microgrooves in the lumen of the conduits.

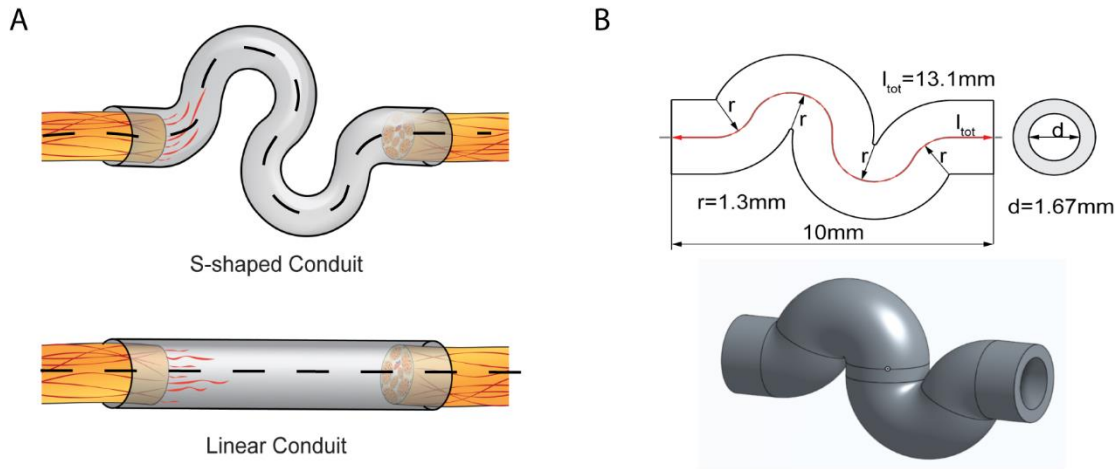


Figure 4.2. A) An S-shaped conduit provides longer regeneration length within the same linear space available in a rat model. B) Digital model of the NGC designed using Onshape software.

#### 4.2.2 Surgical Procedures

In a pilot study, we first tested the ability of nerves to regrow along a curved path. To this end, we implanted three female Lewis rats with a 5mm curved PDMS conduit (Fig. 4.3 A). Regeneration was observed across conduits at 4 weeks, showing complete crossing of the nerve from the proximal to the distal end (Fig.4.3 B). After confirming that axons can re-grow along curved paths, ten female Lewis rats ( $n=5$  per group) were implanted with either 1) straight 10mm tube or 2) S-shaped 10mm tubes, both filled with collagen solution (85 % type I, 15% type II; Millipore; Temecula, CA). The animals were anaesthetized using isoflurane (2% induction with 2% oxygen) and the surgical area was disinfected with povidone-iodine and sterilized with ethanol. An incision was made in between the semitendinosus and biceps femoris muscle. The two muscles were

retracted, and the sciatic nerve was exposed from the sciatic notch to the trifurcation point. With careful dissection, the nerve was cleared from the surrounding tissue and transected at the midpoint of the exposed length. The two ends of the nerve were each inserted in the conduits filled with collagen and then sutured with a 9-0 silk suture. The muscles were then closed with 4-0 resorbable sutures and the skin was stapled. For post-operative care, the animals received subcutaneous sustained-release buprenorphine (0.1mg/kg) and cefazolin (5mg/kg) as an intramuscular antibiotic.

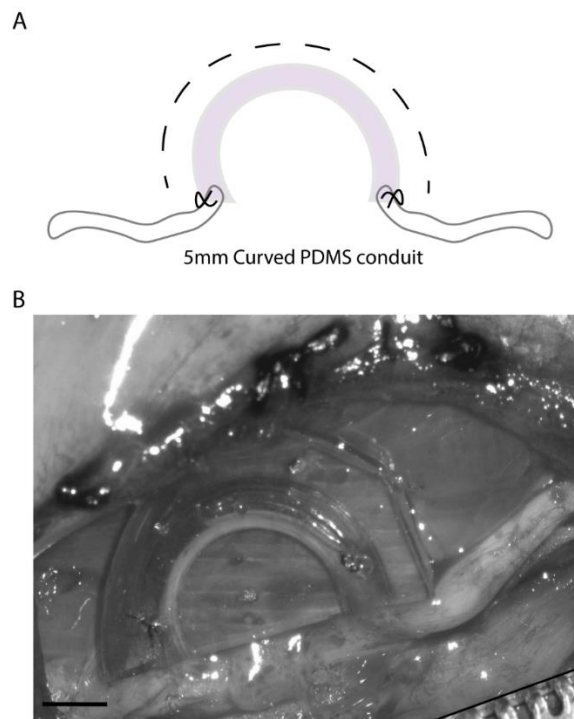


Figure 4.3. Pilot Experiment Showing regeneration of the rat sciatic nerve across a 5mm curved conduit. A) Schematic of conduit geometry and surgical images after the nerve regenerated across the gap. Scale Bar: B) 2mm.

#### 4.2.3 Walking Track Analysis

Starting at week 1 post-surgery, gait analysis was done to monitor functional recovery till the end of the study. The CleverSys® gait scan system allows recording videos as the animal walks on an

automated treadmill. Video recordings of at least one minute (or 10 steps where possible), were obtained the software can then be used to post-process the videos to calculate various gait parameters like swing time, stride length, stance time, etc. A baseline recording was done once before surgery followed by recordings every week till the end of the study.

#### **4.2.4 Terminal Electrophysiology and Tissue Harvest**

At seven weeks post-surgery the implant site was re-exposed as described and the nerve was isolated. Two pairs of hook electrodes, one each on the proximal and distal ends of the nerve was inserted to record evoked compound nerve action potentials. The proximal electrode was stimulated at 2Hz with an inter-pulse duration of 30 $\mu$ s. Threshold was calculated based on an observable motor twitch. Thresholds for the motor response observed were recorded. After electrophysiological recordings, the animals were trans-cardially perfused using 4% paraformaldehyde (PFA) and the nerve tissue obtained was post-fixed.

#### **4.2.5 Immunohistochemistry**

The harvested nerve samples were cryoprotected in 30% sucrose and then embedded in optimum cutting temperature (OCT) compound (Tissue Tek.) using dry ice. The cryo-blocks were then cut into 12 $\mu$ m thin sections and co-labeled for axons and myelination using standard immunohistochemistry techniques. Briefly, the tissue sections were washed in 1X phosphate buffered saline (PBS) and permeabilized using normal goat serum. The slides were then incubated with  $\beta$ -III tubulin; 1:400; Abcam #78078) and myelination (P0; 1:200; EMD Millipore #AB9352) overnight at 4°C. Thereafter, the slides were incubated with goat anti-Mouse 488 (1:400) and goat anti chicken 594 (1:400) at room temperature for one hour and then mounted using ImmuMount media and glass coverslips. Images were taken in a Nikon A1R Confocal microscope using a 20X

objective. The number of axons were measured using a cell counting software, CellC, version 2.5 (<http://en.bio-soft.net/draw/CellC.html>).

#### **4.2.6 Statistical Analysis**

GraphPad Prism statistical analysis software was used to perform analysis of variance (ANOVA) with repeated measures to compare the different groups for the toe-spread index (TSI). Post-hoc Tukeys tests were used for multiple comparisons. For histological analysis, unpaired Student t-test was performed to compare the two groups. A value of  $p \leq 0.05$  was considered as statistically significant.

### **4.3 Results**

#### **4.3.1 Characterization of 3D printed conduits**

The axial tool path direction for 3D printing was selected based on previous work on 3D printed nerve conduits that showed that the tool path direction achieves a resultant conduit tensile strength that matches peripheral nerve and establishes an axial topographical cue (Fig. 4.4 A)[82]. The 3D printed S-shaped conduits exhibit an internal non-linear microgroove topographical cue (Fig. 4.4B). Analysis of the microgroove depth and spacing using ImageJ software revealed the micro grooves were separated by  $156 \pm 27 \mu\text{m}$ , and had an average depth of  $17 \pm 8 \mu\text{m}$ .



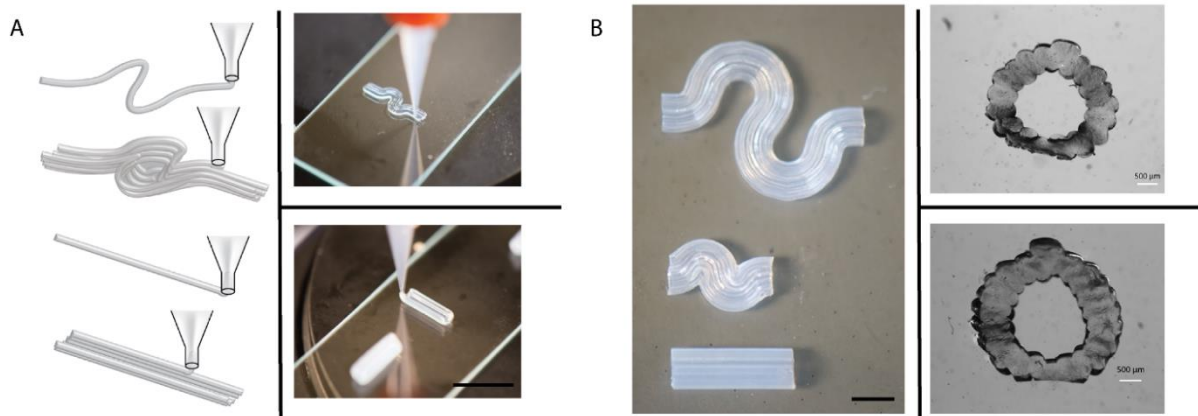


Figure 4.4. Micro-extrusion printing of the nerve guide conduits. A) Fabrication of the NGCs using a custom micro-extrusion 3-D printing system. B) Sample straight and S-shaped NGCs of varying length. Microscopic images of straight (inset, top) and S-shaped (inset, bottom) conduits showing the cross-sectional profile. The printing method results in a micro-groove profile along the conduit, thus providing topological cues for growing axons. Scale Bar: A) 10mm B) 5mm, inset;500 $\mu$ m.

#### 4.3.2 Gross Evaluation of regenerated tissue

At 7 weeks post-surgery, gross evaluation showed successful regeneration across the 10mm gap across all groups(Figure 4.5). The average regenerated length was quantified from gross tissue images using the ImageJ software and was  $11.8 \pm 0.24$ mm for the S-shaped conduits; greater in length than the straight conduits ( $9.5 \pm 0.28$ mm Figure 4.5C). The average thickness of the regenerated nerves was  $1.1 \pm 0.2$ mm for the straight tube group while the S-shaped conduit group had an average thickness of  $0.92 \pm 0.12$ mm and a Students t-test showed no statistical difference between the two groups (Figure 4.5 D).

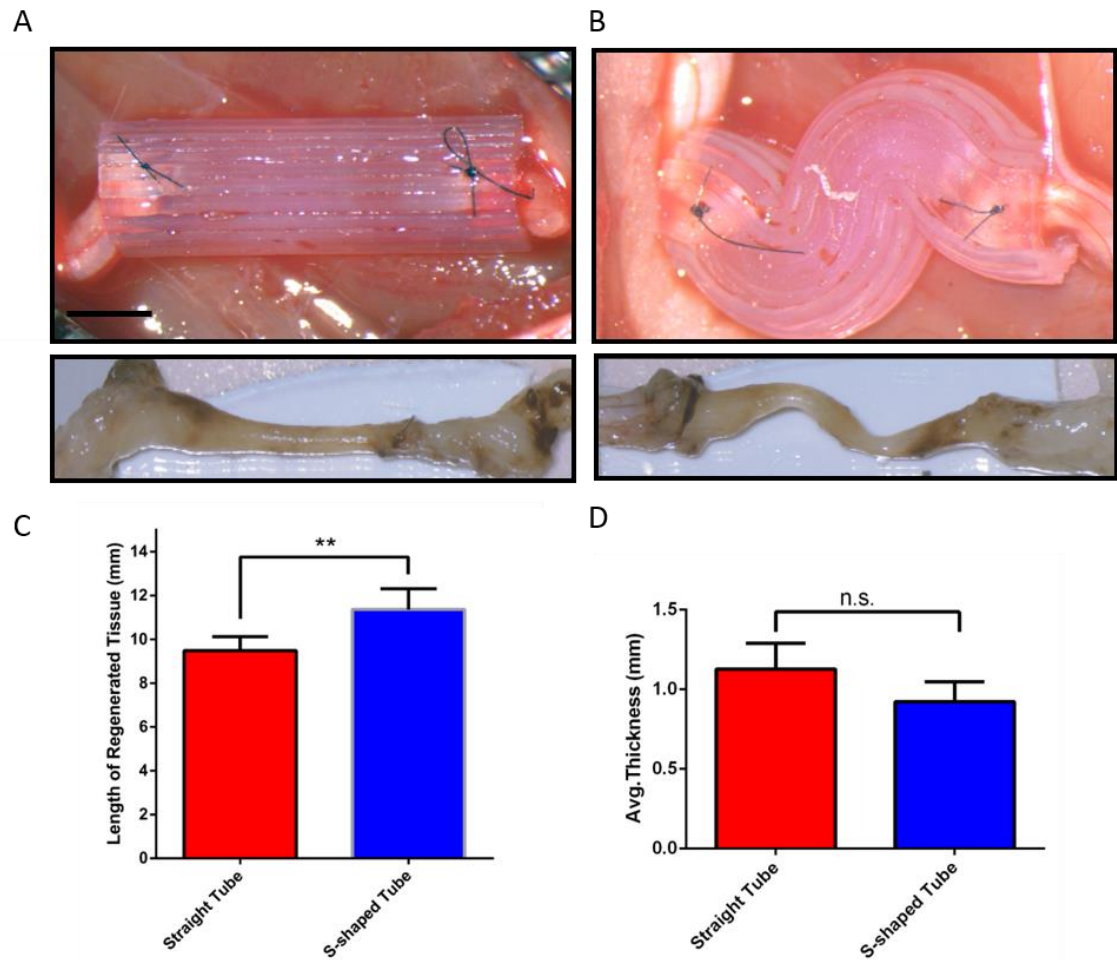


Figure 4.5. Surgical implantation and gross regenerated nerve tissue from the straight (A) and S-shaped (B) NGCs. Quantification of the length (C) and thickness (D) of the regenerated nerve tissue. Scale Bar: A) 2mm.

#### 4.3.3 Straight and S-shaped conduits provide similar functional recovery

Gait cycle parameters and toe-spread index was calculated from video analysis using the CleverSys® system. Although both groups showed a time-dependent increase in recovery, there were no differences between the two groups. Toe-spread index (TSI) was significantly higher at week 7 as compared to week 1 after injury, for both conduit groups (Fig.4.6 B). Although swing time was different at weeks 1, 5 and 7 within each group, there was no significant differences

between the two conduit groups (Fig. 4.6 C) . Furthermore, stance time (Fig. 4.6 D) and stride length (Fig. 4.6 E) showed no differences across time points or between the two conduit groups.

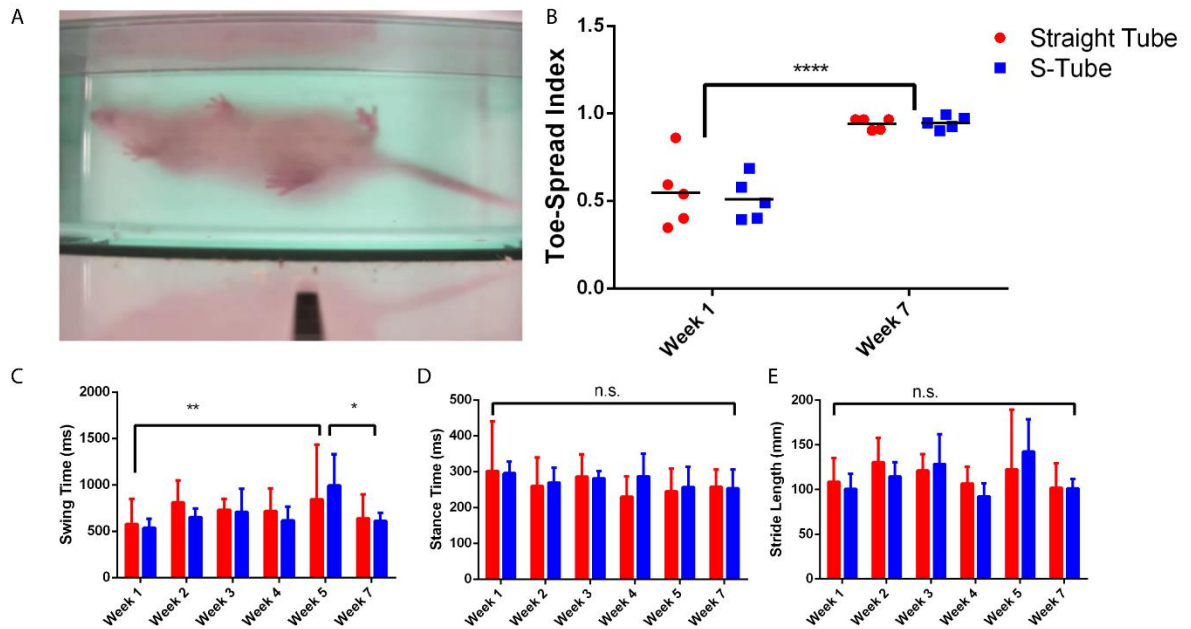


Figure 4.6. A) Toe-spread index (TSI) calculated from treadmill videos was significantly different at week 7 as compared to week 1 after injury but showed now differences between the two conduit groups. Gait analysis showed that though swing time (B) was different at weeks 1, 5 and 7 within each group, there was no significant differences between the two conduit groups. Stance time (C) and stride length (D) were not different across time of between groups.

#### 4.3.4 Shape of conduit does not affect regenerative capacity of axons

Transverse sections of the regenerated nerves were labelled with for axons ( $\beta$ -III tubulin) and myelin (P0). Axon count using an automated software showed similar number of axons in the proximal segment of the regenerated nerves. The total number of axons in the straight tube ( $4977 \pm 1260$ ), were not significantly different from the S-shaped conduits ( $3299 \pm 1219$ , Fig. 4.7 A&C). Consistently, at the distal segment, nerves regenerating through the S-shaped conduit ( $3779 \pm 335$ ) compared to those in the straight tubes ( $2889 \pm 670$ , Fig. 4.7 B&E). Furthermore, similar number

of myelinated axons were present in the proximal segment of the straight tube ( $5148 \pm 715$ ), as compared to the S-shaped conduit ( $4304 \pm 669$ , Figure 4.7 A&D). Interestingly, at the distal end, both the straight tube ( $3063 \pm 571$ ) and S-tube ( $3652 \pm 387$ ) had very similar number of myelinated axons (Fig.4.7 B&F). These findings suggest that axons can regenerate regardless of the geometric shape of the regenerating paths.

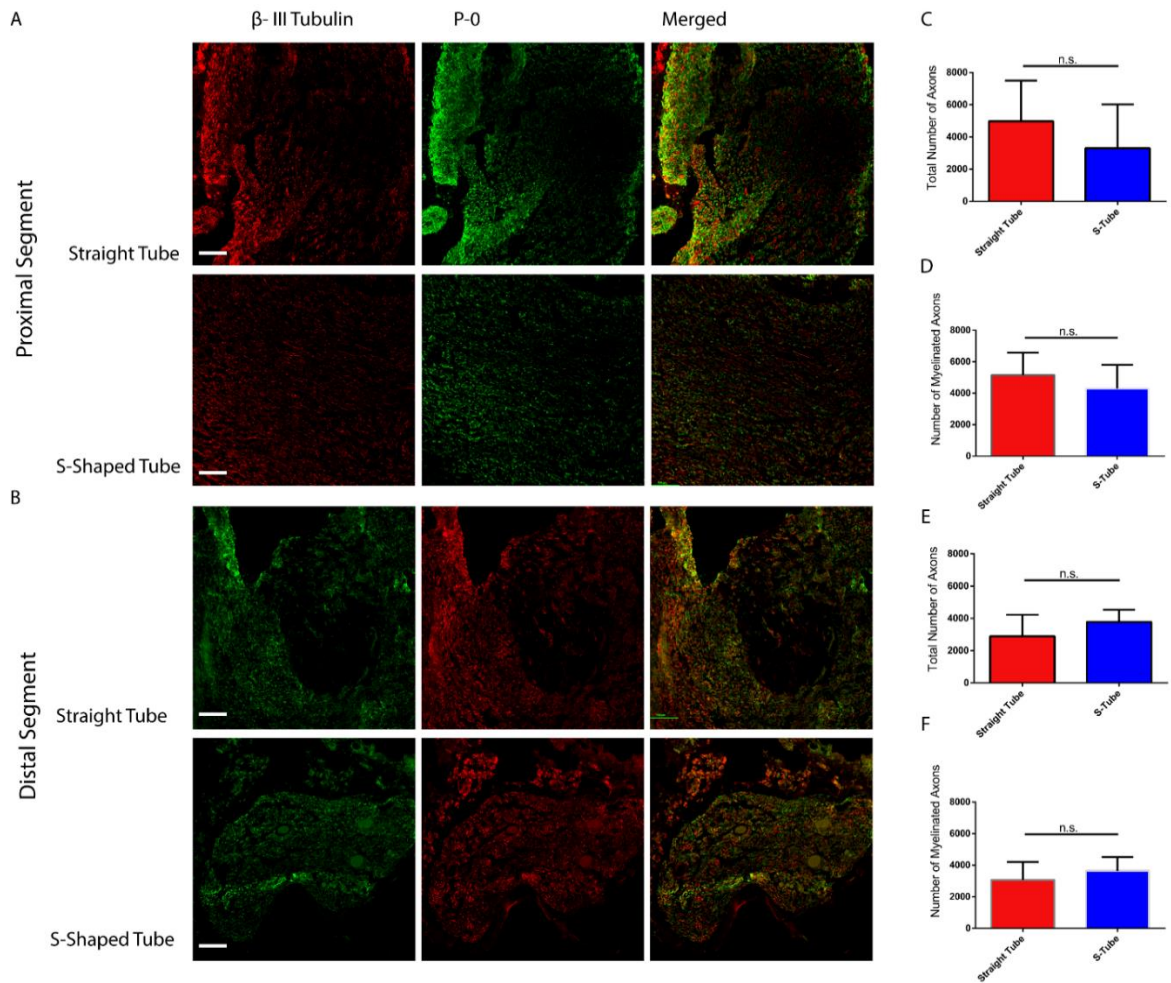


Figure 4.7. Immunohistochemistry of the regenerated nerves. Transverse sections of the A) proximal and B) distal segments of the tissue were labelled for axons ( $\beta$ -III tubulin) and myelin (P0). Quantification using a cell counting software of the C&E) total axons and D&F) myelinated axons gave no significant differences between the straight vs the S-tube groups. Scale Bar: 100 $\mu$ m.

#### 4.3.5 Electro-competency of nerve not affected by shape of conduit

In order to determine if the regenerated axons functionally reinnervated their muscle target in the hindlimb, we electrically stimulated the proximal nerve segment and measured the threshold of the evoked motor response. Stimulation of the proximal segment of the regenerated nerves elicited a motor response in all animals, at a threshold of 1mV (Fig. 4.8) The amplitude of the response peaks observed in nerve regenerated in the S-shaped conduits was  $442.8 \pm 73.5\mu\text{V}$ , which was similar to those measured in peripheral nerve regenerated through the straight conduits ( $554 \pm 165\mu\text{V}$ ).

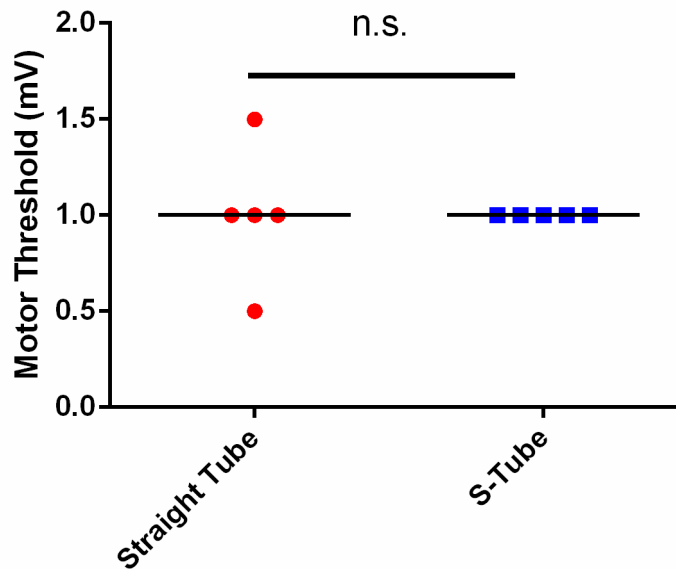


Figure 4.8. Threshold voltage values that evoked a motor response in the two groups, with an average of 1mV, with no significant differences between the two conduit groups.

#### 4.4 Discussion

The extensive use of the rat model in nerve repair experiments has been of importance in providing basic mechanisms of nerve repair. One of the main limitations of using the rat model in critical

nerve injuries has been the small size of the animal, making it difficult to model critical gap injuries that truly translate to clinical scenarios. Here we proposed using 3D printed S-shaped conduits to mimic such long gaps in the rat model, and uncover the mechanisms of delayed, long term regeneration, Schwann cell fate and secretory profile of various neurotrophic factors.

Our results indicate that the geometric path of the conduit does not affect the regenerative capacity of the axons. Interestingly, although the S-shaped conduits were longer in length than the straight tubes, at 7 weeks, both groups showed equivalent axonal growth, with similar behavioral recovery. This may indicate that the topography and shape of these conduits may be enhancing the regeneration rate, but more thorough experiments are needed to determine this effect.

In these pilot experiments, we determined that axons can in fact grow over curved paths, at the same regenerative rate. With these results, we can then extend the conduits to lengths  $\geq 3\text{cm}$  to mimic critical gaps, incorporate physical and chemical cues like growth factors and hydrogel scaffolds that will provide strategies for regeneration. The 3D printing technology provides an automated assembly of the conduits as well as internal scaffolds and growth factors [82]. One of the main advantages of this technology is the imaging derived anatomical customization of the nerve guide conduits, which has significance in clinical translation given the varying nature of such injuries.

Despite much is known about the regenerative profile of peripheral axons after injury, most of these mechanisms fail over severe, long gap nerve injuries. This can be attributed to the long term denervation, lack of adequate neurotrophic factors, senescence of existing Schwann cells and atrophy of the target muscle that profoundly affects functional recovery. Although autografts are the clinical “gold standard” and most preferred surgical repair technique, it has been shown that a

reasonable functional recovery is attainable in only about 50% of patients [185]. Decellularized nerve allografts have been an effective alternative, but clinically fall short due to senescence of Schwann cells that inhibits long distance axon growth[61]. As described in Chapter 2 and 3, we have demonstrated exceptional regeneration of axons across critical gaps promoted by growth factor enriched multi-luminal conduits [122], [134]. However, as seen from behavioral analysis, presence of axons does not directly correlate with functional recovery. Also, due to lack of standardized tests in the rabbit model, we were unable to determine the extent of sensory recovery. The 3D printed S-shaped conduits offer a promising solution, by mimicking a long gap in the rat model while exploiting the multitude of assessment techniques listed in Table 4.1[15]. Skilled motor tasks like grasp test and staircase tests provide evidence of muscle strength and coordination and forelimb dexterity. Furthermore, evoked somatosensory potentials in the rat model are critical to map central pathways, to determine structure-function-behavioral associations affected by injury that will have implications in developing new therapeutic treatments[15], [201]. Interestingly, although the axons had to grow 3mm longer in the S-shaped conduits as compared to the 10mm straight conduits within the same period, there was no difference in the number of axons or functional recovery. These findings can be attributed to the geometrical structural advantage of the S-shaped conduits, perhaps providing a topographical substrate for the axons as they grow, that is absent in the continuous straight conduits. However, this effect is yet to be tested across longer gaps, and using different geometrical structures.

Overall, we can use the model developed here, to extend the nerve gap length, explore the mechanisms of long term denervation and find key molecules that may provide potential therapeutic solutions for this formidable clinical challenge.

## CHAPTER 5

### DISSERTATION SUMMARY

#### 5.1 Introduction

Despite the robust regenerative potential of the peripheral nervous system, repairing critical nerve injuries resulting from large segment tissue loss is still challenging, and current repair techniques fail to provide complete motor and sensory recovery. During development and after injury, neurotrophic factors and pleiotropic factors dictate the fate of peripheral axons, cellular population within the nerve, and function and re-innervation of the target muscle. However, these mechanisms prove to be insufficient for critical injuries due to time required for regeneration. Nerve guide conduits that mimic the native microenvironment of the nerve and provide structural support are favorable biosynthetic alternatives.

In this dissertation, a multi-luminal Biosynthetic Nerve Implant (BNI), previously developed in our lab, was loaded with neurotrophic factors and utilized to promote axon regeneration across 4cm critical gaps. In a previous study, we had determined that the use of pleiotrophin (PTN) and glial-derived neurotrophic factor (GDNF) promoted regeneration and provided a significant improvement in functional recovery as seen from the toe-spread index, although not comparable to the cut-resuture control. In **Chapter 2**, we further analyzed electron micrographs and identified large diameter unmyelinated axons that were present in an arrested state, within Schwann cell basement membranes. These results suggested that although PTN-GDNF together enhance regeneration of axons across the 4cm bridge, abnormal sorting of large caliber axons resulted in failed remyelination. In conclusion, we proposed that exogenous



application of Neuregulin 1 may promote Schwann cell proliferation and differentiation, further influencing radial sorting, and re-myelination.

In **Chapter 3**, we hypothesized that NRG1 Type-III enriched BNI conduits will direct radial sorting of axons, furthering re-myelination and providing functional recovery comparable to that by the autologous nerve graft, across a 4cm peroneal gap. We also combined NRG1 Type-III with PTN to investigate whether it provided an additional neurotrophic effect, augmenting function. Neuregulin 1 Type-III alone provided regeneration of comparably greater number of large unmyelinated axons, which appeared to be sorted out from axon bundles and associated with individual Schwann cells. Electrophysiological analysis revealed that conduction strength along these axons was faster and greater in amplitude in the NRG1 Type-III and PTN-NRG1 group, with greater muscle recruitment as compared to the non-growth factor group. However, the NRG1 Type-III group showed the most significant functional recovery as compared to the no growth factor or the combination group. This suggests that the NRG1 Type-III may be accelerating axon pathfinding to the target muscle, improving the toe-spread index. However, the muscle fiber area indicated that the muscles in all the BNI groups were significantly lower than that of the autograft group, indicating atrophy and poor neuromuscular reconnection. It has been shown the Neuregulin1 modulates Muscle specific kinase activity (MuSK), clustering of acetylcholine receptors at the end-plate and collateral sprouting of axon terminals enhancing re-innervation [202], [203]. In future studies, treatment of denervated muscles with intramuscular NRG1 injections, in addition to nerve repair using conduits, could further improve functional outcomes. In Chapter 2 & 3, we have demonstrated the growth promoting effect of neurotrophic factors on nerve repair in a rabbit model. One of the limitations of this pre-clinical model is the lack of

standardized sensori-motor assessment techniques to fully understand extent of functional recovery, and to characterize it based on histological findings. The rat model has been overwhelmingly used over the last few decades, leading to the development of well characterized molecular and behavioral techniques. However, it has been a challenge to mimic critical injuries in the rat model due to lack of surgical space and because of mixed consensus on the exact nerve gap beyond which a rat nerve cannot regenerate, ranging between 13mm-15mm. In **Chapter 4**, we designed a 3-D printable S-shaped conduit, that offers longer regeneration length within a smaller linear space, providing a clinically translatable injury model for critical regeneration, while using the well-established assessment tools in the rat model. In a rat sciatic nerve transection model, we compared regeneration across a Straight 10mm conduit and an S-shaped 13mm conduit to confirm whether axons can grow over curved paths. Gross anatomy revealed that axons do grow over curved paths and the thickness of the tissue is comparable to that of the nerves growing in straight conduits. Behavioral data showed that gait parameters remained similar in both groups, with comparable toe-spread indices indicating shape of conduits does not attenuate functional recovery. The number of axons in the proximal and distal segments of the regenerated nerves in both groups were similar in number, with equivalent myelination. Our results suggested that while the shape of the conduit does not reduce regenerative capacity of axons, it may be enhancing the rate of regeneration. Interestingly, although the axons had to grow 3mm longer in the S-shaped conduits as compared to the 10mm straight conduits within the same period, there was no difference in the number of axons or functional recovery. These findings can be attributed to the geometrical structural advantage of the S-shaped conduits, perhaps providing a topographical substrate for the axons as they grow, that is absent in the continuous straight conduits. We can

further use this model to extend the nerve gap length and explore the mechanisms of critical gap regeneration and find key molecules that may provide potential therapeutic solutions.

## **5.2 Limitations And Future Directions**

Growth factor enriched BNI conduits promote regeneration of peripheral axons, however, the degree of functional recovery is unmatched to that of the autologous nerve graft. One limitation of the BNI conduit, is the lumen space available to growing axons. The collagen filled microchannels constitute only 38% of the conduit cross sectional area, which may contribute to substantially less axonal growth as compared to autografts. However, regeneration through hollow conduits has been shown to fail even at 3cm, suggesting the need for biodegradable internal scaffolds that can be tuned to degrade at the of axonal growth. Polymers like poly-glycolic acid or poly-lactic acid scaffolds or biodegradable hydrogels will be a favorable option for such applications. Furthermore, while PLGA microspheres provide a sustained release of growth factors within the BNI, since dissolved with collagen, their dispersion within the microchannels is difficult to control. Our lab and others have reported the effect of neurotrophic factor eluting polymeric fibers that provide uniform protein delivery and can be manipulated to create a gradient concentration that provides axons increasing growth cues[204].

Neuregulin1 Type-III has been implicated in Schwann cell proliferation and differentiation and is crucial during development as well as after injury. In our model of critical nerve repair, NRG1 Type-III was effective in enticing axons and myelination, which resulted in enhanced motor recovery and nerve conduction. However, lack of sensory testing makes it difficult to fully understand whether this effect extends to sensory recovery as well. While it is implicated in radial sorting and myelination, the mechanism by which NRG1 Type-III induces greater axonal growth

and provides re-innervation is unclear. A future direction would be retrograde labelling to trace the axons that reached the target muscle back through the dorsal root ganglia and into the spinal cord, to classify their type and function. We also propose that the NRG1 Type-III- ErbB2/3 system is involved in bidirectional signaling that induces neurotrophic factor secretion from Schwann cells. Using western blot analysis, the secretory profile of neurotrophic factors can be mapped, to understand the timeline of the molecular events during regeneration of axons across the BNI conduits[183].

Long term denervation caused by critical nerve injuries has a profound effect on the target muscle, with atrophy of these muscles within the first few weeks post-injury. While the benefits of low frequency electrical stimulation of the injured nerve or target muscle has been shown to rescue atrophy and accelerate regeneration in crush and transection injuries, its efficacy in critical nerve gap injuries is yet to be determined[100], [205]. A combined treatment of growth factor enriched conduits and electrical stimulation of the muscle may be a valuable strategy and may further improve re-innervation and functional recovery.

### **5.3 Overall Summary And Dissertation Contribution**

Despite the robust regenerative capacity of the peripheral nervous system, repairing large nerve defects remains a formidable challenge. In this dissertation we utilized a growth factor enriched multi-luminal biosynthetic nerve implant to entice axons across a 4cm nerve gap. While we demonstrated that PTN and GDNF promote axon regeneration, abnormal sorting of these axons hinders maturation and myelination, leading to poor re-innervation. Using NRG1 Type-III we were able to enhance axonal sorting, which resulted in greater number of myelinated axons. In this work, we determined that while growth factors can get axons to grow across critical gaps, the

number of axons does not necessarily translate to recovery and that maturation and myelination of these axons is critical. Through this work we also determined a possible neurotrophic role of Neuregulin1 Type III in addition to its known effect in radial sorting and myelination. In addition, we designed S-shaped 3-D printed nerve guide conduits that provide micro and macro-topographical features to guide axons and potentially accelerate growth by changing cellular morphology and migration. This model also provides us with the ability to mimic a critical gap in the rat model, and truly understand long term mechanisms involved in peripheral nerve regeneration, using the well standardized assessment tools available in this model.

## REFERENCES

- [1]R. S. Martins, D. Bastos, M. G. Siqueira, C. O. Heise, and M. J. Teixeira, “Traumatic injuries of peripheral nerves: a review with emphasis on surgical indication.,” *Arquivos de neuro-psiquiatria*, vol. 71, no. 10, pp. 811–4, 2013.
- [2]I. Allodi, E. Udina, and X. Navarro, “Specificity of peripheral nerve regeneration: Interactions at the axon level,” *Progress in Neurobiology*, vol. 98, no. 1, pp. 16–37, 2012.
- [3]G. Lundborg, “Nerve injury and repair - A challenge to the plastic brain,” *Journal of the Peripheral Nervous System*, vol. 8, no. 4, pp. 209–226, 2003.
- [4]L. Rasulic, V. Puzovic, K. Rotim, M. Jovanovic, M. Samardzic, B. Zivkovic, and A. Savic, “The epidemiology of forearm nerve injuries--a retrospective study,” *Acta Clin Croat*, vol. 54, no. 1, pp. 19–24, 2015.
- [5]G. Antoniadis, T. Kretschmer, M. T. Pedro, R. W. Konig, C. P. Heinen, and H. P. Richter, “Iatrogenic nerve injuries-prevalence, diagnosis and treatment,” *Dtsch Arztebl Int*, vol. 111, no. 16, pp. 273–279, 2014.
- [6] L. M. Marquardt, X. Ee, N. Iyer, D. Hunter, S. E. Mackinnon, M. D. Wood, and S. E. Sakiyama-Elbert, “Finely Tuned Temporal and Spatial Delivery of GDNF Promotes Enhanced Nerve Regeneration in a Long Nerve Defect Model.,” *Tissue engineering. Part A*, vol. 21, no. 23–24, pp. 2852–64, 2015.
- [7]M. D. Wood, S. W. P. Kemp, C. Weber, G. H. Borschel, and T. Gordon, “Annals of Anatomy Outcome measures of peripheral nerve regeneration,” *Annals of Anatomy*, vol. 193, no. 4, pp. 321–333, 2011.
- [8]J. D. Stewart, “Peripheral nerve fascicles: anatomy and clinical relevance,” *Muscle & Nerve*, vol. 28, no. 5, pp. 525–541, 2003.
- [9]D. Klein and R. Martini, “Myelin and macrophages in the PNS: An intimate relationship in trauma and disease,” *Brain Research*, vol. 1641, pp. 130–138, Jun. 2016.
- [10] K. R. Jessen and R. Mirsky, “The origin and development of glial cells in peripheral nerves.,” *Nature Reviews*, vol. 6, no. 9, pp. 671–682, 2005.
- [11] J. W. Griffin, R. George, and T. Ho, “Macrophage Systems in Peripheral Nerves. A Review,” *Journal of Neuropathology and Experimental Neurology*, vol. 52, no. 6, pp. 553–560, Nov. 1993.
- [12]S. Sunderland, “A classification of peripheral nerve injuries producing loss of function.,” *Brain : a journal of neurology*, vol. 74, no. 4, pp. 491–516, Dec. 1951.

- [13]H. J. Seddon, "Three Types of Nerve Injury," *Brain*, vol. 66, no. 4, pp. 237–288, Dec. 1943.
- [14]B. J. Pfister, T. Gordon, J. R. Loverde, A. S. Kochar, S. E. Mackinnon, and D. K. Cullen, "Biomedical Engineering Strategies for Peripheral Nerve Repair: Surgical Applications, State of the Art, and Future Challenges," *Critical Reviews<sup>TM</sup> in Biomedical Engineering*, vol. 39, no. 2, pp. 81–124, 2011.
- [15]X. Navarro, "Functional evaluation of peripheral nerve regeneration and target reinnervation in animal models: a critical overview.," *The European journal of neuroscience*, vol. 43, pp. 1–16, 2015.
- [16]X. Navarro, M. Vivó, and A. Valero-Cabré, "Neural plasticity after peripheral nerve injury and regeneration," *Progress in Neurobiology*, vol. 82, no. 4, pp. 163–201, 2007.
- [17] J. G. Boyd and T. Gordon, "Neurotrophic Factors and Their Receptors in Axonal Regeneration and Functional Recovery After Peripheral Nerve Injury," vol. 27, no. 3, 2003.
- [18] M. G. Burnett, E. L. Zager, M. A. R. K. G. B. Urnett, and E. R. I. C. L. Z. Ager, "Pathophysiology of peripheral nerve injury : a brief review," *Neurosurgical focus*, vol. 16, no. 5, pp. 1–7, 2004.
- [19]A. Waller, "Experiments on the Section of the Glossopharyngeal and Hypoglossal Nerves of the Frog , and Observations of the Alterations Produced Thereby in the Structure of Their Primitive Fibres Author ( s ): Augustus Waller Source : Philosophical Transactions of th," *Philosophical Transactions of the Royal Society of London*, vol. 140, no. 1850, pp. 423–429, 1850.
- [20]G. Stoll, S. Jander, and R. R. Myers, "Degeneration and regeneration of the peripheral nervous system: From Augustus Waller's observations to neuroinflammation," *Journal of the Peripheral Nervous System*, vol. 7, no. 1, pp. 13–27, 2002.
- [21]M. C. Brown, E. R. Lunn, and V. H. Perry, "Consequences of slow wallerian degeneration for regenerating motor and sensory axons," *Journal of Neurobiology*, vol. 23, no. 5, pp. 521–536, 1992.
- [22]E. R. Lunn, V. H. Perry, M. C. Brown, H. Rosen, and S. Gordon, "Absence of Wallerian Degeneration does not Hinder Regeneration in Peripheral Nerve," *European Journal of Neuroscience*, vol. 1, no. 1, pp. 27–33, 1989.
- [23]Q. Zhai, J. Wang, A. Kim, Q. Liu, R. Watts, E. Hoopfer, T. Mitchison, L. Luo, and Z. He, "Involvement of the Ubiquitin-Proteasome System in the Early Stages of Wallerian Degeneration," *Neuron*, vol. 39, no. 2, pp. 217–225, Jul. 2003.

- [24]E. B. George, J. D. Glass, and J. W. Griffin, "Axotomy-induced axonal degeneration is mediated by calcium influx through ion-specific channels.," *The Journal of neuroscience : the official journal of the Society for Neuroscience*, vol. 15, no. 10, pp. 6445–52, 1995.
- [25]J. Gerdts, D. W. Summers, Y. Sasaki, A. DiAntonio, and J. Milbrandt, "Sarm1-mediated axon degeneration requires both SAM and TIR interactions.," *The Journal of neuroscience : the official journal of the Society for Neuroscience*, vol. 33, no. 33, pp. 13569–80, 2013.
- [26]G. J. Brunn, M. K. Bungum, G. B. Johnson, and J. L. Platt, "Conditional signaling by Toll-like receptor 4," *The FASEB Journal*, vol. 19, no. 7, pp. 872–874, 2005.
- [27]N. Abe and V. Cavalli, "Nerve injury signaling," *Current Opinion in Neurobiology*, vol. 18, no. 3, pp. 276–283, 2008.
- [28]E. Perlson, S. Hanz, K. Ben-Yaakov, Y. Segal-Ruder, R. Seger, and M. Fainzilber, "imentin-dependent spatial translocation of an activated MAP kinase in injured nerve," *Neuron*, vol. 45, no. 5, pp. 715–726, 2005.
- [29]S. Hanz, E. Perlson, D. Willis, J. Q. Zheng, R. Massarwa, J. J. Huerta, M. Koltzenburg, M. Kohler, J. Van-Minnen, J. L. Twiss, and M. Fainzilber, "Axoplasmic importins enable retrograde injury signaling in lesioned nerve," *Neuron*, vol. 40, no. 6, pp. 1095–1104, 2003.
- [30]V. Cavalli, P. Kujala, J. Klumperman, and L. S. B. Goldstein, "Sunday driver links axonal transport to damage signaling," *Journal of Cell Biology*, vol. 168, no. 5, pp. 775–787, 2005.
- [31] C. Lindwall and M. Kanje, "Retrograde axonal transport of JNK signaling molecules influence injury induced nuclear changes in p-c-Jun and ATF3 in adult rat sensory neurons," *Molecular and Cellular Neuroscience*, vol. 29, no. 2, pp. 269–282, 2005.
- [32]Y. J. Sung, D. T. W. Chiu, and R. T. Ambron, "Activation and retrograde transport of protein kinase G in rat nociceptive neurons after nerve injury and inflammation," *Neuroscience*, vol. 141, no. 2, pp. 697–709, 2006.
- [33]A. D. Guertin, D. P. Zhang, K. S. Mak, J. A. Alberta, and H. A. Kim, "Microanatomy of Axon / Glial Signaling during Wallerian Degeneration," *Culture*, vol. 25, no. 13, pp. 3478–3487, 2005.
- [34]M. Gey, R. Wanner, C. Schilling, M. T. Pedro, D. Sinske, and B. Knöll, "Atf3 mutant mice show reduced axon regeneration and impaired regeneration-associated gene induction after peripheral nerve injury," *Open Biology*, vol. 6, no. 8, p. 160091, 2016.
- [35]X. Lu and P. M. Richardson, "Responses of macrophages in rat dorsal root ganglia following peripheral nerve injury," *Journal of Neurocytology*, vol. 22, no. 5, pp. 334–341, 1993.



- [36]A. Humbertson, E. Zimmermann, and M. Leedy, "A chronological study of mitotic activity in satellite cell hyperplasia associated with chromatolytic neurons," *Zeitschrift für Zellforschung und mikroskopische Anatomie* 100.4 (1969): 507-515., vol. 100, no. 4, pp. 507–515, 1969.
- [37] R. C. Schreiber, A. M. Shadiack, T. A. Bennett, C. E. Sedwick, and R. E. Zigmond, "Changes in the macrophage population of the rat superior cervical ganglion after postganglionic nerve injury," *Journal of Neurobiology*, vol. 27, no. 2, pp. 141–153, 1995.
- [38]S. Y. Jang, Y. K. Shin, S. Y. Park, J. Y. Park, H. J. Lee, Y. H. Yoo, J. K. Kim, and H. T. Park, "Autophagic myelin destruction by schwann cells during wallerian degeneration and segmental demyelination," *Glia*, vol. 64, no. 5, pp. 730–742, 2016.
- [39]J. A. Gomez-Sanchez, L. Carty, M. Iruarrizaga-Lejarreta, M. Palomo-Irigoyen, M. Varela-Rey, M. Griffith, J. Hantke, N. Macias-Camara, M. Azkargorta, I. Aurrekoetxea, V. G. De Juan, H. B. J. Jefferies, P. Aspichueta, F. Elortza, A. M. Aransay, M. L. Martínez-Chantar, F. Baas, J. M. Mato, R. Mirsky, A. Woodhoo, and K. R. Jessen, "Schwann cell autophagy, myelinophagy, initiates myelin clearance from injured nerves," *Journal of Cell Biology*, vol. 210, no. 1, pp. 153–168, 2015.
- [40]C. Benito, C. M. Davis, J. A. Gomez-Sanchez, M. Turmaine, D. Meijer, V. Poli, R. Mirsky, and K. R. Jessen, "STAT3 Controls the Long-Term Survival and Phenotype of Repair Schwann Cells during Nerve Regeneration.," *The Journal of neuroscience : the official journal of the Society for Neuroscience*, vol. 37, no. 16, pp. 4255–4269, 2017.
- [41]A. L. Cattin, J. J. Burden, L. Van Emmenis, F. E. MacKenzie, J. J. A. Hoving, N. Garcia Calavia, Y. Guo, M. McLaughlin, L. H. Rosenberg, V. Quereda, D. Jamecna, I. Napoli, S. Parrinello, T. Enver, C. Ruhrberg, and A. C. Lloyd, "Macrophage-Induced Blood Vessels Guide Schwann Cell-Mediated Regeneration of Peripheral Nerves," *Cell*, vol. 162, no. 5, pp. 1127–1139, 2015.
- [42]M. P. Clements, E. Byrne, L. F. Camarillo Guerrero, A. L. Cattin, L. Zakka, A. Ashraf, J. J. Burden, S. Khadayate, A. C. Lloyd, S. Marguerat, and S. Parrinello, "The Wound Microenvironment Reprograms Schwann Cells to Invasive Mesenchymal-like Cells to Drive Peripheral Nerve Regeneration," *Neuron*, vol. 96, no. 1, p. 98–114.e7, 2017.
- [43]R. Martini, S. Fischer, R. López-Vales, and S. David, "Interactions between Schwann cells and macrophages in injury and inherited demyelinating disease," *Glia*, vol. 56, no. 14, pp. 1566–1577, 2008.
- [44]A. T. Dailey, A. M. Avellino, L. Benthem, J. Silver, and M. Klot, "Complement Depletion Reduces Macrophage Infiltration and Activation during Wallerian Degeneration and Axonal Regeneration," *Journal of Neuroscience*, vol. 18, no. 17, pp. 6713–6722, 1998.

- [45]J. A. Stratton, A. Holmes, N. L. Rosin, T. Trang, R. Midha, J. Biernaskie, J. A. Stratton, A. Holmes, N. L. Rosin, S. Sinha, and M. Vohra, “Macrophages Regulate Schwann Cell Maturation after Nerve Injury Report Macrophages Regulate Schwann Cell Maturation after Nerve Injury,” *CellReports*, vol. 24, no. 10, p. 2561–2572.e6, 2018.
- [46]G. N. Panagopoulos, P. D. Megaloikonomos, and A. F. Mavrogenis, “The Present and Future for Peripheral Nerve Regeneration,” *Orthopedics*, vol. 40, no. 1, pp. e141–e156, 2017.
- [47]C. H. Allan, “Primary nerve repair: Indications and results,” *Journal of the American Society for Surgery of the Hand*, vol. 4, no. 3Allan, C. H. (2004). Primary nerve repair: Indications and results. *Journal of the American Society for Surgery of the Hand*, 4(3), 195–199.  
<http://doi.org/10.1016/j.jassh.2004.06.010>, pp. 195–199, 2004.
- [48]R. M. R. Mcallister, S. E. A. Gilbert, J. S. Calder, and P. J. Smith, “The Epidemiology and Management of Upper Limb Peripheral Nerve Injuries in Modern Practice,” 1996.
- [49]W. L. Clark, T. E. Trumble, M. F. Swiontkowski, and A. F. Tencer, “Nerve tension and blood flow in a rat model of immediate and delayed repairs,” *The Journal of Hand Surgery*, vol. 17, no. 4, pp. 677–687, 1992.
- [50]P. J. Driscoll, M. A. Glasby, and G. M. Lawson, “An in vivo study of peripheral nerves in continuity: biomechanical and physiological responses to elongation,” *Journal of Orthopaedic Research*, vol. 20, no. 2, pp. 370–375, 2002.
- [51]H. Millesi, “Techniques for nerve grafting,,” *Hand clinics*, vol. 16, no. 1, p. 73–91, viii, 2000.
- [52]T. Norkus, M. Norkus, and T. Ramanauskas, “Donor, recipient and nerve grafts in brachial plexus reconstruction: anatomical and technical features for facilitating the exposure,” *Surgical and Radiologic Anatomy*, vol. 27, no. 6, pp. 524–530, 2005.
- [53] S. E. Mackinnon, V. B. Doolabh, C. B. Novak, and E. P. Trulock, “Clinical outcome following nerve allograft transplantation,,” *Plastic and reconstructive surgery*, vol. 107, no. 6, pp. 1419–29, 2001.
- [54] K. Brattain, “Analysis of the Peripheral Nerve Repair Market in the United States.”
- [55]B.-S. Kim, J. J. Yoo, and A. Atala, “Peripheral nerve regeneration using acellular nerve grafts,” *Journal of Biomedical Materials Research*, vol. 68A, no. 2, pp. 201–209, 2004.
- [56]O. Frerichs, H. Fansa, C. Schicht, G. Wolf, W. Schneider, and G. Keilhoff, “Reconstruction of peripheral nerves using acellular nerve grafts with implanted cultured Schwann cells,” *Microsurgery*, vol. 22, no. 7, pp. 311–315, 2002.

- [57]M. Szykaruk, S. W. P. Kemp, M. D. Wood, T. Gordon, and G. H. Borschel, “Experimental and clinical evidence for use of decellularized nerve allografts in peripheral nerve gap reconstruction,” *Tissue engineering. Part B, Reviews*, vol. 19, no. 1, 2013.
- [58]M. D. Wood, S. W. P. Kemp, E. H. Liu, M. Szykaruk, T. Gordon, and G. H. Borschel, “Rat-derived processed nerve allografts support more axon regeneration in rat than human-derived processed nerve xenografts,” pp. 1085–1091, 2013.
- [59]D. N. Brooks, R. V Weber, J. D. Chao, B. D. Rinker, J. Zoldos, M. R. Robichaux, S. B. Ruggeri, K. A. Anderson, E. Bonatz, S. M. Wisotsky, M. S. Cho, C. Wilson, E. O. Cooper, J. V Ingari, B. Safa, B. M. Parrett, and G. M. Buncke, “Processed Nerve Allografts For Peripheral Nerve Reconstruction: A Multicenter Study Of Utilization And Outcomes In Sensory, Mixed, And Motor Nerve Reconstructions,” 2011.
- [60] S. E. Mackinnon, V. B. Doolabh, C. B. Novak, and E. P. Trulock, “Clinical outcome following nerve allograft transplantation,” *Plastic and reconstructive surgery*, vol. 107, no. 6, pp. 1419–29, 2001.
- [61]M. Saheb-Al-Zamani, Y. Yan, S. J. Farber, D. A. Hunter, P. Newton, M. D. Wood, S. A. Stewart, P. J. Johnson, and S. E. Mackinnon, “Limited regeneration in long acellular nerve allografts is associated with increased Schwann cell senescence,” *Experimental Neurology*, vol. 247, pp. 165–177, 2013.
- [62]L. H. Poppler, X. Ee, L. Schellhardt, G. M. Hoben, D. Pan, D. A. Hunter, Y. Yan, A. M. Moore, A. K. Snyder-Warwick, S. A. Stewart, S. E. Mackinnon, and M. D. Wood, “Axonal Growth Arrests After an Increased Accumulation of Schwann Cells Expressing Senescence Markers and Stromal Cells in Acellular Nerve Allografts,” *Tissue Engineering Part A*, vol. 22, no. 13–14, pp. 949–961, 2016.
- [63]J. Campisi and F. D’Adda Di Fagagna, “Cellular senescence: When bad things happen to good cells,” *Nature Reviews Molecular Cell Biology*, vol. 8, no. 9, pp. 729–740, 2007.
- [64]S. Kehoe, X. F. Zhang, and D. Boyd, “FDA approved guidance conduits and wraps for peripheral nerve injury: A review of materials and efficacy,” *Injury*, vol. 43, no. 5, pp. 553–572, 2012.
- [65]D. Arslantunali, T. Dursun, D. Yucel, N. Hasirci, and V. Hasirci, “Peripheral nerve conduits: Technology update,” *Medical Devices: Evidence and Research*, vol. 7, pp. 405–424, 2014.
- [66]S. E. Mackinnon, A. R. Hudson, V. Bojanowski, D. A. Hunter, and E. Maraghi, “Peripheral nerve injection injury with purified bovine collagen--an experimental model in the rat,” *Annals of plastic surgery*, vol. 14, no. 5, pp. 428–36, 1985.

- [67]S. J. Archibald, J. Shefner, C. Krarup, and R. D. Madison, "Monkey median nerve repaired by nerve graft or collagen nerve guide tube.," *The Journal of neuroscience : the official journal of the Society for Neuroscience*, vol. 15, no. 5 Pt 2, pp. 4109–23, 1995.
- [68]S. J. Archibald, C. Krarup, J. Shefner, S. T. Li, and R. D. Madison, "A collagen-based nerve guide conduit for peripheral nerve repair: an electrophysiological study of nerve regeneration in rodents and nonhuman primates.," *The Journal of comparative neurology*, vol. 306, no. 4, pp. 685–696, 1991.
- [69]P. A. Wieringa, A. R. Gonçalves de Pinho, S. Micera, R. J. A. van Wezel, and L. Moroni, "Biomimetic Architectures for Peripheral Nerve Repair: A Review of Biofabrication Strategies," *Advanced Healthcare Materials*, vol. 1701164, pp. 1–19, 2018.
- [70]G. R. . Evans, K. Brandt, S. Katz, P. Chauvin, L. Otto, M. Bogle, B. Wang, R. K. Meszlenyi, L. Lu, A. G. Mikos, and C. W. Patrick, "Bioactive poly(l-lactic acid) conduits seeded with Schwann cells for peripheral nerve regeneration," *Biomaterials*, vol. 23, no. 3, pp. 841–848, 2002.
- [71] F. J. Rodríguez, E. Verdú, D. Ceballos, and X. Navarro, "Nerve Guides Seeded with Autologous Schwann Cells Improve Nerve Regeneration," *Experimental Neurology*, vol. 161, no. 2, pp. 571–584, 2000.
- [72]J. Fujimura, R. Ogawa, H. Mizuno, Y. Fukunaga, and H. Suzuki, "Neural differentiation of adipose-derived stem cells isolated from GFP transgenic mice.," *Biochemical and biophysical research communications*, vol. 333, no. 1, pp. 116–21, 2005.
- [73]J. H. Gu, Y. H. Ji, E.-S. Dhong, D. H. Kim, and E.-S. Yoon, "Transplantation of adipose derived stem cells for peripheral nerve regeneration in sciatic nerve defects of the rat.," *Current stem cell research & therapy*, vol. 7, no. 5, pp. 347–55, 2012.
- [74]M. Dezawa, I. Takahashi, M. Esaki, M. Takano, and H. Sawada, "Sciatic nerve regeneration in rats induced by transplantation of in vitro differentiated bone-marrow stromal cells," *European Journal of Neuroscience*, vol. 14, no. 11, pp. 1771–1776, 2001.
- [75]C.-J. Chen, Y.-C. Ou, S.-L. Liao, W.-Y. Chen, S.-Y. Chen, C.-W. Wu, C.-C. Wang, W.-Y. Wang, Y.-S. Huang, and S.-H. Hsu, "Transplantation of bone marrow stromal cells for peripheral nerve repair.," *Experimental neurology*, vol. 204, no. 1, pp. 443–53, 2007.
- [76] G. Stoll and H. W. Müller, "1999 Nerve injury, axonal degeneration and neural regeneration," vol. 325, pp. 313–325, 1999.
- [77]V. T. Ribeiro-resende, B. Koenig, S. Nichterwitz, S. Oberhoffner, and B. Schlosshauer, "Biomaterials " ngner in peripheral Strategies for inducing the formation of bands of Bu nerve regeneration," *Biomaterials*, vol. 30, no. 29, pp. 5251–5259, 2009.

- [78]K. E. Tansey, J. L. Seifert, B. Botterman, M. R. Delgado, and M. I. Romero, “Peripheral nerve repair through multi-luminal biosynthetic implants,” *Annals of Biomedical Engineering*, vol. 39, no. 6, pp. 1815–1828, 2011.
- [79]I. P. Clements, Y. Kim, A. W. English, X. Lu, A. Chung, and R. V. Bellamkonda, “Thin-film enhanced nerve guidance channels for peripheral nerve repair,” *Biomaterials*, vol. 30, no. 23–24, pp. 3834–3846, 2009.
- [80] A. Kriebel, M. Rumman, M. Scheld, D. Hodde, G. Brook, and J. Mey, “Three-dimensional configuration of orientated fibers as guidance structures for cell migration and axonal growth,” *Journal of Biomedical Materials Research - Part B Applied Biomaterials*, vol. 102, no. 2, pp. 356–365, 2014.
- [81]L. Yao, G. C. W. de Ruitter, H. Wang, A. M. Knight, R. J. Spinner, M. J. Yaszemski, A. J. Windebank, and A. Pandit, “Controlling dispersion of axonal regeneration using a multichannel collagen nerve conduit,” *Biomaterials*, vol. 31, no. 22, pp. 5789–5797, 2010.
- [82]B. N. Johnson, K. Z. Lancaster, G. Zhen, J. He, M. K. Gupta, Y. L. Kong, E. A. Engel, K. D. Krick, A. Ju, F. Meng, L. W. Enquist, X. Jia, and M. C. McAlpine, “3D Printed Anatomical Nerve Regeneration Pathways,” *Advanced Functional Materials*, vol. 25, no. 39, pp. 6205–6217, 2015.
- [83]D. Y. Nguyen, R. T. Tran, F. Costanzo, and J. Yang, “Tissue-Engineered Peripheral Nerve Guide Fabrication Techniques,” *Nerves and Nerve Injuries*, vol. 2, pp. 971–992, 2015.
- [84] V. Chiono and C. Tonda-Turo, “Trends in the design of nerve guidance channels in peripheral nerve tissue engineering,” *Progress in Neurobiology*. 2015.
- [85]L. Zhang, Z. Ma, G. M. Smith, X. Wen, Y. Pressman, P. M. Wood, and X. M. Xu, “GDNF-enhanced axonal regeneration and myelination following spinal cord injury is mediated by primary effects on neurons,” *Glia*, vol. 57, no. 11, pp. 1178–1191, 2009.
- [86]T. Gordon, “The physiology of neural injury and regeneration: The role of neurotrophic factors,” *Journal of Communication Disorders*, vol. 43, no. 4, pp. 265–273, 2010.
- [87]M. S. Airaksinen and M. Saarma, “the Gdnf Family: Signalling, Biological Functions and Therapeutic Value,” *Nature Reviews Neuroscience*, vol. 3, no. 5, pp. 383–394, 2002.
- [88]T. M. Brushart, M. Aspalter, J. W. Griffin, R. Redett, H. Hameed, C. Zhou, M. Wright, A. Vyas, and A. Höke, “Schwann cell phenotype is regulated by axon modality and central-peripheral location, and persists in vitro,” *Experimental Neurology*, vol. 247, pp. 272–281, 2013.

- [89]P. Xu, K. M. Rosen, K. Hedstrom, O. Rey, S. Guha, C. Hart, and G. Corfas, "Nerve injury induces glial cell line-derived neurotrophic factor (GDNF) expression in schwann cells through purinergic signaling and the PKC-PKD pathway," *Glia*, vol. 61, no. 7, pp. 1029–1040, 2013.
- [90]Y. Yamada, K. Shimizu, A. Nitta, H. Soumiya, H. Fukumitsu, and S. Furukawa, "Axonal regrowth downregulates the synthesis of glial cell line-derived neurotrophic factor in the lesioned rat sciatic nerve," *Neuroscience Letters*, vol. 364, no. 1, pp. 11–15, 2004.
- [91]A. Höke, T. Ho, T. O. Crawford, C. LeBel, D. Hilt, and J. W. Griffin, "Glial cell line-derived neurotrophic factor alters axon schwann cell units and promotes myelination in unmyelinated nerve fibers.," *The Journal of neuroscience : the official journal of the Society for Neuroscience*, vol. 23, no. 2, pp. 561–567, 2003.
- [92]M. D. Wood, H. Kim, A. Bilbily, S. W. P. Kemp, C. Lafontaine, T. Gordon, M. S. Shoichet, and G. H. Borschel, "GDNF released from microspheres enhances nerve regeneration after delayed repair," *Muscle and Nerve*, vol. 46, no. 1, pp. 122–124, 2012.
- [93]S. Madduri, K. Feldman, T. Tervoort, M. Papaloïzos, and B. Gander, "Collagen nerve conduits releasing the neurotrophic factors GDNF and NGF," *Journal of Controlled Release*, vol. 143, no. 2, pp. 168–174, 2010.
- [94]M. D. Wood, T. Gordon, S. W. P. Kemp, E. H. Liu, H. Kim, M. S. Shoichet, and G. H. Borschel, "Functional motor recovery is improved due to local placement of GDNF microspheres after delayed nerve repair," *Biotechnology and Bioengineering*, vol. 110, no. 5, pp. 1272–1281, 2013.
- [95]G. Piquilloud, T. Christen, L. A. Pfister, B. Gander, and M. Y. Papaloïzos, "Variations in glial cell line-derived neurotrophic factor release from biodegradable nerve conduits modify the rate of functional motor recovery after rat primary nerve repairs," *European Journal of Neuroscience*, vol. 26, no. 5, pp. 1109–1117, 2007.
- [96]S. Averill, G. J. Michael, P. J. Shortland, R. C. Leavesley, V. R. King, E. J. Bradbury, S. B. McMahon, and J. V. Priestley, "NGF and GDNF ameliorate the increase in ATF3 expression which occurs in dorsal root ganglion cells in response to peripheral nerve injury," *European Journal of Neuroscience*, vol. 19, no. 6, pp. 1437–1445, 2004.
- [97]B. Wang, J. Yuan, X. Chen, J. Xu, Y. Li, and P. Dong, "Functional regeneration of the transected recurrent laryngeal nerve using a collagen scaffold loaded with laminin and laminin-binding BDNF and GDNF," *Scientific Reports*, vol. 6, p. 32292, 2016.
- [98]L. M. Marquardt, X. Ee, N. Iyer, D. Hunter, S. E. Mackinnon, M. D. Wood, and S. E. Sakiyama-Elbert, "Finely Tuned Temporal and Spatial Delivery of GDNF Promotes Enhanced Nerve Regeneration in a Long Nerve Defect Model," *Tissue Engineering Part A*, 2015.

- [99] J. M. Vianney, M. J. McCullough, A. M. Gyorkos, and J. M. Spitsbergen, "Exercise-dependent regulation of glial cell line-derived neurotrophic factor (GDNF) expression in skeletal muscle and its importance for the neuromuscular system," *Frontiers in Biology*, vol. 8, no. 1, pp. 101–108, 2013.
- [100] M. P. Willand, E. Rosa, B. Michalski, J. J. Zhang, T. Gordon, M. Fahnstock, and G. H. Borschel, "Electrical muscle stimulation elevates intramuscular BDNF and GDNF mRNA following peripheral nerve injury and repair in rats," *Neuroscience*, vol. 334, pp. 93–104, 2016.
- [101] J.-S. Park and A. Höke, "Treadmill Exercise Induced Functional Recovery after Peripheral Nerve Repair Is Associated with Increased Levels of Neurotrophic Factors," *PLoS ONE*, vol. 9, no. 3, p. e90245, 2014.
- [102] Chen J, C. Yf, C. Jm, and B. C. Li, "Synergistic effects of NGF, CNTF and GDNF on functional recovery following sciatic nerve injury in rats," vol. 55, no. 1, pp. 32–42, 2010.
- [103] S. Catrina, B. Gander, and S. Madduri, "Nerve conduit scaffolds for discrete delivery of two neurotrophic factors," *European Journal of Pharmaceutics and Biopharmaceutics*, vol. 85, no. 1, pp. 139–142, 2013.
- [104] H. Rauvala, "An 18-kd heparin-binding protein of developing brain that is distinct from fibroblast growth factors.," *The EMBO journal*, vol. 8, no. 10, pp. 2933–41, 1989.
- [105] C. González-Castillo, D. Ortúño-Sahagún, C. Guzmán-Brambila, M. Pallás, and A. E. Rojas-Mayorquén, "Pleiotrophin as a central nervous system neuromodulator, evidences from the hippocampus," *Frontiers in Cellular Neuroscience*, vol. 8, pp. 1–7, 2015.
- [106] K. Ochiai, H. Muramatsu, S. Yamamoto, H. Ando, and T. Muramatsu, "The role of midkine and pleiotrophin in liver regeneration," *Liver International*, vol. 24, no. 5, pp. 484–491, 2004.
- [107] A. Hoke, "Schwann Cells Express Motor and Sensory Phenotypes That Regulate Axon Regeneration," *Journal of Neuroscience*, vol. 26, no. 38, pp. 9646–9655, 2006.
- [108] B. Blondet, G. Carpentier, F. Lafdil, and J. Courty, "Pleiotrophin Cellular Localization in Nerve Regeneration after Peripheral Nerve Injury," *The Journal of Histochemistry & Journal of Histochemistry & Cytochemistry*, vol. 53, no. 8, pp. 971–977, 2005.
- [109] R. Mi, W. Chen, and A. Höke, "Pleiotrophin is a neurotrophic factor for spinal motor neurons.," *Proceedings of the National Academy of Sciences of the United States of America*, vol. 104, no. 11, pp. 4664–9, 2007.
- [110] L. Jin, C. Jianghai, L. Juan, and K. Hao, "Pleiotrophin and peripheral nerve injury," *Neurosurgical Review*, vol. 32, no. 4, pp. 387–393, 2009.

- [111]C. Xu, S. Zhu, M. Wu, W. Han, and Y. Yu, “Functional receptors and intracellular signal pathways of midkine (MK) and pleiotrophin (PTN).,” *Biological & pharmaceutical bulletin*, vol. 37, no. 4, pp. 511–20, 2014.
- [112]S. Anand, V. Desai, N. Alsmadi, A. Kanneganti, D. H. T. Nguyen, M. Tran, L. Patil, S. Vasudevan, C. Xu, Y. Hong, J. Cheng, E. Keefer, and M. I. Romero-Ortega, “Asymmetric Sensory-Motor Regeneration of Transected Peripheral Nerves Using Molecular Guidance Cues,” *Scientific Reports*, vol. 7, no. 1, 2017.
- [113]B. Blondet, G. Carpentier, A. Ferry, and J. Courty, “Exogenous pleiotrophin applied to lesioned nerve impairs muscle reinnervation,” *Neurochemical Research*, vol. 31, pp. 907–91, 2006.
- [114]M. Sarker, S. Naghieh, A. D. Mcinnes, D. J. Schreyer, and X. Chen, “Strategic Design and Fabrication of Nerve Guidance Conduits for Peripheral Nerve Regeneration,” vol. 13, p. 1700635, 2018.
- [115]A. Pabari, S. Y. Yang, A. Mosahebi, and A. M. Seifalian, “Recent advances in artificial nerve conduit design: Strategies for the delivery of luminal fillers,” *Journal of Controlled Release*, vol. 156, no. 1, pp. 2–10, 2011.
- [116] T. Gordon, T. M. Brushart, and K. M. Chan, “Augmenting nerve regeneration with electrical stimulation.,” *Neurological research*, vol. 30, no. 10, pp. 1012–1022, 2008.
- [117] A. O’Daly, C. Rohde, and T. M. Brushart, “The topographic specificity of muscle reinnervation predicts function,” *European Journal of Neuroscience*, vol. 43, no. 3, pp. 443–450, 2016.
- [118]P. Ahlborn, M. Schachner, and A. Irintchev, “One hour electrical stimulation accelerates functional recovery after femoral nerve repair,” *Experimental Neurology*, vol. 208, no. 1, pp. 137–144, 2007.
- [119]M. P. Willand, C. D. Chiang, J. J. Zhang, S. W. P. Kemp, G. H. Borschel, and T. Gordon, “Daily Electrical Muscle Stimulation Enhances Functional Recovery Following Nerve Transection and Repair in Rats,” *Neurorehabilitation and Neural Repair*, vol. 29, pp. 690–700, 2015.
- [120] T. Gordon and A. W. English, “Strategies to promote peripheral nerve regeneration: Electrical stimulation and/or exercise,” *European Journal of Neuroscience*, vol. 43, no. 3. pp. 336–350, 2016.
- [121]K. Elzinga, N. Tyreman, A. Ladak, B. Savaryn, J. Olson, and T. Gordon, “Brief electrical stimulation improves nerve regeneration after delayed repair in Sprague Dawley rats,” *Experimental Neurology*, vol. 269, pp. 142–153, 2015.



- [122]K. E. Tansey, J. L. Seifert, B. Botterman, M. R. Delgado, and M. I. Romero, "Peripheral nerve repair through multi-luminal biosynthetic implants," *Annals of Biomedical Engineering*, vol. 39, no. 6, pp. 1815–1828, 2011.
- [123]A. Höke and T. Brushart, "Introduction to special issue: Challenges and opportunities for regeneration in the peripheral nervous system.," *Experimental neurology*, vol. 223, no. 1, pp. 1–4, 2010.
- [124]D. Grinsell and C. P. Keating, "Peripheral Nerve Reconstruction after Injury: A Review of Clinical and Experimental Therapies," *BioMed Research International*, vol. 2014, p. 698256, 2014.
- [125] A. M. Moore, R. Kasukurthi, C. K. Magill, F. H. Farhadi, G. H. Borschel, and S. E. Mackinnon, "Limitations of conduits in peripheral nerve repairs," *Hand*, vol. 4, no. 2, pp. 180–186, 2009.
- [126] K. R. Jessen and R. Mirsky, "Schwann cells and their precursors emerge as major regulators of nerve development," *Trends in Neurosciences*, vol. 22, no. 9, pp. 402–410, 1999.
- [127]C. Taveggia, G. Zanazzi, A. Petrylak, H. Yano, J. Rosenbluth, S. Einheber, X. Xu, R. M. Esper, J. A. Loeb, P. Shrager, M. V. Chao, D. L. Falls, L. Role, and J. L. Salzer, "Neuregulin-1 type III determines the ensheathment fate of axons," *Neuron*, vol. 47, no. 5, pp. 681–694, 2005.
- [128]D. L. Sherman and P. J. Brophy, "Mechanisms of axon ensheathment and myelin growth.," *Nature reviews. Neuroscience*, vol. 6, no. 9, pp. 683–90, 2005.
- [129]F. R. Fricker, A. Antunes-Martins, J. Galino, R. Paramsothy, F. La Russa, J. Perkins, R. Goldberg, J. Brelstaff, N. Zhu, S. B. McMahon, C. Orengo, A. N. Garratt, C. Birchmeier, and D. L. H. Bennett, "Axonal neuregulin 1 is a rate limiting but not essential factor for nerve remyelination," *Brain*, vol. 136, no. 7, pp. 2279–2297, 2013.
- [130]J. T. Voyvodic, "Target size regulates calibre and myelination of sympathetic axons.," *Nature*, vol. 342, no. 6248, pp. 430–433, 1989.
- [131]S. Quintes, B. G. Brinkmann, M. Ebert, F. Fröb, T. Kungl, F. A. Arlt, V. Tarabykin, D. Huylebroeck, D. Meijer, U. Suter, M. Wegner, M. W. Sereda, and K.-A. Nave, "Zeb2 is essential for Schwann cell differentiation, myelination and nerve repair," *Nature Neuroscience*, vol. 19, no. 8, 2016.
- [132]J. A. Pereira, R. Baumann, C. Norrmen, C. Somandin, M. Mieke, C. Jacob, T. Luhmann, H. Hall-Bozic, N. Mantei, D. Meijer, and U. Suter, "Dicer in Schwann Cells Is Required for Myelination and Axonal Integrity," *Journal of Neuroscience*, vol. 30, no. 19, pp. 6763–6775, 2010.

- [133]A. F. Dawood, P. Lotfi, S. N. Dash, S. K. Kona, K. T. Nguyen, and M. I. Romero-Ortega, “VEGF Release in Multiluminal Hydrogels Directs Angiogenesis from Adult Vasculature In Vitro,” *Cardiovascular Engineering and Technology*, vol. 2, no. 3, pp. 173–185, 2011.
- [134]N. Z. Alsmadi, G. S. Bendale, A. Kanneganti, T. Shihabeddin, A. H. Nguyen, E. Hor, S. Dash, B. Johnston, R. Granja-Vazquez, and M. I. Romero-Ortega, “Glial-derived growth factor and pleiotrophin synergistically promote axonal regeneration in critical nerve injuries,” *Acta Biomaterialia*, vol. 78, pp. 165–177, 2018.
- [135]A. Höke, “Mechanisms of Disease: what factors limit the success of peripheral nerve regeneration in humans?,” *Nature clinical practice. Neurology*, vol. 2, no. 8, pp. 448–454, 2006.
- [136]S. Madduri, P. di Summa, M. Papaloizos, D. Kalbermatten, and B. Gander, “Effect of controlled co-delivery of synergistic neurotrophic factors on early nerve regeneration in rats,” *Biomaterials*, vol. 31, no. 32, pp. 8402–8409, 2010.
- [137]T. Gordon, “The role of neurotrophic factors in nerve regeneration,” *Neurosurgical focus*, vol. 26, no. 2. p. E3, 2009.
- [138]C. Baudet, a Mikaelis, H. Westphal, J. Johansen, T. E. Johansen, and P. Ernfors, “Positive and negative interactions of GDNF, NTN and ART in developing sensory neuron subpopulations, and their collaboration with neurotrophins,” *Development (Cambridge, England)*, vol. 127, no. 20, pp. 4335–4344, 2000.
- [139]D. Bonanomi, O. Chivatakarn, G. Bai, H. Abdesslem, K. Lettieri, T. Marquardt, B. A. Pierchala, and S. L. Pfaff, “Ret is a multifunctional coreceptor that integrates diffusible- and contact-axon guidance signals,” *Cell*, vol. 148, no. 3, pp. 568–582, 2012.
- [140]E. D. Rabinovsky, “The multifunctional role of IGF-1 in peripheral nerve regeneration,” *Neurological Research*, vol. 26, no. 2, pp. 204–210, 2004.
- [141]M. Paveliev, A. Hienola, E. Jokitalo, A. Planken, M. M. Bernalov, H. Rauvala, and M. Saarma, “Sensory neurons from N-syndecan-deficient mice are defective in survival,” *NeuroReport*, vol. 19, no. 14, pp. 1397–1400, 2008.
- [142]P. Perez-Pinera, O. Garcia-Suarez, P. Menendez-Rodriguez, J. Mortimer, Y. Chang, A. Astudillo, and T. F. Deuel, “The receptor protein tyrosine phosphatase (RPTP)??/?? is expressed in different subtypes of human breast cancer,” *Biochemical and Biophysical Research Communications*, vol. 362, no. 1, pp. 5–10, 2007.
- [143]R. L. Friede and T. Samorajski, “Relation between the number of myelin lamellae and axon circumference in fibers of vagus and sciatic nerves of mice,” *The Journal of Comparative Neurology*, vol. 130, no. 3, pp. 223–231, 1967.

- [144]G. V Michailov, M. W. Sereda, B. G. Brinkmann, T. M. Fischer, B. Haug, C. Birchmeier, L. Role, C. Lai, M. H. Schwab, and K.-A. Nave, “Axonal Neuregulin-1 Regulates Myelin Sheath Thickness,” vol. 304, pp. 700–703, 2004.
- [145]G. A. Elder, V. L. Friedrich, and R. A. Lazzarini, “Schwann cells and oligodendrocytes read distinct signals in establishing myelin sheath thickness,” *Journal of Neuroscience Research*, vol. 65, no. 6, pp. 493–499, 2001.
- [146]B. Singh, Q.-G. Xu, C. K. Franz, R. Zhang, C. Dalton, T. Gordon, V. M. K. Verge, R. Midha, and D. W. Zochodne, “Accelerated axon outgrowth, guidance, and target reinnervation across nerve transection gaps following a brief electrical stimulation paradigm,” *Journal of Neurosurgery*, vol. 116, no. 3, pp. 498–512, 2012.
- [147]M.-C. Lu, C.-Y. Ho, S.-F. Hsu, H.-C. Lee, J.-H. Lin, C.-H. Yao, and Y.-S. Chen, “Effects of Electrical Stimulation at Different Frequencies on Regeneration of Transected Peripheral Nerve,” *Neurorehabilitation and Neural Repair*, vol. 22, no. 4, pp. 367–373, 2007.
- [148]K. Elzinga, N. Tyreman, A. Ladak, B. Savaryn, J. Olson, and T. Gordon, “Brief electrical stimulation improves nerve regeneration after delayed repair in Sprague Dawley rats,” *Experimental Neurology*, vol. 269, pp. 142–153, 2015.
- [149] E. Asensio-Pinilla, E. Udina, J. Jaramillo, and X. Navarro, “Electrical stimulation combined with exercise increase axonal regeneration after peripheral nerve injury,” *Experimental Neurology*, vol. 219, no. 1, pp. 258–265, 2009.
- [150] A. Arbat-Plana, S. Cobiañchi, M. Herrando-Grabulosa, X. Navarro, and E. Udina, “Endogenous modulation of TrkB signaling by treadmill exercise after peripheral nerve injury,” *Neuroscience*, vol. 340, pp. 188–200, 2017.
- [151]D. Meyer, T. Yamaai, A. Garratt, E. Riethmacher-sonnenberg, D. Kane, L. E. Theill, and C. Birchmeier, “Isoform-specific expression and function of neuregulin,” vol. 3586, pp. 3575–3586, 1997.
- [152] R. M. Esper, M. S. Pankonin, and J. A. Loeb, “Neuregulins : Versatile growth and differentiation factors in nervous system development and human disease,” vol. 51, pp. 162–168, 2006.
- [153]L. Mei and W. C. Xiong, “Neuregulin 1 in neural development, synaptic plasticity and schizophrenia,” *Nature Reviews Neuroscience*, vol. 9, no. 6, pp. 437–452, 2008.
- [154]Y. Miyamoto, T. Torii, A. Tanoue, K. Kawahara, M. Arai, H. Tsumura, T. Ogata, M. Nagao, N. Terada, M. Yamamoto, S. Takashima, and J. Yamauchi, “Neuregulin-1 type III knockout mice exhibit delayed migration of Schwann cell precursors,” *Biochemical and Biophysical Research Communications*, vol. 486, no. 2, pp. 506–513, 2017.

- [155]Y. Li, G. I. Tennekoon, M. Birnbaum, M. A. Marchionni, and J. L. Rutkowski, “Neuregulin signaling through a PI3K/Akt/Bad pathway in Schwann cell survival,” *Molecular and Cellular Neuroscience*, vol. 17, no. 4, pp. 761–767, 2001.
- [156]H. M. Chang, M. K. Shyu, G. F. Tseng, C. H. Liu, H. S. Chang, C. T. Lan, W. M. Hsu, and W. C. Liao, “Neuregulin Facilitates Nerve Regeneration by Speeding Schwann Cell Migration via ErbB2/3-Dependent FAK Pathway,” *PLoS ONE*, vol. 8, no. 1, 2013.
- [157]A. Casanovas, S. Salvany, V. Lahoz, O. Tarabal, L. Piedrafita, R. Sabater, S. Hernández, J. Calderó, and J. E. Esquerda, “Neuregulin 1-ErbB module in C-bouton synapses on somatic motor neurons: molecular compartmentation and response to peripheral nerve injury,” *Scientific Reports*, vol. 7, no. December 2016, p. 40155, 2017.
- [158]R. M. Stassart, R. Fledrich, V. Velanac, B. G. Brinkmann, M. H. Schwab, D. Meijer, M. W. Sereda, and K.-A. Nave, “A role for Schwann cell-derived neuregulin-1 in remyelination,” *Nature Neuroscience*, vol. 16, no. 1, pp. 48–54, 2013.
- [159]A. Buonanno and G. D. Fischbach, “Neuregulin and ErbB receptor signaling pathways in the nervous system,” *Current Opinion in Cell Biology*, vol. 11, pp. 287–296, 2001.
- [160] C. Taveggia, “Schwann cells-axon interaction in myelination,” *Current Opinion in Neurobiology*, vol. 39, pp. 24–29, 2016.
- [161]P. Maurel and J. L. Salzer, “Axonal regulation of Schwann cell proliferation and survival and the initial events of myelination requires PI 3-kinase activity.,” *The Journal of neuroscience : the official journal of the Society for Neuroscience*, vol. 20, no. 12, pp. 4635–4645, 2000.
- [162]Y. Y. Chen, D. McDonald, C. Cheng, B. Magnowski, J. Durand, and D. W. Zochodne, “Axon and Schwann cell partnership during nerve regrowth.,” *Journal of neuropathology and experimental neurology*, vol. 64, no. 7, pp. 613–622, 2005.
- [163]J. R. Perlin, M. E. Lush, W. Z. Stephens, T. Piotrowski, and W. S. Talbot, “Neuronal Neuregulin 1 type III directs Schwann cell migration,” *Development*, vol. 138, no. 21, pp. 4639–4648, 2011.
- [164]G. Ronchi, K. Haastert-Talini, B. E. Fornasari, I. Perroteau, S. Geuna, and G. Gambarotta, “The Neuregulin1/ErbB system is selectively regulated during peripheral nerve degeneration and regeneration,” *European Journal of Neuroscience*, vol. 43, no. 3, pp. 351–364, 2016.
- [165]S. Heermann, J. Schmücker, U. Hinz, M. Rickmann, T. Unterbarnscheidt, M. H. Schwab, and K. Kriegstein, “Neuregulin 1 type III/ErbB signaling is crucial for schwann cell colonization of sympathetic axons,” *PLoS ONE*, vol. 6, no. 12, 2011.

- [166]D. E. Bergles, J. Hopkins, D. Gerber, M. Ghidinelli, E. Tinelli, C. Somandin, J. Gerber, J. A. Pereira, A. Ommer, G. Figlia, M. Mieke, L. G. Nägeli, V. Suter, V. Tadini, P. N. Sidiropoulos, C. Wessig, K. V Toyka, and U. Suter, “Schwann cells, but not Oligodendrocytes, Depend Strictly on Dynamin 2 Function,” *eLife*, vol. 8, p. e42404, 2019.
- [167]E. Tinelli, J. A. Pereira, and U. Suter, “Muscle-specific function of the centronuclear myopathy and Charcot–Marie–Tooth neuropathy-associated dynamin 2 is required for proper lipid metabolism, mitochondria, muscle fibers, neuromuscular junctions and peripheral nerves,” *Human Molecular Genetics*, vol. 22, no. 21, pp. 4417–4429, Nov. 2013.
- [168]J. B. Grinspan, M. A. Marchionni, M. Reeves, M. Coulaloglou, and S. S. Scherer, “Axonal Interactions Regulate Schwann Cell Apoptosis in Developing Peripheral Nerve : Neuregulin Receptors and the Role of Neuregulins,” vol. 16, no. 19, pp. 6107–6118, 1996.
- [169]K. A. Nave and J. L. Salzer, “Axonal regulation of myelination by neuregulin 1,” *Current Opinion in Neurobiology*, vol. 16, no. 5, pp. 492–500, 2006.
- [170]T. Gordon, N. Tyreman, and M. A. Raji, “The Basis for Diminished Functional Recovery after Delayed Peripheral Nerve Repair,” vol. 31, no. 14, pp. 5325–5334, 2011.
- [171]A. R. Raphael, D. A. Lyons, and W. S. Talbot, “ErbB signaling has a role in radial sorting independent of Schwann cell number,” *Glia*, vol. 59, no. 7, pp. 1047–1055, 2011.
- [172]M. L. Hancock, D. W. Nowakowski, L. W. Role, D. A. Talmage, and J. G. Flanagan, “Type III neuregulin 1 regulates pathfinding of sensory axons in the developing spinal cord and periphery,” *Development*, vol. 138, no. 22, pp. 4887–4898, 2011.
- [173]J. G. Boyd and T. Gordon, “Neurotrophic factors and their receptors in axonal regeneration and functional recovery after peripheral nerve injury,” *Molecular neurobiology*, vol. 27, no. 3, pp. 277–324, 2003.
- [174]S. Y. Fu and T. Gordon, “The cellular and molecular basis of peripheral nerve regeneration,” *Molecular neurobiology*, vol. 14, no. 1-2[1] S. Y. Fu and T. Gordon, “The cellular and molecular basis of peripheral nerve regeneration,” *Molecular neurobiology*, vol. 14, numbers 1–2, p. 67–116, 1997., pp. 67–116, 1997.
- [175]K. Tajdaran, T. Gordon, M. D. Wood, M. S. Shoichet, and G. H. Borschel, “A glial cell line-derived neurotrophic factor delivery system enhances nerve regeneration across acellular nerve allografts,” *Acta Biomaterialia*, vol. 29, pp. 62–70, 2016.
- [176]F. R. Fricker, N. Lago, S. Balarajah, C. Tsantoulas, S. Tanna, N. Zhu, S. K. Fageiry, M. Jenkins, A. N. Garratt, C. Birchmeier, and D. L. H. Bennett, “Axonally Derived Neuregulin-1 Is Required for Remyelination and Regeneration after Nerve Injury in Adulthood,” *Journal of Neuroscience*, vol. 31, no. 9, pp. 3225–3233, 2011.

- [177]R. Leimeroth, C. Lobsiger, A. Lu, V. Taylor, U. Suter, and L. Sommer, “Membrane-Bound Neuregulin1 Type III Actively Promotes Schwann Cell Differentiation of Multipotent Progenitor Cells,” vol. 258, pp. 245–258, 2002.
- [178]F. R. Fricker, N. Lago, S. Balarajah, C. Tsantoulas, S. Tanna, N. Zhu, S. K. Fageiry, M. Jenkins, A. N. Garratt, C. Birchmeier, and D. L. H. Bennett, “Axonally Derived Neuregulin-1 Is Required for Remyelination and Regeneration after Nerve Injury in Adulthood,” vol. 31, no. 9, pp. 3225–3233, 2011.
- [179]N. Syed, K. Reddy, D. P. Yang, C. Taveggia, J. L. Salzer, P. Maurel, and H. A. Kim, “Soluble Neuregulin-1 Has Bifunctional , Concentration-Dependent Effects on Schwann Cell Myelination,” vol. 30, no. 17, pp. 6122–6131, 2010.
- [180]Y. Hu, Y. Wu, Z. Gou, J. Tao, J. Zhang, Q. Liu, T. Kang, S. Jiang, S. Huang, J. He, S. Chen, Y. Du, and M. Gou, “3D-engineering of cellularized conduits for peripheral nerve regeneration,” *Scientific Reports*, vol. 6, p. 32184, 2016.
- [181]B. N. Johnson, K. Z. Lancaster, G. Zhen, J. He, M. K. Gupta, Y. L. Kong, E. A. Engel, K. D. Krick, A. Ju, F. Meng, L. W. Enquist, X. Jia, and M. C. McAlpine, “3D Printed Anatomical Nerve Regeneration Pathways,” *Advanced Functional Materials*, vol. 25, pp. 6205–6217, 2015.
- [182]M. Morano, G. Ronchi, V. Nicolò, B. E. Fornasari, A. Crosio, I. Perroteau, S. Geuna, G. Gambarotta, and S. Raimondo, “Modulation of the Neuregulin 1/ErbB system after skeletal muscle denervation and reinnervation,” *Scientific Reports*, vol. 8, no. 1, pp. 1–13, 2018.
- [183]R. M. Esper and J. A. Loeb, “Rapid Axoglial Signaling Mediated by Neuregulin and Neurotrophic Factors,” *Journal of Neuroscience*, vol. 24, p. 6218–6227 Cellular/Molecular, 2004.
- [184]R. M. Esper and J. A. Loeb, “Neurotrophins induce neuregulin release through protein kinase Cdelta activation.,” *The Journal of biological chemistry*, vol. 284, no. 39, pp. 26251–60, 2009.
- [185]S. K. Lee and S. W. Wolfe, “Peripheral nerve injury and repair.,” *The Journal of the American Academy of Orthopaedic Surgeons*, vol. 8, no. 4, pp. 243–52.
- [186] I. Allodi, E. Udina, and X. Navarro, “Specificity of peripheral nerve regeneration: Interactions at the axon level,” *Progress in Neurobiology*, vol. 98, no. 1. pp. 16–37, 2012.
- [187]S. Kehoe, X. F. Zhang, and D. Boyd, “FDA approved guidance conduits and wraps for peripheral nerve injury: A review of materials and efficacy,” *Injury*. 2012.
- [188]K. Brattain, “Analysis of the Peripheral Nerve Repair Market in the United States,” vol., pp. 1–11, 2014.

- [189] S. Y. Fu and T. Gordon, "Contributing Factors to Poor Functional Recovery after Delayed Nerve Repair: Prolonged Axotomy," *Journal of Neuroscience*, vol. 15, pp. 3876–3885, 1995.
- [190] S. Y. Fu and T. Gordon, "The cellular and molecular basis of peripheral nerve regeneration," *Molecular Neurobiology*, vol. 14, no. 1–2, pp. 67–116, 1997.
- [191] D. Angius, H. Wang, R. J. Spinner, Y. Gutierrez-Cotto, M. J. Yaszemski, and A. J. Windebank, "A systematic review of animal models used to study nerve regeneration in tissue-engineered scaffolds," *Biomaterials*, vol. 33, no. 32, pp. 8034–8039, 2012.
- [192] S. E. Thomson, C. Charalambous, C.-A. Smith, P. M. Tsimbouri, T. Déjardin, P. J. Kingham, A. M. Hart, and M. O. Riehle, "Microtopographical cues promote peripheral nerve regeneration via transient mTORC2 activation," *Acta biomaterialia*, vol. 60, pp. 220–231, 2017.
- [193] S. Y. Chew, R. Mi, A. Hoke, and K. W. Leong, "The effect of the alignment of electrospun fibrous scaffolds on Schwann cell maturation," *Biomaterials*, vol. 29, no. 6, pp. 653–661, 2008.
- [194] J. M. Murbach, S. Currilin, A. Widener, Y. Tong, S. Chhatre, V. Subramanian, D. C. Martin, B. N. Johnson, and K. J. Otto, "In situ electrochemical polymerization of poly(3,4-ethylenedioxythiophene) (PEDOT) for peripheral nerve interfaces," *MRS Communications*, vol. 8, no. 03, pp. 1043–1049, 2018.
- [195] Y. Tong, J. M. Murbach, V. Subramanian, S. Chhatre, F. Delgado, D. C. Martin, K. J. Otto, M. Romero-Ortega, and B. N. Johnson, "A Hybrid 3D Printing and Robotic-assisted Embedding Approach for Design and Fabrication of Nerve Cuffs with Integrated Locking Mechanisms," *MRS Advances*, vol. 3, no. 40, pp. 2365–2372, 2018.
- [196] M. Singh, Y. Tong, K. Webster, E. Cesewski, A. P. Haring, S. Laheri, B. Carswell, T. J. O'Brien, C. H. Aardema, R. S. Senger, J. L. Robertson, and B. N. Johnson, "3D printed conformal microfluidics for isolation and profiling of biomarkers from whole organs," *Lab on a Chip*, vol. 17, no. 15, pp. 2561–2571, 2017.
- [197] A. P. Haring, A. U. Khan, G. Liu, and B. N. Johnson, "3D Printed Functionally Graded Plasmonic Constructs," *Advanced Optical Materials*, vol. 5, no. 18, pp. 1–9, 2017.
- [198] B. N. Johnson, K. Z. Lancaster, I. B. Hogue, F. Meng, Y. L. Kong, L. W. Enquist, and M. C. McAlpine, "3D printed nervous system on a chip," *Lab on a Chip*, vol. 16, no. 8, pp. 1393–1400, 2016.
- [199] M. K. Gupta, F. Meng, B. N. Johnson, Y. L. Kong, L. Tian, Y. W. Yeh, N. Masters, S. Singamaneni, and M. C. McAlpine, "3D Printed Programmable Release Capsules," *Nano Letters*, vol. 15, no. 8, pp. 5321–5329, 2015.

- [200] H. Kim, B. N. Johnson, Y. L. Kong, H.-A. Chin, M. K. Gupta, D. A. Steingart, I. A. Tamargo, B. P. Rand, T.-W. Koh, and M. C. McAlpine, “3D Printed Quantum Dot Light-Emitting Diodes,” *Nano Letters*, vol. 14, no. 12, pp. 7017–7023, 2014.
- [201] X. Navarro, “Chapter 27 - Neural Plasticity After Nerve Injury and Regeneration,” *International Review of Neurobiology*, vol. 87, pp. 483–505, 2009.
- [202] S. T. Ngo, R. N. Cole, N. Sunn, W. D. Phillips, and P. G. Noakes, “Neuregulin-1 potentiates agrin-induced acetylcholine receptor clustering through muscle-specific kinase phosphorylation,” *Journal of cell science*, vol. 125, no. Pt 6, pp. 1531–43, 2012.
- [203] R. Mancuso, A. Martínez-Muriana, T. Leiva, D. Gregorio, L. Ariza, M. Morell, J. Esteban-Pérez, A. García-Redondo, A. C. Calvo, G. Atencia-Cibreiro, G. Corfas, R. Osta, A. Bosch, and X. Navarro, “Neuregulin-1 promotes functional improvement by enhancing collateral sprouting in SOD1G93A ALS mice and after partial muscle denervation,” *Neurobiology of Disease*, vol. 95, pp. 168–178, 2016.
- [204] N. Zoghoul, L. S. Patil, E. M. Hor, P. Lofti, J. M. Razal, C. Chuong, G. G. Wallace, and M. I. Romero-ortega, “Coiled polymeric growth factor gradients for multi-luminal neural chemotaxis,” *Brain Research*, vol. 1619, pp. 72–83, 2015.
- [205] N. M. Geremia, T. Gordon, T. M. Brushart, A. A. Al-Majed, and V. M. K. Verge, “Electrical stimulation promotes sensory neuron regeneration and growth-associated gene expression,” *Experimental Neurology*, vol. 205, pp. 347–359, 2007.



## **BIOGRAPHICAL SKETCH**

Geetanjali Bendale received her Bachelor of Technology in Biotechnology from the University of Pune, India, in Summer 2012. The following Fall, she enrolled in the Master of Science program in Bioengineering at UT Arlington and shortly joined the Regenerative Neurobiology and Neuroelectronic Lab . After graduation, she enrolled in the PhD program at UT Dallas in the fall of 2014 to continue her work in Dr.Romero-Ortega's laboratory. Her graduate work has focused on using neurotrophic factors to enhance axon regeneration and maturation and restore sensory and motor recovery. She has presented this work in national conferences and has co-authored a peer reviewed research article. As part of collaborative work, she has also authored several other papers on her work in neural interfaces. Her goal is to continue her work to uncover specific mechanisms of delayed regeneration to provide clinically applicable treatment strategies for peripheral nerve repair.

## CURRICULUM VITAE

**Geetanjali S Bendale**

### EDUCATION

**Ph.D. Biomedical Engineering** **May 2019**  
University of Texas at Dallas

**Master of Science in Bioengineering** **August 2014**  
University of Texas at Arlington

**Bachelor of Technology in Biotechnology** **June 2012**  
University of Pune, Maharashtra, India

### PUBLICATIONS AND PROFESSIONAL PRESENTATIONS

- **Geetanjali S. Bendale**, Brandon Tran, Jefferey Miyata, Farial Rehman, Ana Hernandez, Eileen Shimizu, Sanjay Anand, Mario Romero-Ortega\*. Neurotrophic effect of Neuregulin1 Type-III in repairing a 4 cm gap injury in the rabbit common peroneal nerve. (2019, Acta Biomaterialia, In preparation).
- **Geetanjali S. Bendale**, Yuxin Tong, Eileen Shimizu, Sanjay Anand, Blake Johnson, Mario Romero-Ortega Extending the maximum critical nerve gap in the rat sciatic nerve model using curved conduits. (2019, Tissue Engineering Part A, In submission)
- Eric C. Meyers, Nimit Kasliwal, Bleyda R. Solorzano, Elaine Lai, **Geetanjali S Bendale**, Patrick Ganzer, Rafael Granja, Mario Romero-Ortega, Robert L. Rennaker II, Michael P. Kilgard and Seth Hays. Enhancing plasticity in central networks improves motor and sensory recovery after nerve damage. (2019, Nature Communications Submitted)
- SD Bredeson, R Frederick, A Kanneganti, **G.S. Bendale**, M Romero-Ortega, S Cogan and PR Troyk. An assessment of the biological reaction to chronic implantation of peripheral nerve interface devices. (2019, Journal of Neural Engineering, In review)
- Aswini Kanneganti, PhD, **Geetanjali S Bendale**, MS1,2, Eileen Shimizu, Ashlesha Deshmukh, Ana Hernandez-Reynoso, Philippe Zimmern, MD, Dan Freeman, Stuart F. Cogan, Mario Romero-Ortega. A new frontier in neuromodulation with a miniature wireless stimulator for small peripheral nerves. Poster presentation at **2019** SUFU winter meeting, Miami, Florida.

- **Geetanjali S. Bendale**, Brandon Tran, Jefferey Miyata, Farial Rehman, Ana Hernandez, Eileen Shimizu, Sanjay Anand, Mario Romero-Ortega\*. Effect of Neuregulin 1 in repairing long gap nerve injuries in a rabbit model. Oral Presentation at Society for Neuroscience Annual Meeting, November 6, **2018** in San Diego, California.
- **Geetanjali S. Bendale**, Yuxin Tong, Eileen Shimizu, Sanjay Anand, Blake Johnson, Mario Romero-Ortega. Extending the Maximum Critical Nerve Gap in The Rat Sciatic Nerve Model Using Curved Conduits. Poster Presentation at Society for Neuroscience Annual Meeting, November 7, **2018** in San Diego, California.
- María A. González-González, Aswini Kanneganti, Alexandra Joshi-Imre, Ana G. Hernandez-Reynoso, **Geetanjali S Bendale**, Lokesh Patil, Romil Modi, Melanie Ecker, Ali Khurram, Stuart F. Cogan, Walter Voit, Mario I. Romero-Ortega<sup>1\*</sup> Multi-size Softening Cuff Electrodes for Selective Neuromodulation. November **2018**, Scientific Reports. <https://www.nature.com/articles/s41598-018-34566-6>
- Alsmadi, N. Z., **Bendale, G. S.**, Kanneganti, A., Shihabeddin, T., Nguyen, A. H., Hor, E., ... Romero-Ortega, M. I. Glial-derived growth factor and pleiotrophin synergistically promote axonal regeneration in critical nerve injuries. August **2018**, Acta Biomaterialia. <http://doi.org/10.1016/J.ACTBIO.2018.07.048>
- Ana Hernandez-Reynoso, Shrenevas Nandam, Aswini Kanneganti, **Geetanjali S Bendale**, Daniel Freeman, Stuart F Cogan, Mario Romero-Ortega. Wireless Cuff Electrode for Peripheral Neural Interfacing. Poster presentation, Neural Interfaces Conference 2018, Minneapolis.
- **G. S. Bendale**, N. Alsmadi, R. Granja-Vazquez, E. Hor, M. Romero-Ortega. Delayed radial sorting and re-myelination in a 4cm long gap repair despite synergistic effect of neurotrophins and pleiotrophins in nerve regeneration. Oral Presentation at Society for Neuroscience Annual Meeting, November 12, **2017** in Washington D.C.
- **Invited Talk** titled 'Peripheral Nerve Injuries and Alternation Due to Mechanical or Surgical Damage' at the **2017** Environmental Electromagnetic Field and Chronic Pain Symposium at UT Dallas.
- **Finalist** at the **3MT Competition**, UT Dallas, **2017**.
- **G.S. Bendale**, Kanneganti A, Deku F, Bredeson S, Seifert J, Troyk P, Cogan, Romero-Ortega M. A novel wireless microelectrode array implanted chronically provides reliable and selective stimulation. Poster presentation at Society for Neuroscience Annual Meeting, October **2015**, Chicago, Illinois.
- Romero-Ortega M, Kanneganti A, **Bendale G.S**, Seifert J, Bredeson S, Troyk P, Deku F, Cogan S. "Chronic and low charge injection wireless intraneural stimulation in vivo." 2015 37th Annual International Conference of the IEEE Engineering in Medicine and Biology Society (EMBC). IEEE, **2015**. <https://ieeexplore.ieee.org/document/7318536>

- M.I. Romero-Ortega, N.Z. Alsmadi, R. Granja, B. Johnston, A. Kanneganti, **G.S. Bendale**, E. Hor, H. Sumdani, S. Trinh, M. Le. Synergistic effects of neurotrophins and pleiotrophins in stimulating nerve regeneration across long gap peripheral nerve defects. BMES Annual Meeting, **2014** (Podium presentation)
- Kanneganti, **G.S. Bendale**, J. L. Seifert, V. Desai, M. Romero-Ortega. Reestablishment of the blood nerve barrier in Regenerative Multielectrode Interfaces. BMES Annual Meeting, **2014** (Podium presentation)
- M.I. Romero-Ortega, N.Z. Alsmadi, R. Granja, B. Johnston, A. Kanneganti, **G.S. Bendale**, E. Hor, H. Sumdani, S. Trinh, M. Le. Synergistic effects of neurotrophins and pleiotrophins in stimulating nerve regeneration across long gap peripheral nerve defects. SFN Annual Meeting, **2014** (Poster)
- **G.S. Bendale\*** and Ginikachi Ojinnaka\*, Analyzing the placebo effect on human psychology- a comparative study, Oral Presentation at the University of Texas at Arlington Annual symposium ACES in **2013**.
- **G.S. Bendale**, A Bapat, V Kulkarni, A Raut, 'Pathogenicity islands and virulence factors in Salmonella' at 'International Conference on Regulatory Network Architecture in Bacteria' (9-11 March **2012**), held at Sastra University, Tamil Nadu, India. The project was among the eight best abstracts submitted all over the country.

## TECHNICAL SKILLS

**Laboratory Bench:** Immunohistochemistry and Tissue Processing, Cell Culture, DNA/RNA extraction, ELISA and Spectrophotometry, Pre-clinical studies design and execution, Neural Interfaces/Implantation/Testing, Electrophysiology and Data Analysis, Drug Delivery, Confocal Microscopy, Electron Microscopy, Material Testing/Dynamic Mechanical Analysis, Prototype design and 3-D Printing, Project Management

**Software:** Biopac BSL Pro physical measurement software, Image J/NeuronJ, Graphpad Prism, CellSense, Axiovision/LSM/ZEN Imaging software, Adobe Illustrator/ Photoshop, MATLAB, Oracle Clinical, NeuroExplorer

## Certifications:

Clinical Research Management, New York academy of Science, 2017.

## **PROFESSIONAL EXPERIENCE**

### **Graduate Research Assistant**

**University of Texas At Dallas (Dr. Mario Romero-Ortega)**

**August'14- Present**

- *Project lead* on sustained release based growth factor delivery to enhance nerve regeneration across a critical nerve gap in a rabbit model
- Identified appropriate molecular cues required for improved myelination in long nerve regeneration
- Designed, created and fabricated a new conduit design to facilitate use of rodent model in long gap repair and avoid using rabbit and/or higher animal models
- Tested a wireless floating microelectrode array (WFMA) in peripheral nerve stimulation over 14 months for neuromodulation applications
- Validated, optimized and tested versions of shape memory polymer (SMP) based flexible neural interface for stimulation and recording in bioelectronic medicine.

### **Graduate Teaching Assistant**

**August'14- Present**

**University of Texas at Dallas**

Electrical and Electronic circuits in Biomedical engineering

Fall '14

Engineering Physiology of the human body

Spring '15, Spring'16

Advanced Seminars in Bioengineering

Fall'16, Spring'17, Fall 2018, Spring 2019

### **Admin Assistant**

**November'12- May'13**

**UT Arlington**

- Received visitors, directed them around campus and set up meetings
- Received, sorted and distributed all correspondence
- Assisted management with scheduling school educational events

### **Trainee (Dr. Dhorje, Dr. Suresh Jadhav)**

**June '11-August'11**

**Serum Institute of India Ltd.**

- Conducted quality control and stability tests on drugs by following SOPs
- Completed QC analysis reports for vaccine batches
- Document maintenance for FDA inspections